Copyright Warning & Restrictions

The copyright law of the United States (Title 17, United States Code) governs the making of photocopies or other reproductions of copyrighted material.

Under certain conditions specified in the law, libraries and archives are authorized to furnish a photocopy or other reproduction. One of these specified conditions is that the photocopy or reproduction is not to be "used for any purpose other than private study, scholarship, or research." If a, user makes a request for, or later uses, a photocopy or reproduction for purposes in excess of "fair use" that user may be liable for copyright infringement,

This institution reserves the right to refuse to accept a copying order if, in its judgment, fulfillment of the order would involve violation of copyright law.

Please Note: The author retains the copyright while the New Jersey Institute of Technology reserves the right to distribute this thesis or dissertation

Printing note: If you do not wish to print this page, then select "Pages from: first page # to: last page #" on the print dialog screen

ABSTRACT

DEVELOPMENT OF A NON-INTRUSIVE PARTICLE MOTION TRACKING TECHNIQUE FOR GRANULAR FLOW EXPERIMENTS

by
Jerry R. Volcy

Implementation aspects of monitoring the position and orientation of a one-inch diameter particle in space non-intrusively based on the principle of magnetic induction coupling are discussed. A radio-transmitter embedded within the particle induces voltages in receiver antennae. Position and orientation of the particle are deciphered from these voltages. A previously developed math model that predicts the voltage induced in an antenna given the position and orientation of the transmitter with respect to the antenna as well as the numerical techniques used to obtain the inverse solution of computing position and orientation from a given set of voltages are used.

Practical issues of implementation including the experimental setup, the effect of model-reality discrepancy, empirical model corrections, and methods improving the numerical techniques are the focus of the present study. Experimental results show that the present tracking system has an accuracy of approximately 1 to 2 particle diameters and indicate the accuracy may be greatly improved with the use of multiple transmitters. The technique of tracking developed here has a wide range of applications because of its non-intrusive nature, however, emphasis is placed on the study of the behavior of bulk solids. Directions for future work are discussed.

DEVELOPMENT OF A NON-INTRUSIVE PARTICLE MOTION TRACKING TECHNIQUE FOR GRANULAR FLOW EXPERIMENTS

by
Jerry R. Volcy

A Thesis
Submitted to the Faculty of
New Jersey Institute of Technology
in Partial Fulfillment of the Requirement for the Degree of
Master of Science in Mechanical Engineering

Department of Mechanical and Industrial Engineering

January 1994

APPROVAL PAGE

DEVELOPMENT OF A NON-INTRUSIVE PARTICLE MOTION TRACKING TECHNIQUE FOR GRANULAR FLOW EXPERIMENTS

Jerry R. Volcy

Dr. Rajesh N. Dave, Thesis Advisor — Date
Associate Professor of Mechanical Engineering,
New Jersey Institute of Technology

Dr. Anthony D. Rosato, Committee Member — Date
Associate Professor of Mechanical Engineering,
New Jersey Institute of Technology

Dr. Bruce G. Bukiet, Committee Member — Date
Assistant Professor of Mathematics,
New Jersey Institute of Technology

Dr. Ian S. Fischer, Committee Member — Date
Associate Professor of Mechanical Engineering,
New Jersey Institute of Technology

VITA

Author: Jerry R. Volcy

Degree: Master of Science in Mechanical Engineering

Date: January 1994

Undergraduate and Graduate Education:

- Master of Science in Mechanical Engineering,
  New Jersey Institute of Technology,
  Newark, New Jersey, 1994

- Bachelor of Science in Mechanical Engineering,
  New Jersey Institute of Technology,
  Newark, New Jersey, 1992

Major: Mechanical Engineering

Presentations and Publications:

Dave, R., J. Volcy , A. Rosato,
"Non-Intrusive Rigid Body Tracking in Dry Granular Flows"
Twelfth US National Congress of Applied Mechanics
Seattle, Washington, 26 June - 1 July, 1994.

Dave, R., B. Bukiet, A. Rosato, I. Fischer, J. Volcy,
"Non-Invasive Rigid Body Tracking"
Department of Energy/National Science Foundation: The Flow of Particulates and Fluids
Ithaca, New York, 30 September - 1 October, 1993.

Volcy J.,
"Three Dimensional Particle Tracking Using High Speed Digital Photography"
American Society of Mechanical Engineers Winter Annual Meeting
Anaheim, California, 10 November, 1992.

This thesis is dedicated to

my mother

my father

and my aunt

ACKNOWLEDGMENT

I wish to express my deepest gratitude to Dr. Rajesh N. Dave for his expertise and support throughout this research. His guidance has been truly exceptional. I also thank Dr. Bruce G. Bukiet, Dr. Anthony D. Rosato and Dr. Ian S. Fischer as committee members and collaborators in this work.

I acknowledge the work of my colleagues Anthony La Rosa, Elliotte Harold, Anthony Troiano, Subramanyam Chamarti and Kurra Bhaswan. This thesis would not have been possible without their contributions.

I acknowledge Don Rosander, Joe Glaz, Dave Singh, and Hugh Magee of the Mechanical Engineering Technical Staff for their support during the course of this research.

I am grateful to the United States Department of Energy for having funded this project.

TABLE OF CONTENTS

TABLE OF CONTENTS
(continued)

Chapter **Page**

TABLE OF CONTENTS
(continued)

Chapter **Page**

LIST OF FIGURES

Figure **Page**

LIST OF TABLES

Table **Page**

Chapter 1
Introduction

1.1 The Study of Bulk Solids

Bulk Solids or granular materials refer to the class of substances characterized by a collection of discrete solid particles dispersed in a fluid continuum. When the fluid is a liquid, the mix is termed a slurry and the liquid may become important in characterizing the behavior of the mixture. When the interstitial fluid is a static gas, the behavior of the bulk is governed primarily by the interactions between the solid elements composing the mass. Thus, a study of the behavior of bulk solids can begin with a study of the dynamics between the constituents within the bulk.

The size of the particulates within a bulk solid can range from fine dusts to large rocks [Woodcock (10)]. Some examples of bulk solids include coal, pack ice, metal powders, ceramic powders, pharmaceuticals, grain, sand, ores, kaolin, potatoes, sugar, table salt and rocks [Savage (6)]. Hence, the study of bulk solids finds applications in every industry that handle or work with these materials. The study of bulk materials finds relevance in many areas of science and engineering as well. Geology, geophysics, sedimentology, conveyor belt design, hopper design, pharmaceutical processing and handling, processing industries, ceramics, powder metal forming and bulk solids transportation are a few of the areas that can benefit from an improved understanding of the flow behavior of granular materials. In the case of conveyor belt and hopper design, the designing engineer typically is forced to rely strictly on the trials and errors of the past when a new design is in need. The result is often an expensive failure of the new design because of a lack of understanding of how the old design parameters are to be adapted to the newer design. Little or no scientific theory is at hand to guide the engineer [Savage (6)].

Given the increasing importance of the study of granular materials in flow, it is surprising that studies in this area have lagged so far behind studies in parallel fields such as fluid mechanics and gas dynamics. The little theory that exists in the field has, however, well surpassed experimental studies. The time has come that the theory can no longer progress rapidly without the substantiation and corrections that can come only from actual experimentation. Such experiments have been lacking in the past primarily because of the formidable nature of the problem. For example, the parameter space of a free flowing mass is so wide that it almost defies the controlled space needed to carry out experimentation. The size of the constituents within the flowing mass, the shape of these constituents, the nature of the dispersant, the coefficient of friction between the constituents, the coefficient of restitution, the boundary conditions, the angle of flow, the speed of the flow, the friction and restitution coefficients against the boundary and the packing density of the mass are some of the primary parameters that must be considered. The parameter space increases further when particles of differing size, shape and physical properties are combined in a composite flow.

There are two basic approaches to studying the behavior of a flowing system. One can approach the problem either from a LaGrangian or Eulerian point of view. In an Eulerian study, a fixed volume of space within the flow, called the Eulerian space or Eulerian volume, is observed. The focus is not on any individual particle, but on the activity of particles that cross the boundaries of the control space. Such studies give us an understanding of how the mass behaves as a whole, but give little insight to the dynamics within the flow. Macroscopic properties such as flow rate, packing density, pressures and other flow properties are typically devised from Eulerian studies. A LaGrangian study, on the other hand, attempts to study the

behavior of a collection of particles by observing the activities of a single particle typical of the moving pack and embedded therein. Such studies have proven to be of extreme difficulty to perform because of the large parameter space and the difficulties of monitoring a single particle in a flowing mass.

Historically, experimenters have attempted to perform such studies by collapsing the parameter space to two dimensions or by intruding into or simply stopping the flowing mass to determine the state of the tracer particles. The results of either technique is arguably untrue to the real nature of the flow. The first has a two-dimensional limitation. It is not clear how the results of such a study is to be extrapolated into three dimensions. The latter is an intrusive technique and has the disadvantage of disturbing the very flow it seeks to characterize. Some non-intrusive techniques [Tuzun(8)] that use X-rays, γ-rays, radio-isotopes, radio pills or magnetic tracers are either extremely expensive, health hazards or incapable of measuring orientations because of their isotropic properties. A well established technique of monitoring position and orientation of a single particle in a flowing mass has yet to be developed.

1.2 Statement of the Problem

We propose to develop an authentic non-intrusive particle tracking technique that will be valid for use in the study of unconstrained granular chute flows. The tracking system uses magnetic coupling and the relationship that exists between current levels and the positioning of transmitter with respect to receiver to estimate the location of the source. The theoretical viability of this tracking system has been substantiated by Dave *et al.* [Dave (3)] through simulations. Construction of the physical tracking system is near completion. Methods of implementation will be discussed here. Difficulties in the numerical methods used will be examined as well as difficulties that arise form the discrepancies that exist between theory and experimentation.

1.3 Outline of Remaining Chapters

In Chapter two, we describe the proposed tracking system and provide an overview of the technique. Details of the experimental hardware is covered and general hardware specifications are provided. Chapter three examines the mathematical model used to describe the transmitter-receiver relationship we seek to exploit. Discrepancies between the model and reality are identified and methods of error corrections are developed. In chapter four we focus on the signal processing part of the tracking system and look at various techniques used to better the inverse solution of determining position and orientation from measured voltages. Convergence issues are considered and methods of improving the numerical techniques are discussed. In chapter 5, we present some experimental results and discuss the need for a multiple transmitter system. Chapter 6 summarizes the efforts, to date, in developing the tracking system. Direction for future study is provided and conclusions are outlined.

Chapter 2
The Physical System

2.1 Overview

The proposed tracking system is based on the principle of magnetic induction coupling. This principle states that the presence of an electromagnetic source will induce a current in nearby objects. The magnitude of this induced current will be primarily a function of the conductance of the pick-up objects and the orientation of the transmitting source with respect to the receiving object. Typically, objects with low conductance like acrylic, glass, nylon, wood and other non-metals are classified as "radio-transparent" materials because the currents induced in these media is often undetectably small. Objects with high conductance include metals like copper, iron, silver and gold. These metals are good receptors of electromagnetic radiation and produce currents that can be measured by readily available electronic circuitry.

The aim here is to exploit the relationship that exists between the transmitting source and the receiving antenna to determine the location of the source. Because the current induced within a given receiver is not unique with respect to the spatial position and orientation of the transmitting source, multiple receivers are needed to monitor the source. Triangulation-like techniques can then be used to determine the location of the source.

The proposed tracking system is comprised of a radio-transparent flow space instrumented with number of receiving antennae. The problem, then, becomes one of embedding a radio transmitter source within one of the particles in the flowing mass and subsequently translating the antenna voltages into positions and orientations. In this study, the particles to be used are 1-inch acrylic spheres.

Once the mechanics of the system are established, data is collected in the form of signals from the receiving antennae. These signals are filtered, amplified, digitized,

downloaded and stored in a computer. The *inverse solution* refers to the process by which these signals are used to determine transmitter's position and orientation. Through theories of electricity and magnetism, it is possible to estimate the signal levels in a loop antenna given the position and orientation of the transmitting source with respect to the loop. However, it is difficult to obtain an inverse solution in closed form because of the complex relationship that exists between the induced signal and the location of the transmitter. We resort to numerical methods to solve an over-determined system of m non-linear equations for 6 unknowns: x, y, z, α, β, γ. m is the number of receiving antennae in the system. x, y and z are the coordinates describing the position of the particle in space. α, β and γ are parameters that describe how the particle is oriented in space. α, β and γ are defined in figure 2.1 as the angles that the axis of the transmitter makes with the x-axis, y-axis and z-axis respectively.

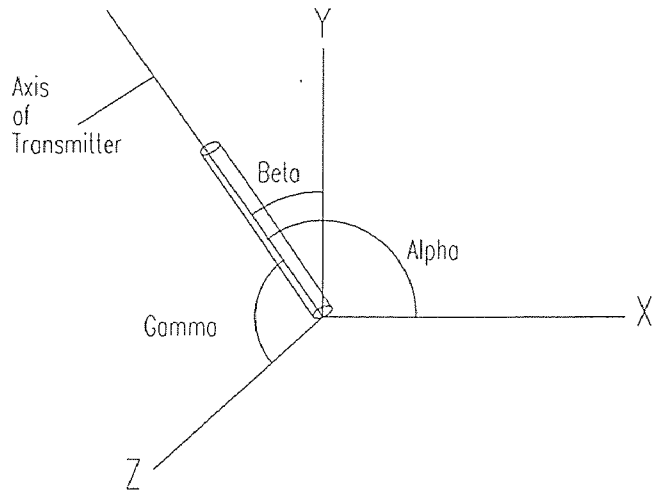

Figure 2.1 Definition of α, β and γ. The angles α, β and γ are parameters that define the transmitter's, and hence the tracking sphere's, orientation in space.

A block diagram of the entire tracking system appears in Figures 2.2 and 2.3. The tracking technique can be separated into two major sections: data acquisition and signal processing. Details of the experimental data acquisition system are presented in

this chapter while details of the voltage model will be discussed in the next. We will focus attention on the signal processing aspects in chapter 4.

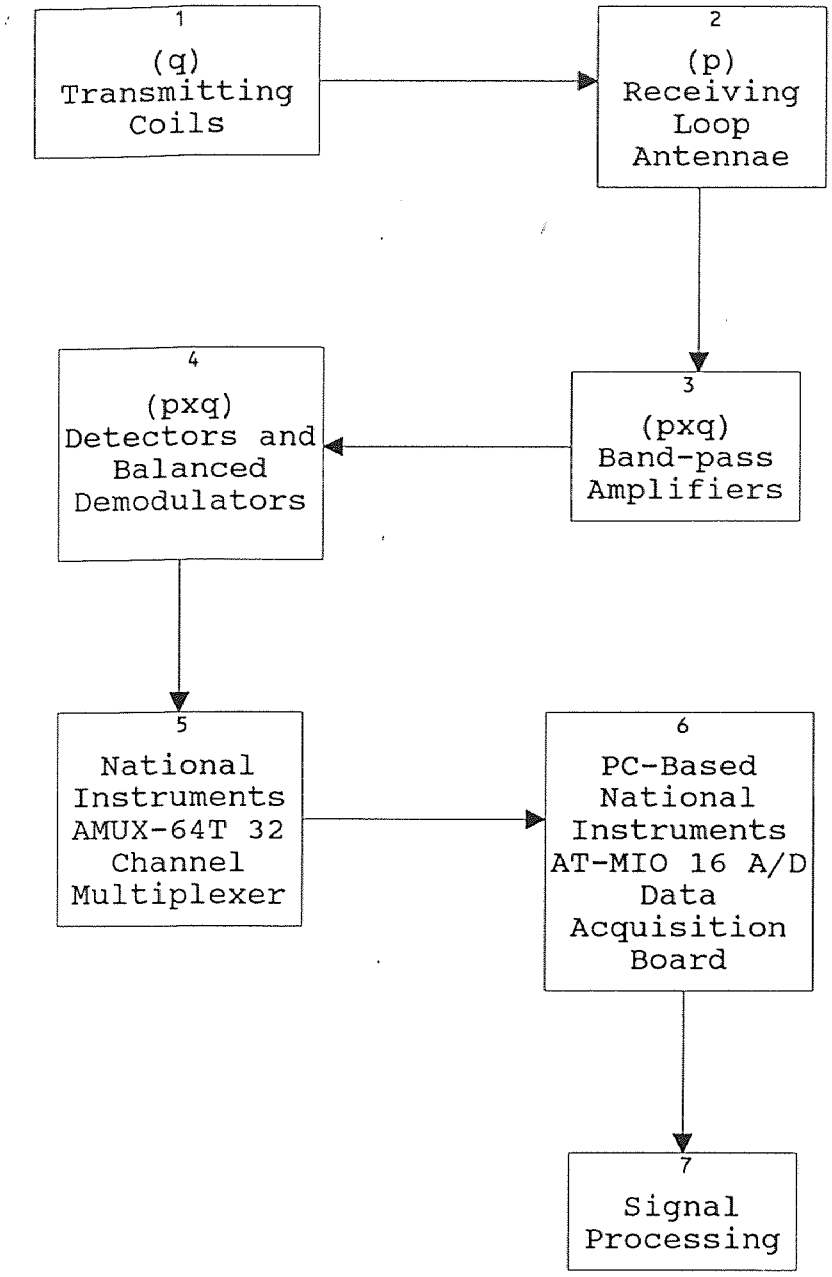

Figure 2.2 Data Acquisition Block Diagram.

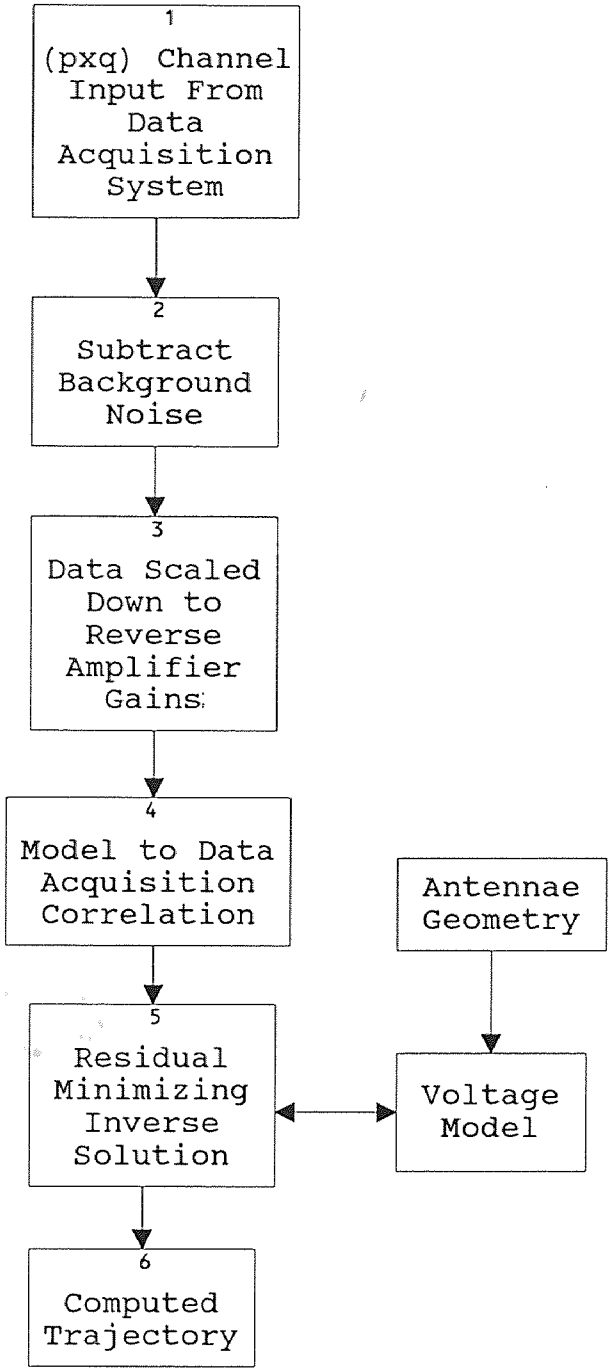

Figure 2.3 Signal Processing Block Diagram.

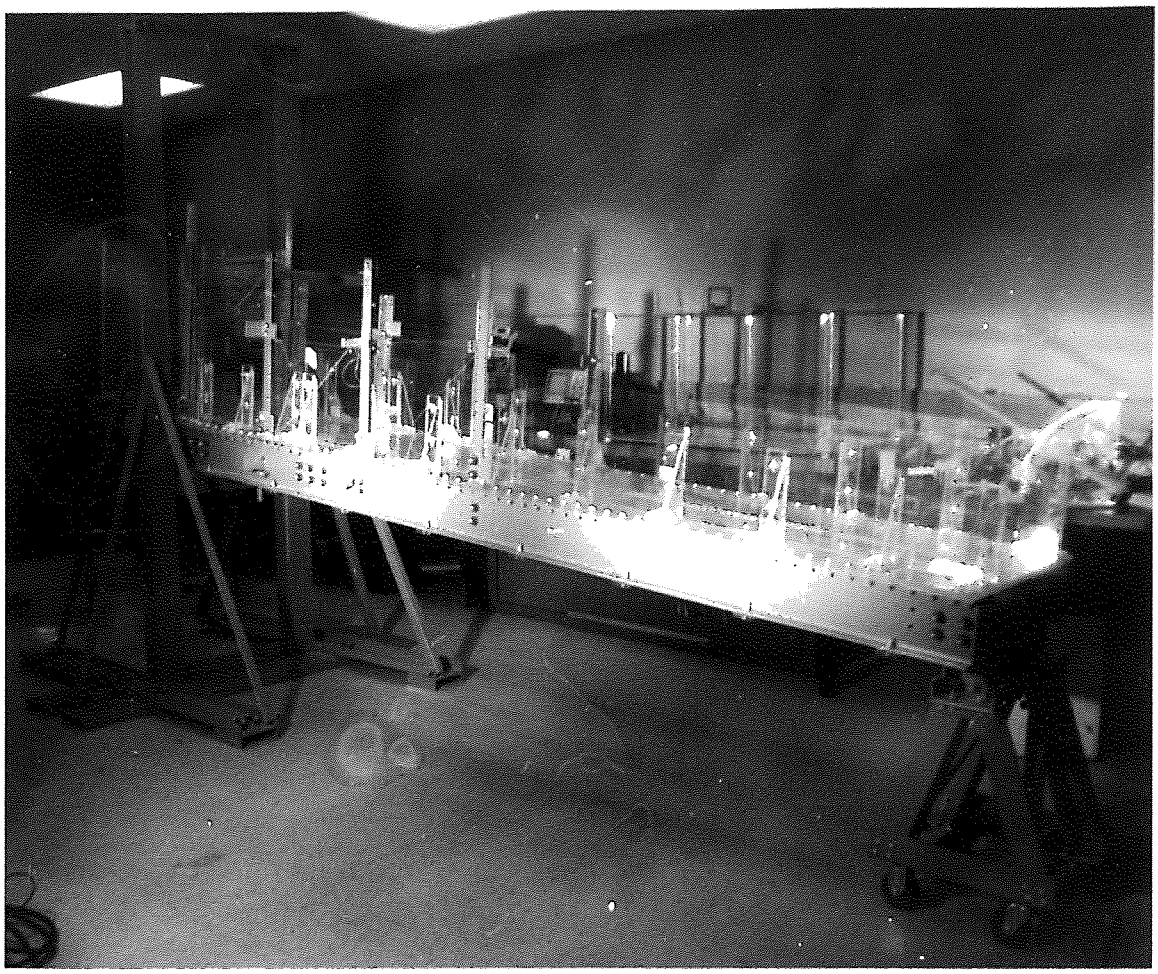

Figure 2.4 The Radio-Transparent Chute.

2.2 Experimental Hardware

Successful implementation of the proposed tracking system is contingent on the ability to successfully build, integrate and "tune" the electrical, mechanical and computer hardware needed. Because of the sensitivity of the receiver-transmitter system, it is found that small modifications to any part of the system (configuration of antennae and choice of electric wires, for example) are often reflected in the results. Consequently, several alternative configurations are tested and evaluated and the optimal configuration is attained largely by trial and error. Here we shall set our focus on the design of the chute, transmitter, antennae, receiver, wiring and data acquisition system.

2.2.1 Chute

Because of the radio-magnetic nature of the tracking system, the chute is a 12"x12"x120" "radio-transparent" structure constructed primarily of Extren 500 and 600 structural shapes (See Appendix F) and acrylic sheets. It is fastened together mostly by nylon nuts and bolts. The only metallic component of the structure are the rectangular loop antennae that tessellate the flow area. The construction of the chute is such that the center deflection in no larger that 5/32" under a 87.4 lb/ft load [La Rosa (4)]. The maximum inclination angle of the chute is 35°. The hopper of the chute is a volume of 24" x 18" x 24" capable of housing 10,000 1" spherical particles. A picture of the chute is shown in Figure 2.4. Construction diagrams of the major components appear in Appendix A. The coordinate system of the chute (which we will call the global system) is such that the x-axis runs along the center length of the chute as shown in figure 2.5.

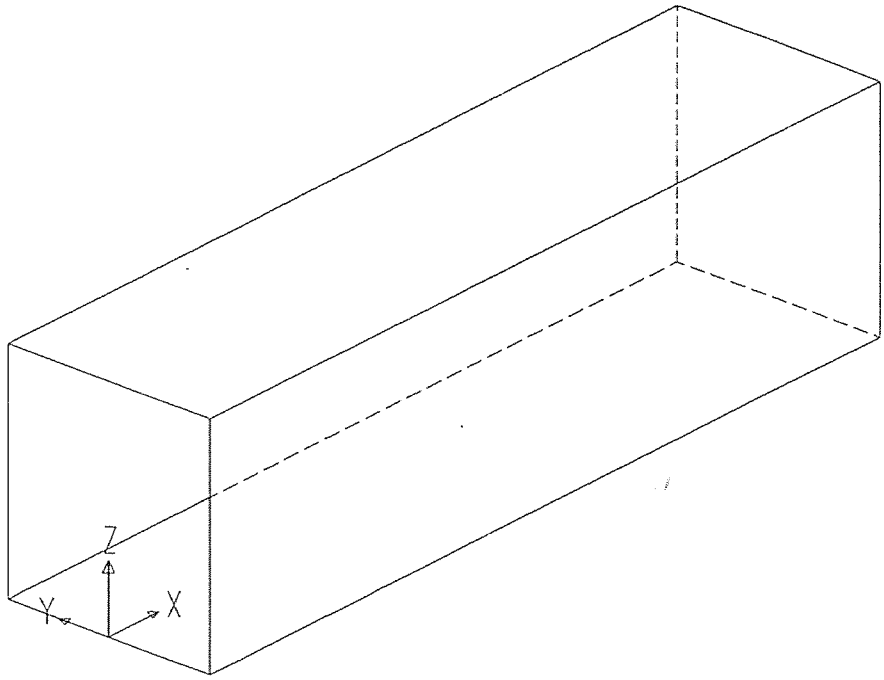

Figure 2.5 Flow space and coordinate system of the chute (not to scale).

2.2.2 Transmitter

The tracking sphere is made from a 1" acrylic sphere typical of those in the flowing mass. A sphere is cut into two halves which are bored hollow and threaded to fit a cylindrical collar as shown in figure 2.6. Within the collar is centered a 5mW Hartley oscillator broadcasting at 2.04 MHz [Troiano (7)]. The oscillator circuitry is constructed entirely of miniature surface-mount components arranged on a 0.55" diameter printed circuit board. The oscillating coil is wound around a ferrite core and mounted above the circuit board as shown in figure 2.7.

The required power for the circuit is provided by two 1.5 volt nickel-cadmium batteries installed on either side of the coil. See figure 2.8. It is assumed that the interference introduced by the proximity of the metallic batteries is negligible given their small size. A schematic of the transmitter circuitry is shown in figure 2.9. The axis of the transmitter, as it will be discussed in this document is defined in figure 2.10.

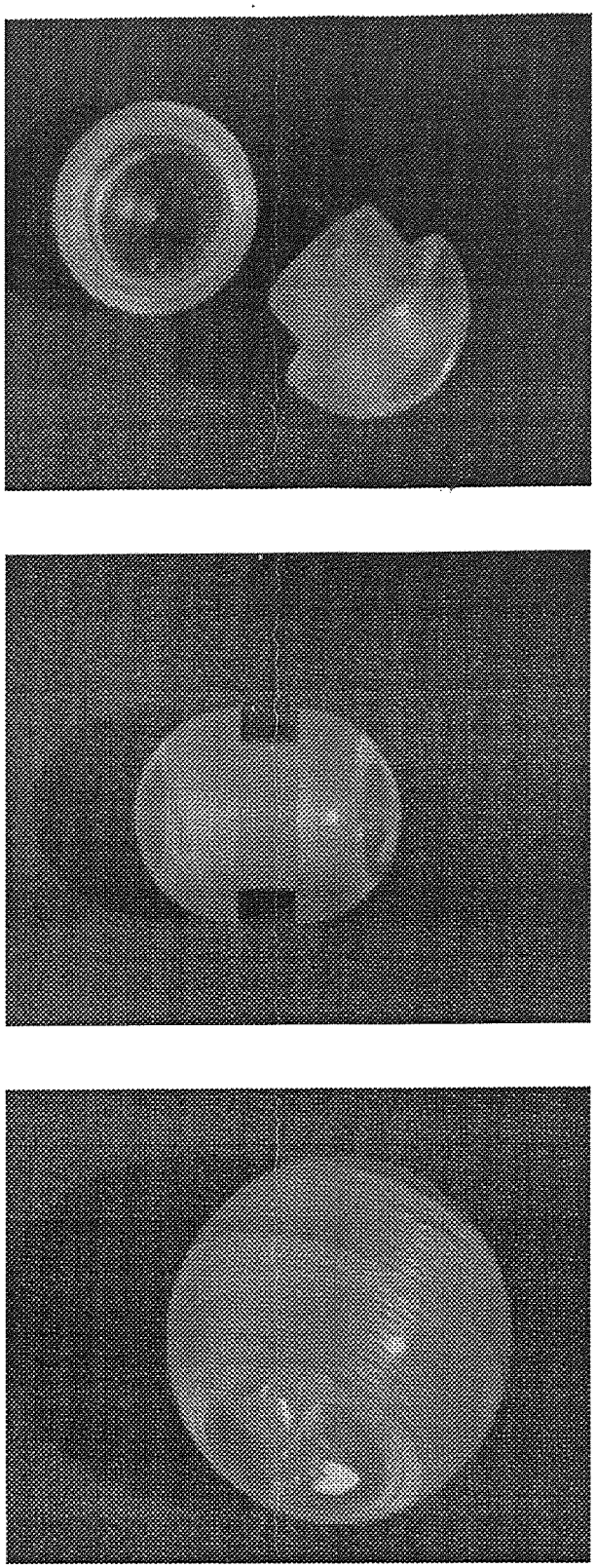

Figure 2.6 Case of the Tracking Sphere: The case of the tracking sphere is fabricated from a 1" acrylic sphere typical of those in the flowing mass.

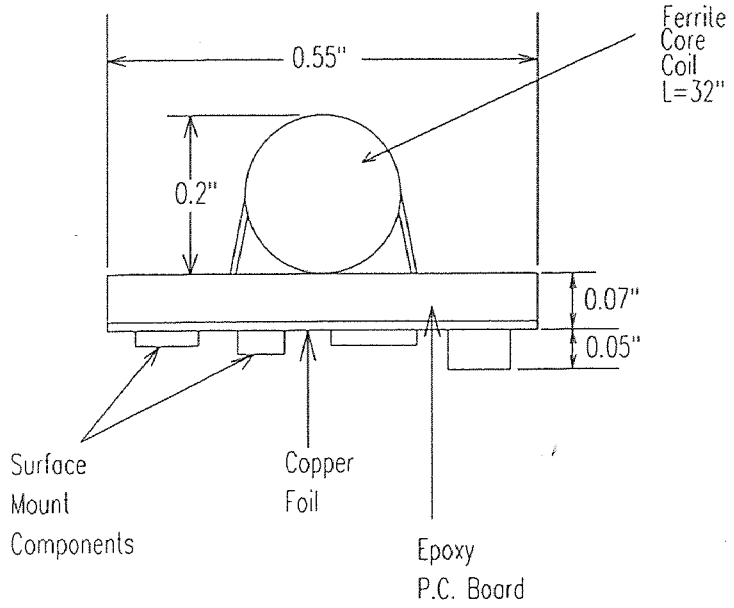

Figure 2.7 Profile of the transmitter-coil and the supporting circuitry.

The transmitter oscillating frequency was chosen to be 2.04 MHz. This frequency is chosen for several reasons. One reason is that extreme frequencies require high capacitances or high inductances which become difficult to incorporate into a miniature circuit. Another reason is related to the transmission of power. The level of power delivered to the receiving antennae, it will be shown, is directly proportional to the frequency of oscillation of the source. It is thus desirable to have as high a frequency of oscillation as possible. The higher the frequency, however, the greater the power requirements and the greater the possibility of standing waves and interference from distant metallic objects that may reflect the radio waves. Thus, an upper limit is placed on the transmitting frequency because of limitations on the size of the power source and because of a desire to keep clear of very high frequencies where interference as described becomes problematic. Yet another reason for choosing a frequency of 2.04 MHz is its availability. For example, a frequency of 88.0 MHz is a bad choice because it is on the FM (Frequency Modulation) band and is constantly in

use, representing an endless source of high power noise. Likewise, a frequency of 176.0 MHz is a poor choice because it is the first harmonic of the busy 88.0 MHz band. 2.04 MHz is a fairly isolated frequency with no immediate "busy" harmonics.

Mechanical balancing of the tracking sphere entails the addition of nonmetallic materials within the package to give it the same weight as any other sphere in the flowing mass. Also, the weight must be positioned such that the finished package does not have a "heavy" side. Given the size and non-metallic limitation of the balancing weights, an effort to accurately balance the tracking sphere is non-trivial and beyond the scope of this document.

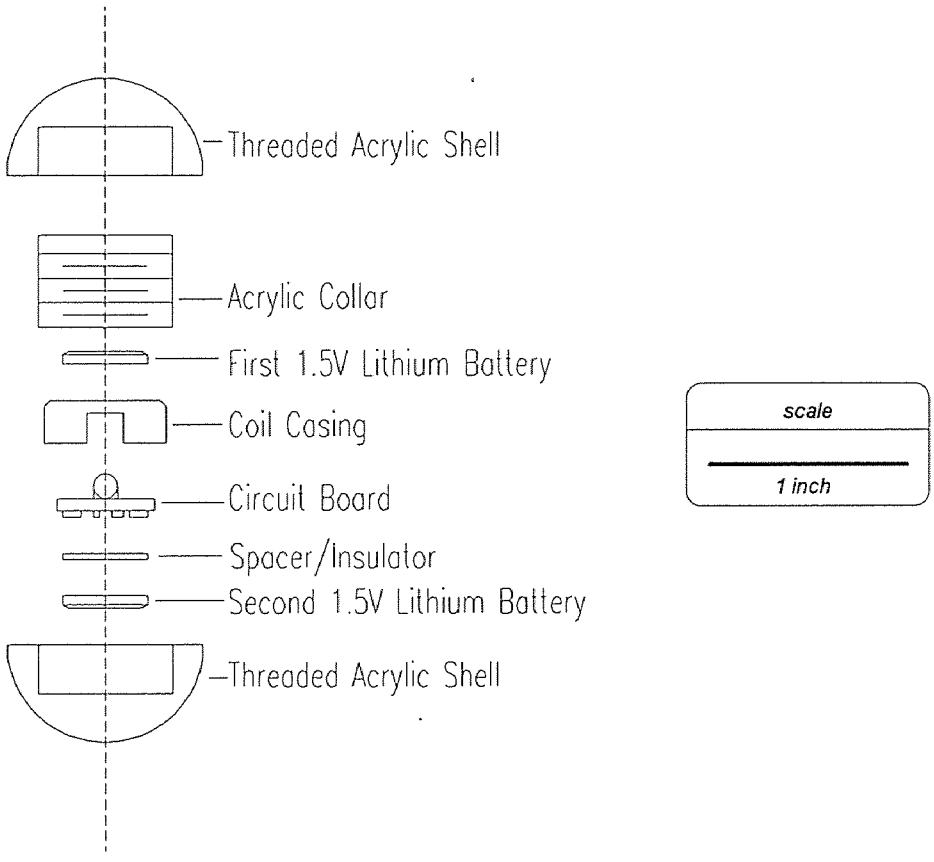

Figure 2.8 2.04 MHz Transmitter Assembly. This exploded view of the 2.04 packaged transmitter is a sketch showing the actual size of components within the tracking sphere.

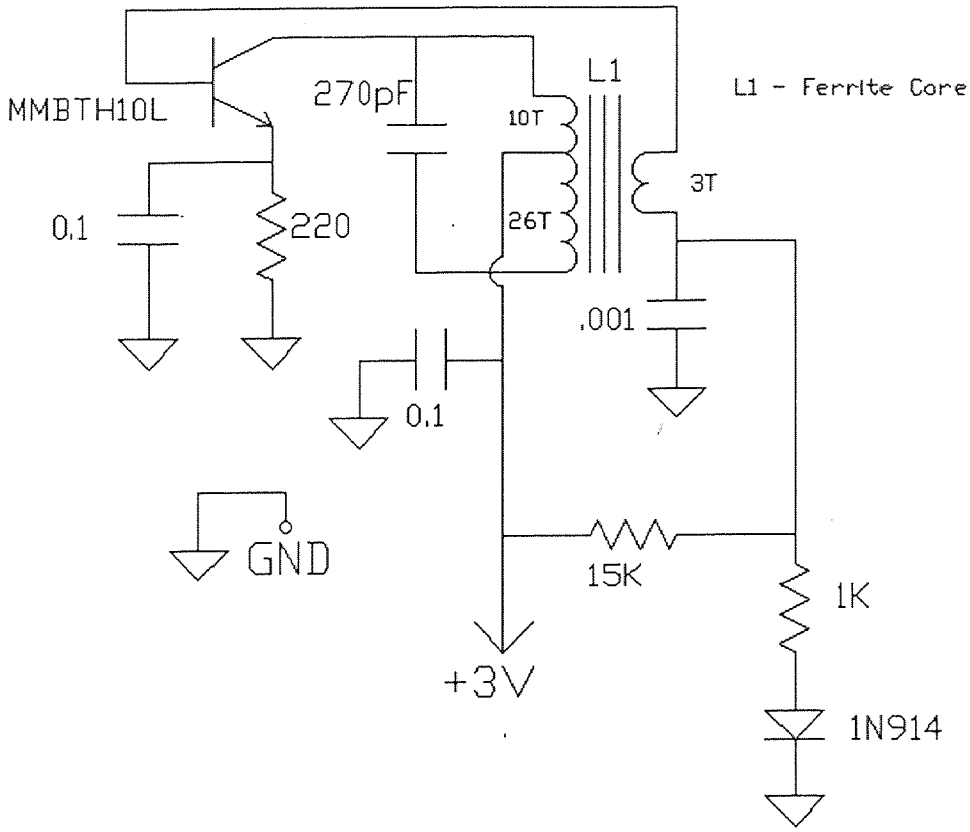

Figure 2.9 Schematic Diagram of the Transmitter Circuitry

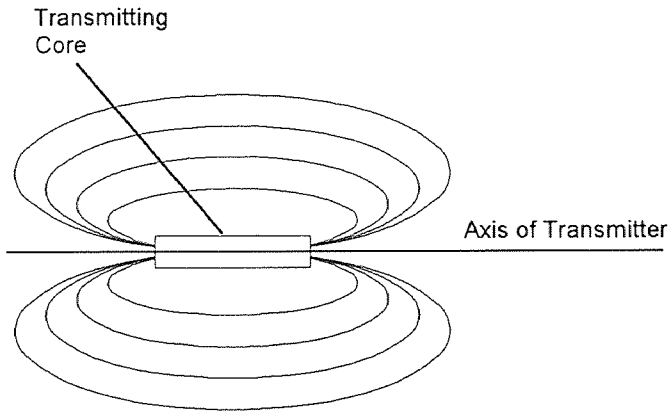

Figure 2.10 The axis of the transmitter.

2.2.3 Antenna System

Complete determination of the position and orientation of the tracking sphere translates into solving six unknowns: three in position and three in orientation. Thus, at every instance, at least six antennae must be used to monitor the path of the tracking sphere. In this experiment, the a antennae used are rectangular loops. The configuration of these antennae, that is their location, size, shape and number has proven to be extremely important to the tracking system. It is found in preliminary studies that smaller antennae with aspect ratios close to 1 work reasonably well, however, further study reveals that generalities on the size of the antennae cannot easily be made. Larger antennae tend to give low signals and thus a small signal to noise ratio. Antennae with large aspect ratios tend to deviate more from the model predicted voltages, resulting in large systematic errors in the final results. Thus, the smaller the antenna, the better the results. However, more antennae are needed to cover the length of the chute. It is found that antennae with dimensions of approximately 22" by 22" cover a good space while providing consistently good results with the model predictions. See figure 2.11. The letters DAQ in the figure is shorthand for "Data AcQuisition". The units of the ordinate are counts which are integers with magnitudes directly proportional to the signal level in the antenna. The data is collected with the axis of the transmitter collinear with the axis of the antenna. Data is collected as the transmitter is moved away from the plane of the antenna. The axis of the transmitter is as defined in figure 2.10. The area of the antenna is defined as the vector centered in the plane of the antenna and perpendicular to it with a magnitude equal to the area of the loop.

The position and orientation of the antennae that cover the chute flow space also have a strong impact on the end results of the inverse solution. Problems arise particularly when an orthogonality occurs between the axis of the tracking sphere's transmitter and the axis of one or more antennae. When this occurs, a very low

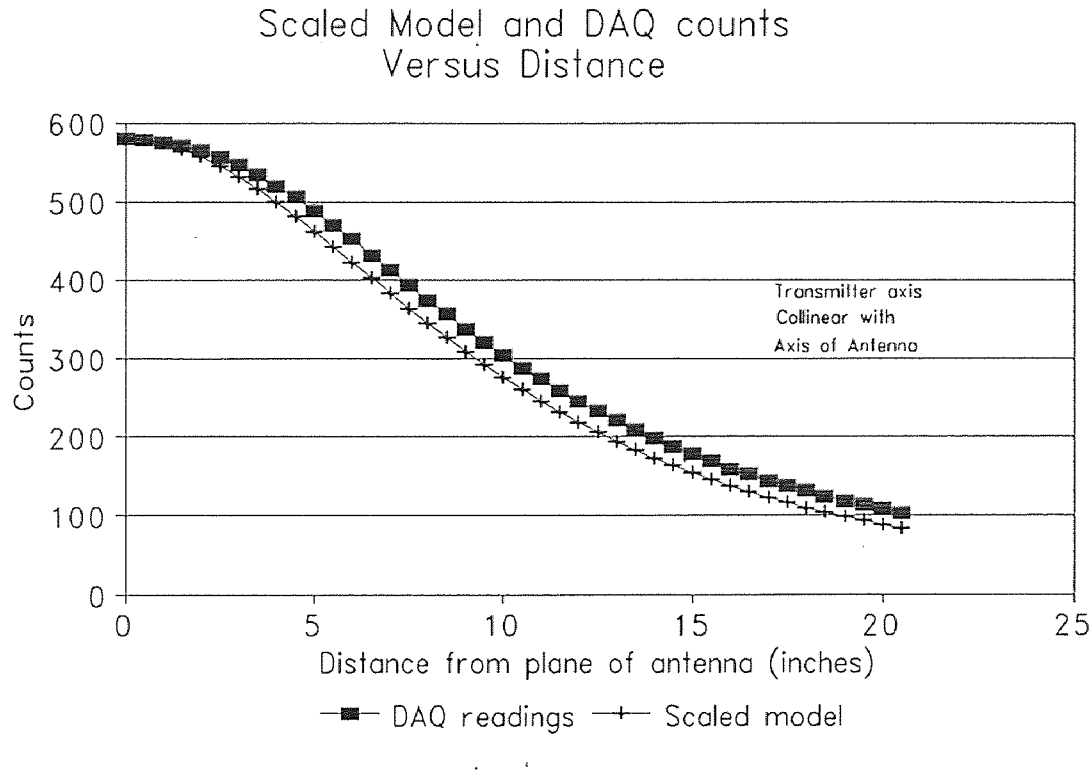

Figure 2.11 Data collected using a 22" x 22" antenna.

current is induced within the antenna, resulting in a very low signal to noise ratio. This is illustrated in figure 2.12. If the space around the transmitter is being monitored by six antennae arranged in a cubic tessellation, then an orthogonality can result in as many as four of the six antennae at the same time. The result of such an occurrence is always the same. The two antennae with axes parallel to the transmitter axis have very strong signal to noise ratio while the other four antennae give signals with unacceptably low signal to noise ratios. In a true granular flow, such an orthogonality is rare in a sustained manner. Techniques are developed in the signal processing stage to overcome this situation. The history of the particle's path can be reconstructed by examining its position and orientation immediately before and after the orthogonality occurred and subsequently interpolating to determine a true position. The need for

this interpolating technique can be slightly reduced by the addition of extra antennae mounted at an angle with respect to the chute.

Also important in the tracking of the sphere is the selection of antennae. A minimum of 31 antennae are required to do a cubic tessellating of the chute if we wish to respect the 22" x 22" guideline for antenna size. This implies that antennae at the extremities of the chute will be separated by a large distance. It is not desirable to use very distant antennae to compute the position and orientation of the tracking sphere because these antennae will provide low signal to noise ratios and will increase the numerical computation effort without increasing the accuracy of the end results. It is therefore desirable to develop a methodology to systematically select sets of antennae as the tracking sphere moves along the chute. This selection is to be handled in the signal processing stage of the experiment when true flows are being studied.

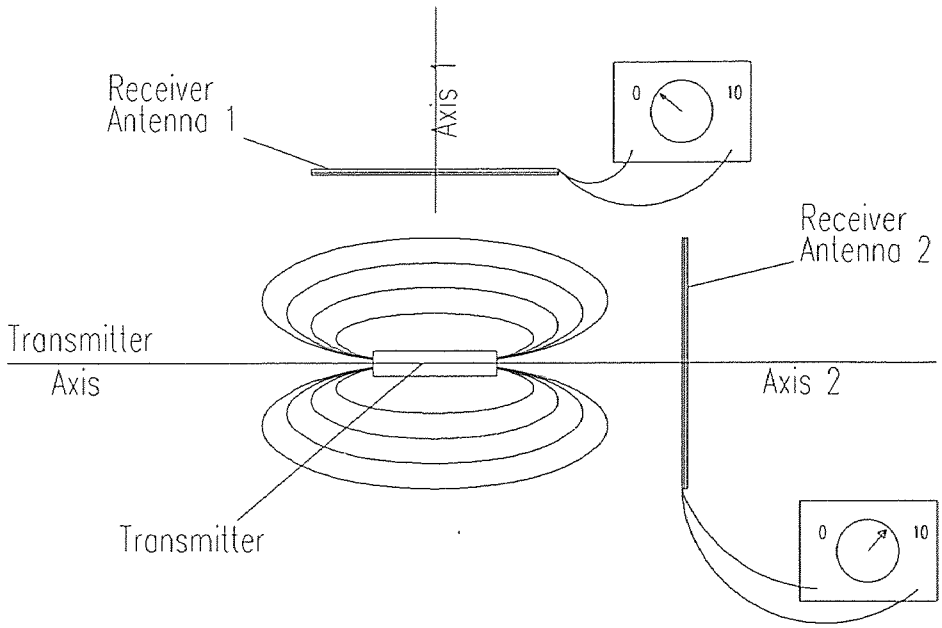

Figure 2.12 The effect of orthogonal transmitter-receiver axes. In the above illustration, the axis of the transmitter is parallel to the axis of antenna #2. A high signal level will be induced in antenna #2 as a result. On the other hand, the transmitter's axis is orthogonal to the axis of antenna #1. As a result, a low signal level will be registered in antenna #1.

2.2.4 Receivers and Data Acquisition

The presence of the tracking sphere within the flow space yields only a few millivolts in the loop antennae. Receiver boards have been built to amplify these signals and isolate the 2.04 MHz transmitter frequency. The output of these boards is a differential positive DC voltage in the range of approximately 0 to 3 volts. It is crucial that the receiver boards amplify the signal and convert the AC input to a scaled DC voltage in a linear fashion. Figure 2.13 is a plot of the system's linearity [Troiano (7)].

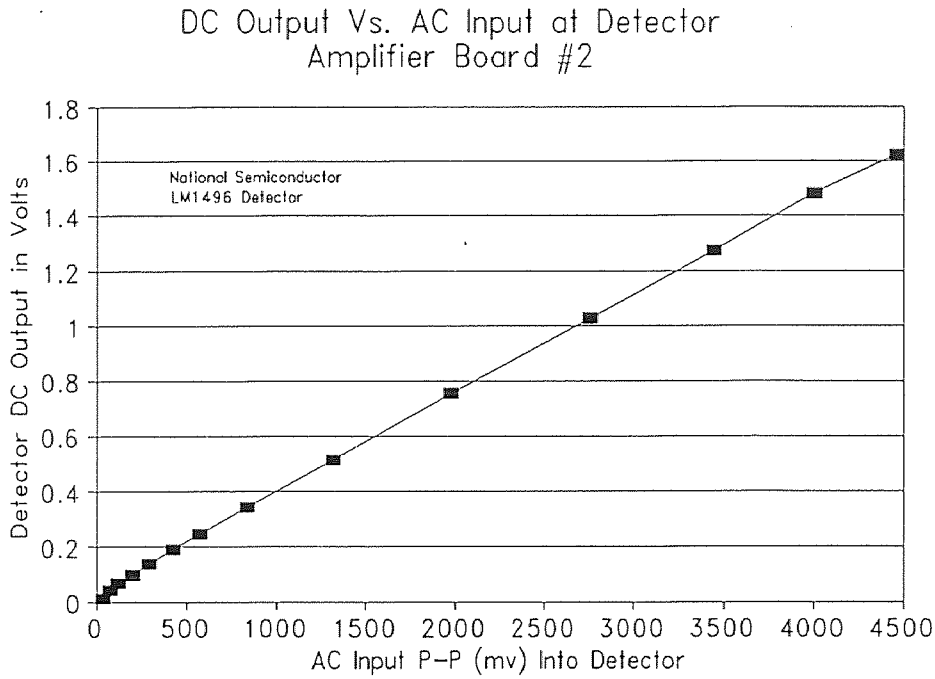

Figure 2.13 Linearity of receiver boards at detector stage.

The sensitivity of the transmitter-receiver system is a limitation of the digital data acquisition system (referred to as the DAQ system). Because the receiver boards are analog devices, they are, in theory, sensitive to infinitesimal changes in the position and orientation of the tracking sphere. The data acquisition system is found to be sensitive to small changes in angles and position. However, this sensitivity is dependent on the transmitter's orientation with respect to the monitoring antenna.

The analog to digital system is a National Instruments (see Appendix F) 12-bit converter that outputs a value of -2047 to 2048 "counts" corresponding to -10 volts to +10 volts DC.

The sampling speed is a limitation of the digital data acquisition system and its host computer. In high speed chute flows, if this limitation becomes an impracticality, it may be overcome by first using magnetic tape to collect the analog data and subsequently downloading to the data acquisition system at a reduced speed.

2.3 Calibrating the System

The mathematical model predicts the signal level induced in each antenna as a function of the position and orientation of the transmitting source. The data collected from the data acquisition system is in the form of *counts*, a set of integers in the range of 0 to 2048 that are representative of the signal level in an antenna multiplied by a scaling factor that is a function primarily of the amplifier gains. Determination of this scaling factor is imperative to converting the counts to volts. We have assumed that this factor is constant with respect to position, orientation and time. Calibration of the data acquisition system is thus done by setting the tracking sphere at a known position and orientation and recording the count level. The model predicted voltage at this same position is divided by the measured reading to obtain the scaling factor. Normally, calibration is done at a point of high signal levels to minimize errors.

Because it is never possible to eliminate random noise from the environment, it is necessary to remove all standing waves from the collected data. This is done by collecting data from each antenna with the transmitter turned off. This reading, henceforth termed the *background reading*, is then subtracted from subsequently collected data. Background readings have accounted for as much as 5.0% of the total reading on a single channel. At very low signal levels, this fraction is even higher. It is thus necessary to eliminate this noise.

2.4 Interference and Wiring

Wiring from the chute antennae run along the length of the chute in approximately parallel paths to the receiver boards and circuitry kept a few feet from the experimental space to avoid interference. When lines travel long paths in parallel and close proximity, it is inevitable that interference will occur. Figure 2.14 shows the result of antennae lines coupled from a long parallel run. The data in this figure is collected in a similar manner as the data set described in section 2.2.3. The transmitter, whose axis is collinear with the axis of the antenna, is moved away from the plane of the antenna in increments of 0.5 inches. An error of approximately 200% is observed between the scaled model and the curve labeled "Unbraided DAQ lines". The situation is rectified in the curve labeled "Braided DAQ lines". Braided data lines greatly reduce the effect of coupling between antennae lines. Coupling currents are induced in both lines simultaneously and have a net cancellation affect.

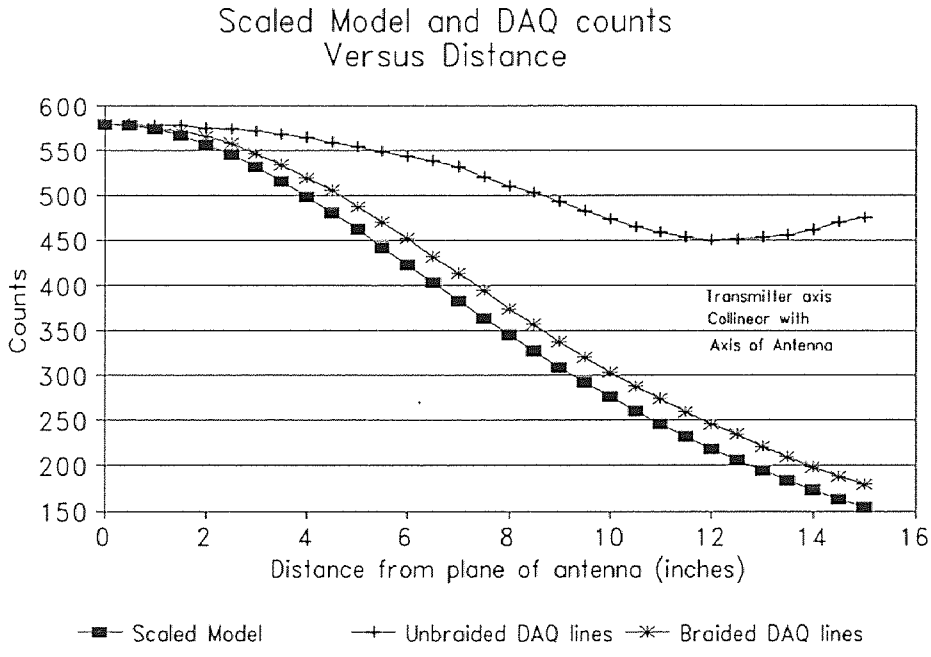

Figure 2.14 Effects of coupled antenna leads.

Chapter 3
The Model

3.1 Derivation of the Voltage Model

A model has been developed to predict the voltage that will exist in the rectangular loop antennae as a function of position and orientation of a point transmitter [Parasar (5)]. A complete derivation including assumptions and approximations can be found in Ashok, 1992 [Ashok (1)]. The resulting equations are reproduced here for convenience.

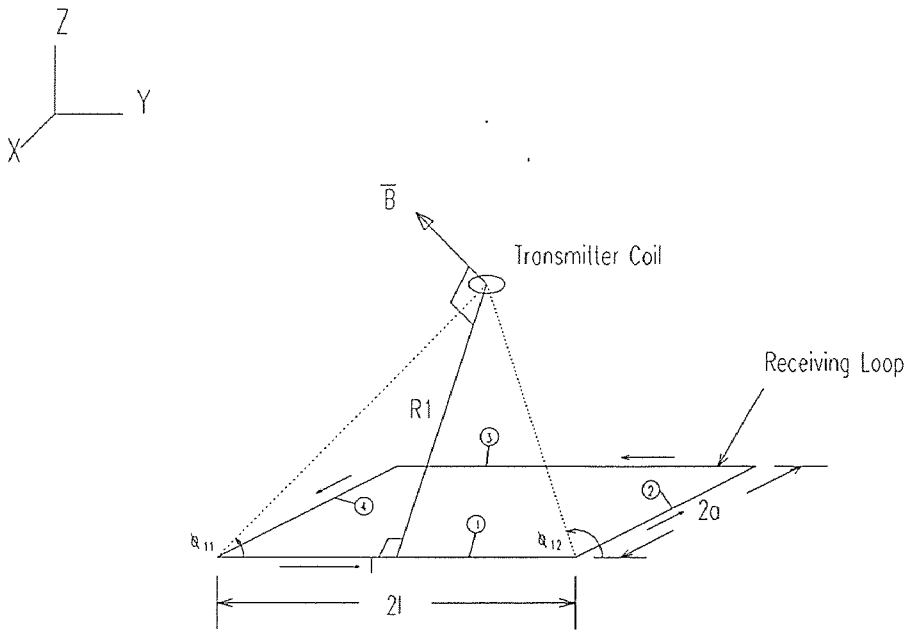

Figure 3.1: Transmitter-Receiver Spatial Orientation

Consider the Transmitting coil and receiving antenna depicted in figure 3.1. The magnetic flux vector $\vec{B}$ in the receiving antenna caused by the presence of the transmitter is obtained by using the principle of reciprocity [Van Valkenberg (9)]. First, the magnetic flux induced in each line segment of the loop is computed. These

are then summed to obtain the total field in the loop, $\vec{B}$. For i transmitters and j receivers,

$$\vec{B} = \sum_{k=1}^{4}\left[\left(\frac{\mu I_i}{4\pi R_k}\right)(\cos\varphi_{k1} - \cos\varphi_{k2})\right]\hat{\theta}_k \qquad (3.1)$$

Where, $\vec{B}$ is the resultant magnetic flux

and, $\vec{B} = B_x\hat{i} + B_y\hat{j} + B_z\hat{k}$ (3.2)

μ is the permeability of the transmission medium, air

I_i is the current in transmitter i

$R_k, \cos\varphi_k, \hat{\theta}_k$ are functions of the relative position of transmitter i with respect to receiver j. These positions are expressed as x_{ij}, y_{ij} and z_{ij} and are shown below without the subscript indices for clarity. The dimensions of receiver j (l_j, a_j) are also shown without the subscripts. The coordinate frame used to derive the above equations is as shown in figure 3.1, and is centered in the plane of the receiving loop.

(3.3a-h)

$$\cos\varphi_{11} = \frac{x+l}{\sqrt{(x+l)^2+(y+a)^2+z^2}}$$

$$\cos\varphi_{12} = \frac{x-l}{\sqrt{(x-l)^2+(y+a)^2+z^2}}$$

$$\cos\varphi_{21} = \frac{y+a}{\sqrt{(x-l)^2+(y+a)^2+z^2}}$$

$$\cos\varphi_{22} = \frac{y-a}{\sqrt{(x-l)^2+(y-a)^2+z^2}}$$

$$\cos\varphi_{31} = \frac{-(x-l)}{\sqrt{(x-l)^2+(y-a)^2+z^2}}$$

$$\cos\varphi_{32} = \frac{-(x+l)}{\sqrt{(x+l)^2+(y-a)^2+z^2}}$$

$$\cos\varphi_{41} = \frac{-(y-a)}{\sqrt{(x+l)^2+(y-a)^2+z^2}}$$

$$\cos\varphi_{42} = \frac{-(y+a)}{\sqrt{(x+l)^2+(y+a)^2+z^2}}$$

(3.4a-d)

$$R_1 = \sqrt{(y+a)^2+z^2}$$

$$R_2 = \sqrt{(x-l)^2+z^2}$$

$$R_3 = \sqrt{(y-a)^2+z^2}$$

$$R_4 = \sqrt{(x+l)^2+z^2}$$

The direction angles are given by:

(3.5a-d)

$$\hat{\theta}_1 = \frac{-z}{\sqrt{z^2+y^2+a^2+2ya}}\hat{y} + \frac{(y+a)}{\sqrt{z^2+y^2+a^2+2ya}}\hat{z}$$

$$\hat{\theta}_2 = \frac{z}{\sqrt{z^2+x^2+l^2-2xl}}\hat{x} + \frac{(-x+l)}{\sqrt{z^2+x^2+l^2-2xl}}\hat{z}$$

$$\hat{\theta}_3 = \frac{z}{\sqrt{z^2+y^2+a^2-2ya}}\hat{y} + \frac{(-y+a)}{\sqrt{z^2+y^2+a^2-2ya}}\hat{z}$$

$$\hat{\theta}_4 = \frac{-z}{\sqrt{z^2+x^2+l^2+2lx}}\hat{x} + \frac{(x+l)}{\sqrt{z^2+x^2+l^2+2lx}}\hat{z}$$

$\hat{x}$, $\hat{y}$ and $\hat{z}$ are the unit direction vectors in the x, y and z directions respectively.

The potential difference at the terminals of receiver j caused by the presence of transmitter i [Carr and Parasar (2)] is given by

$$V_{ij} = -N_i N_j \omega_i (\bar{A}_i \cdot \bar{B}) \tag{3.6}$$

or,

$$V_{ij} = -N_i N_j \omega_i \bar{A}_i \left[B_x \cos\alpha_{ij} + B_y \cos\beta_{ij} + B_z \cos\gamma_{ij} \right] \tag{3.7}$$

where,

N_i is the number of turns in the coil of transmitter i,

N_j is the number of turns in receiver j,

$\omega_i = 2\pi f_i$

and f_i is the oscillation frequency of transmitter i,

A_i is the vector area of transmitter i, which has magnitude equal to the cross sectional area of the transmitter coil and has a direction perpendicular to this area.

The parameters α_{ij} β_{ij} and γ_{ij} are the direction angles from the receiver plane to the normal of the transmitting coil's plane and are related by the equation

$$\cos^2 \alpha_{ij} + \cos^2 \beta_{ij} + \cos^2 \gamma_{ij} = 1 \qquad (3.8)$$

The viability of this voltage model has been repeatedly tested and shown to match experimental data well. Typical model-reality plots are shown in figures 3.2a-c. In figure 3.2a, the axis of the transmitter is collinear with the axis of the antenna. The transmitter travels from within the plane of the antenna to a point 21 inches from this plane. In figure 3.2b, the transmitter is initially at the center of and in the plane of the antenna with which its axis is collinear. The transmitter is then moved away from the center of the antenna, but within its plane. Figure 3.2c is the result of keeping the transmitter in the center of the antenna and rotating about the z (vertical) axis until the angle between transmitter and receiver is 90°.

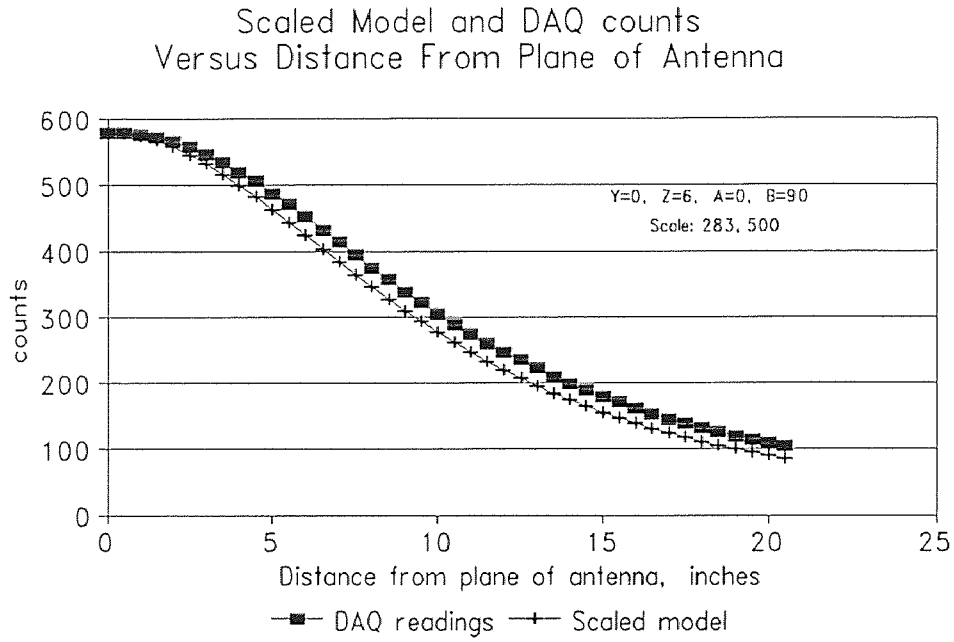

Figure 3.2a Model-Reality Plot as the transmitter is moved away from the plane of the antenna in a path coincident with the axis of the antenna.

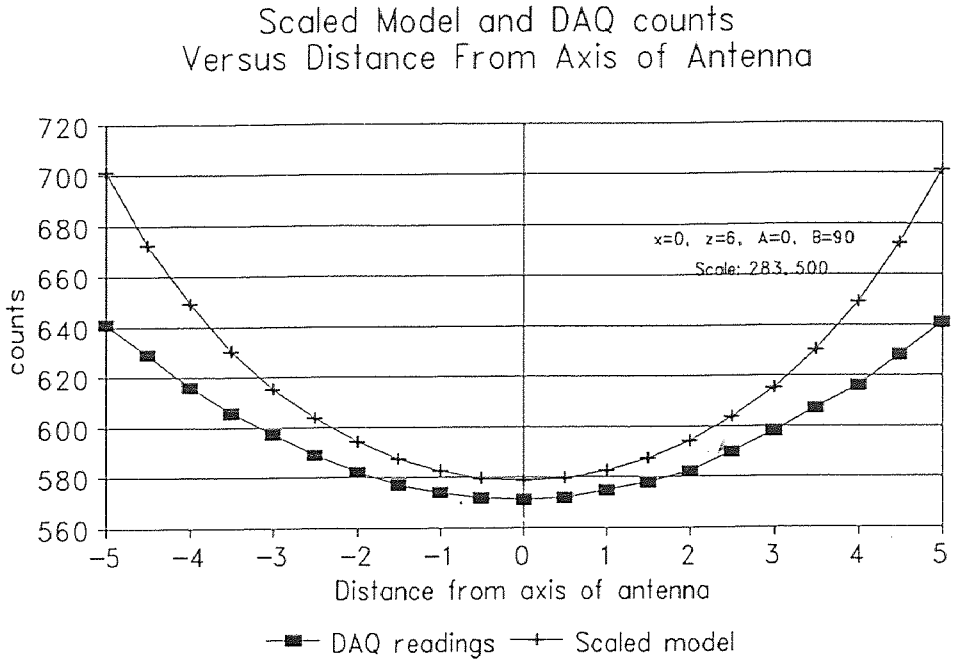

Figure 3.2b Model-Reality Plot as the transmitter is moved in a plane parallel to the plane of the antenna. The transmitter axis is kept parallel to the axis of the antenna.

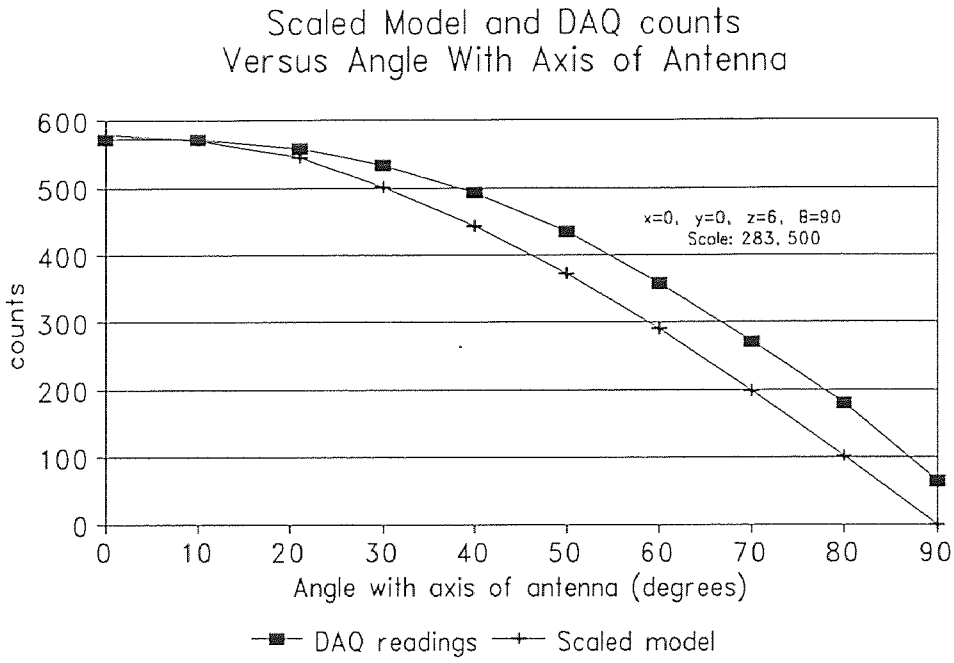

Figure 3.2c Model-Reality Plot as the angle between the transmitter axis and the antenna axis is rotated from 0° to 90°.

3.2 Propagation of Errors in the Inverse Solution

The inverse solution, recall, is the process by which signal data is converted to transmitter position and orientation. In other words, given $\bar{B}$ in the equation (3.1), we wish to find x, y, z α, β, and γ (transmitter position and orientation) by numerical methods. It has been shown by simulations [Dave *et al.* (3)] that given an exact set of voltages, the backward model converges to the exact solution. That is, when voltages from the forward model are processed through the backward model, the computed solution is identical to the simulated trajectory. When small errors are added to the data to simulate noise, the model converges to a best solution from a number of possible solutions based on a residual minimizing technique. The error between this "best solution" and the "exact solution" is not, however, trivially related to the errors added to the supplied voltages. Exactly how noise in the input data translates into errors in the inverse solution is currently under study. Certain instances of high signal noise have resulted in very accurate inverse-solutions while other instances of lower signal noise have resulted in poorer solutions. These inconsistencies are best explained by the cancellation or propagation of errors in the inverse solution. What is known is that to assure consistency of accuracy in the inverse-solution, the supplied voltages must have errors no larger than about 10% of the maximum reading [Dave *et al* (2)]. It is for this reason that the plots of figure 3.2a-c are not accurate enough to assure consistent convergence to the desired solutions. Figures 3.3a-c are reproductions of figures 3.2a-c with the absolute error scaled by a factor of ten superimposed. Errors of up to 19% are visible from fig 3.3a, 9% from figure 3.3b and over 70% from figure 3.3c.

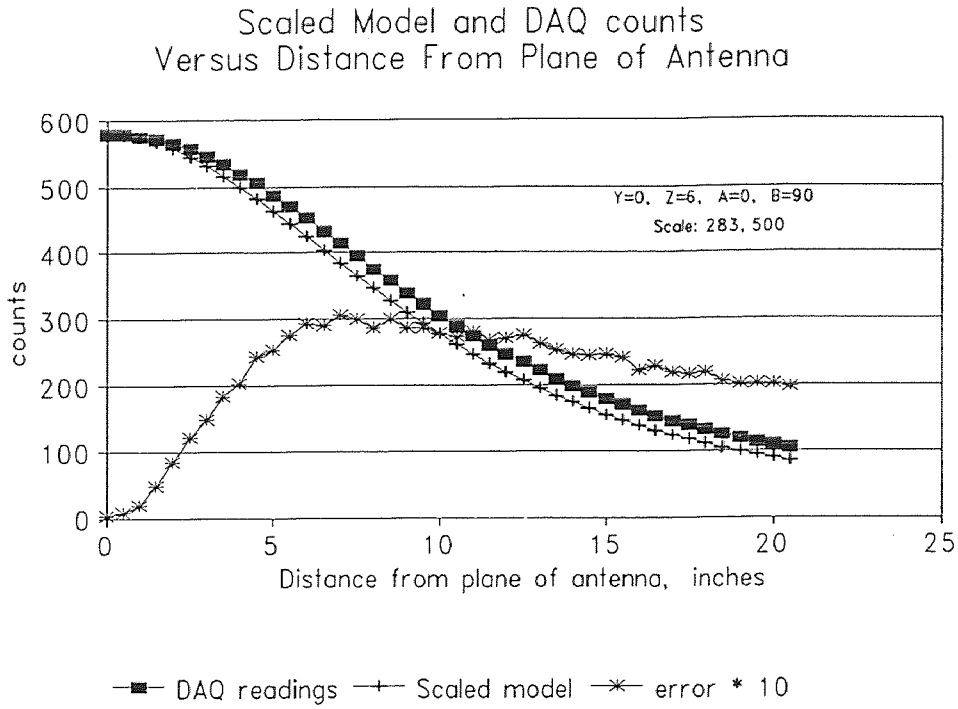

Figure 3.3a Model-Reality Plot as the transmitter is moved away from the plane of the antenna in a path coincident with the axis of the antenna. A maximum relative error of 19% is observed when the distance is 21 inches.

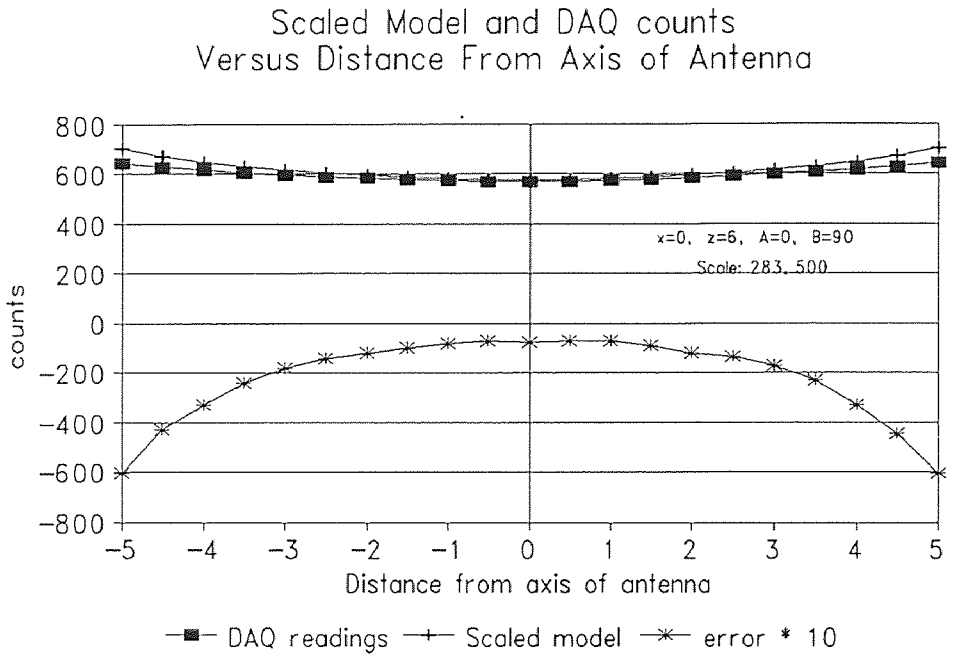

Figure 3.3b Model-Reality Plot as the transmitter is moved in a plane parallel to the plane of the antenna. The transmitter axis is kept parallel to the axis of the antenna. A maximum relative error of 9% is observed when the distance is 5 inches.

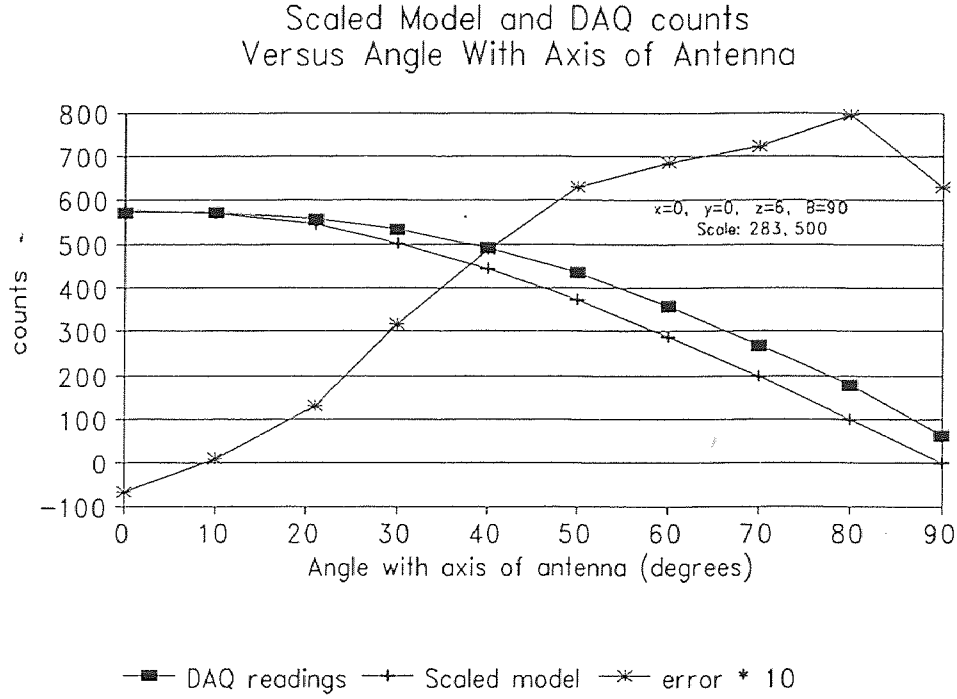

Figure 3.3c Model-Reality Plot as the angle between the transmitter axis and the antenna axis is rotated from 0° to 90°. A relative error of 10% is observed when the angle is 40°. The error at 90° is not finite because the theoretical value is zero at that point.

3.3 Error Analysis

Two types of errors appear into the measurements of any physical entity: random errors and systematic errors. Random errors or noise refers to the unpredictable fluctuation that creep into any measurements. Over time, these errors are self-normalizing because of their random nature. As such noise tends to offset every reading or measurement equally. Noise can often be eliminated by taking "differential" measurements, when possible. Systematic errors unlike random errors are introduced into a system by the human biases or imperfections in the equipment used for measuring. These errors tend to accumulate and bias rather than offset a set of measurements. They cannot usually be simply subtracted out. They must be corrected.

Figures 3.3a-c show examples of systematic errors. Note that in every case because calibration is done at the point of highest antenna signal, the error grows in inverse proportion to signal strengths and that the error curves are all continuous. The ratio of model to data acquisition readings for figures 3.3a-c are shown in figures 3.4a-c. These graphs demonstrate the nature of the systematic errors. For example, the data points in figure 3.4a can be approximated by a line, implying that the error is a constant multiplier. the graph of figure 3.4b shows that the error is of a more complicated nature; perhaps a quadratic.

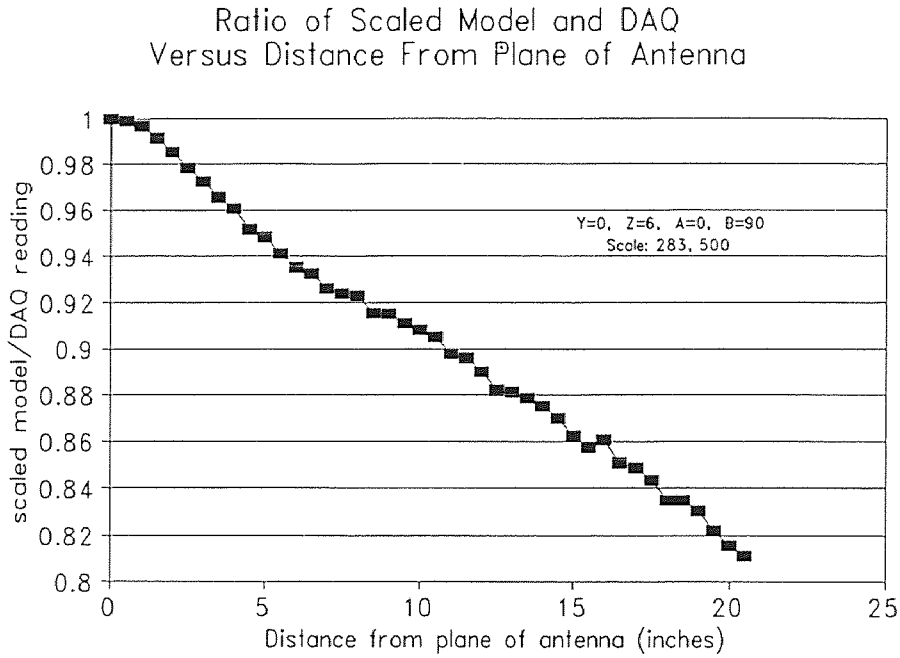

Figure 3.4a Ratio of model and data acquisition voltages as the transmitter is moved away from the plane of the antenna on a path coincident with the axis of the antenna. The graph is very linear, indicating that a constant multiplier equal to the slope is introduced in every measurement from the data acquisition system.

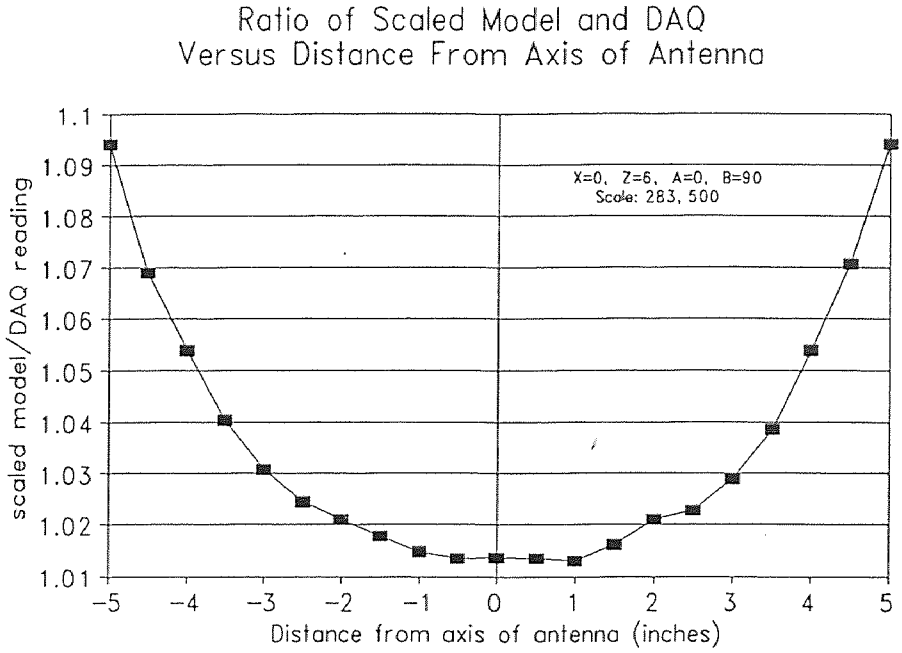

Figure 3.4b Ratio of model and data acquisition voltages as the transmitter is moved away from the axis of the antenna in a plane parallel to that of the antenna. The graph is continuous, implying that a systematic error is introduced in every measurement. This error is non-linear and is potentially dependent on a multitude of variables.

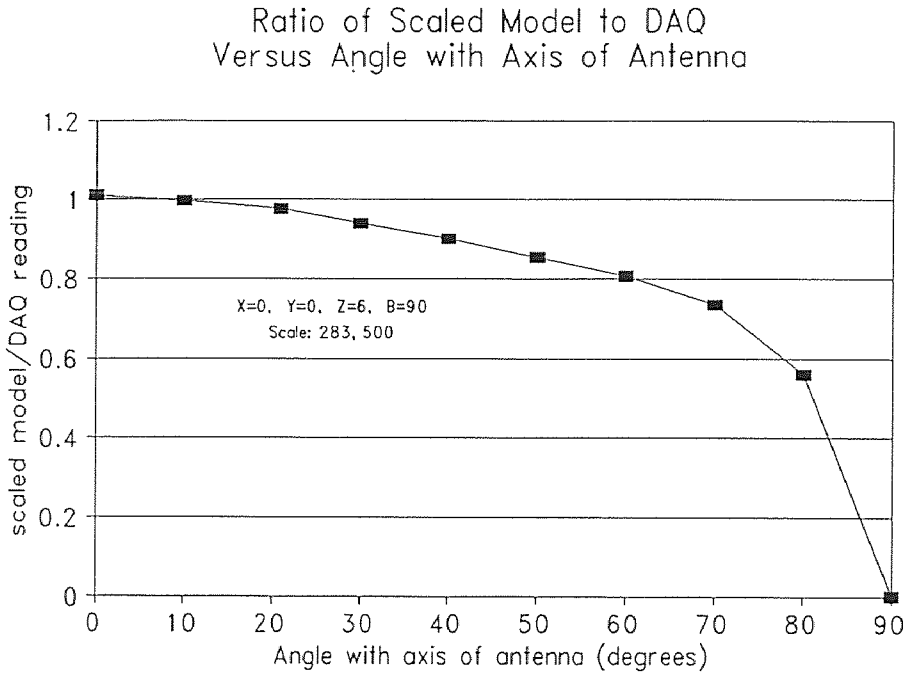

Figure 3.4c Ratio of model and data acquisition voltages as the transmitter orientation is changed with respect to the axis of the antenna. The graph is very non-linear but continuous, implying that the errors are systematic.

3.4 The Two-Part Model

The systematic errors described in the previous section are attributable to any number of factors:

- The field of the transmitter is not perfectly symmetrical
- The amplifier boards are not perfectly linear
- The data acquisition board is not perfectly linear
- Magnetic coupling may exist between antennae
- Higher order terms neglected in the derivation of the model may be producing systematic errors

One way to correct these errors given the difficulties in determining their source, is to add an empirical extension to the existing theoretical model. Such an extension could be an error map of correction terms in six dimensions for the six variables x, y, z, α,β and γ. If the space of the chute were discretized such that nodes in the space were separated by a distance of six inches and the angles α,β and γ were discretized by 30 degrees, the empirical map would have

$$(120/6 +1)*(12/6 +1)*(12/6+1)*(180/30 +1)*(180/30 +1)*(180/180 +1) = 18{,}522$$

nodes, assuming 180 degrees of symmetry in the transmitter. This is illustrated in figure 3.5. At each node, there are 98 possible orientations for the transmitter.

Such a map is coarsely discretized, extremely laborious to construct and likely to be inadequate. Alternative methods are sought.

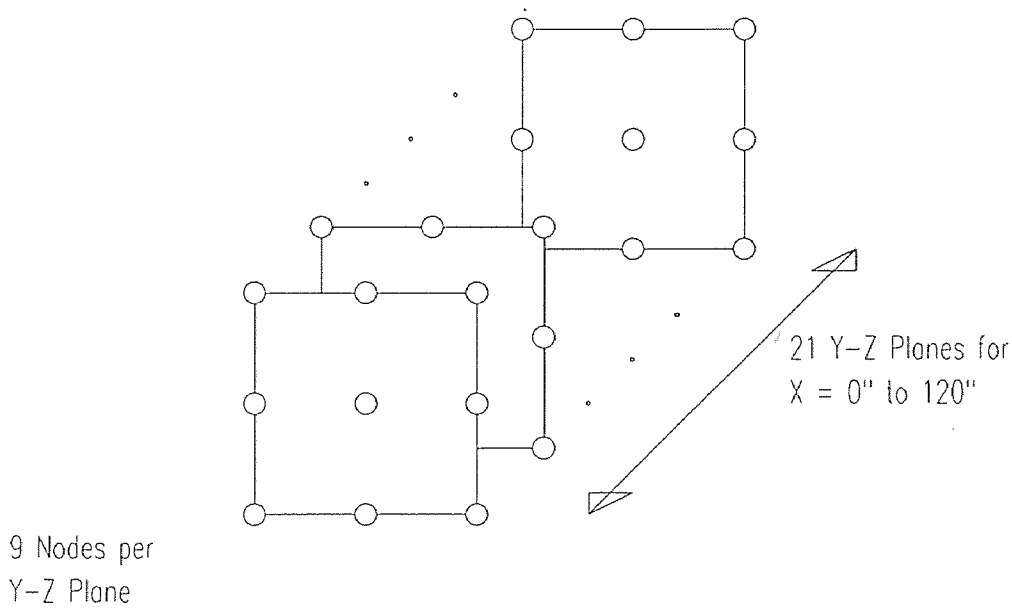

Figure 3.5 Nodes for empirical correction map of chute space. There are 9 nodes per plane and 21 planes for a total of 189 nodes.

3.4.1 27-Point Empirical Corrections

Rather than attempting to discretize the volume of the chute, one could instead discretize the space around the antennae that tessellate the chute. If the geometry of all the antennae is the same, then the discretization of a typical antenna should carry into the space of all the others, assuming that the errors we aim to minimize do not stem from individual antenna or amplifier board. Furthermore, because of symmetry, it is possible to discretize one octant of the space around an antenna and duplicate this 8 times to build the desired space. This is illustrated below in figure 3.6.

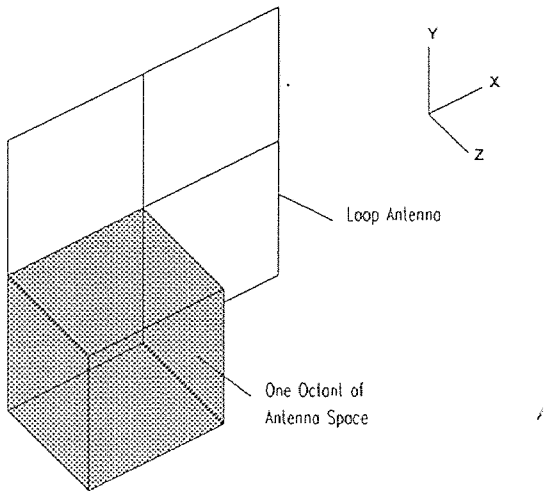

Figure 3.6 One octant of the space around the antenna plane.

A mirror-symmetry relationship exists between each of the 8 sub-spaces that form the volume around the plane of the loop antenna. Thus, if the volume of any one subspace can be discretized, the discretized volumes in the other regions can be obtained by simple coordinate transformations. For antennae centered around a 16"x16" flow space, the space of interest is a volume 8"x8"x8"", assuming a cubic tessellation of antennae (16" antennae are separated by 16"). Calibration nodes are distributed as shown in figure 3.7.

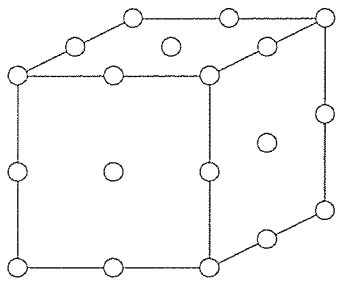

Figure 3.7 Node points for the discretization of one octant of one antenna's space. Nodes on hidden faces are suppressed for clarity.

Eight nodes are placed at the corners of the space, twelve nodes are at the center of each edge, six nodes are at the center of each face and one node is in the center of the volume for a total of 27 nodes.

In the development of the 27-point corrections, it is assumed that the propagation of systematic errors is linear. This assumption is substantiated by figure 3.4a but is disfavored by figure 3.4b. · Figure 3.4b shows a non-linear propagation, which will be approximated by two lines radiating outward from the point (0,1) to the points (5,1.1) and (-5,1.1). Such an approximation should not introduce large errors given the small range of the ordinate.

Systematic errors, it has been shown, are greatest at the lower readings and diminish to zero at higher readings if calibration is done at the point of high signal levels. If the linearity assumptions made are valid, then an error correction factor can be obtained for the position of highest error (i.e. highest reading) and subsequently scaled down for readings of lower magnitudes.

3.4.1.1 Implementation of the 27-Point Empirical Scale

Construction of the 27-point empirical correction multipliers is described below.

First, data is collected at the chosen points with the axis of the transmitter parallel to the axis of a typical antenna. This orientation gives near optimal or optimal transmitter to receiver signal transfer for the entire space of interest. It is selected for convenience of measurement. Random errors are removed from the collected data by subtraction of a background reading as described in section 2.3. Next, simulations are run on the forward model at the prescribed positions and orientations to obtain corresponding theoretical predictions. The data acquisition readings are then scaled down such that the reading at the center and within the plane of the antenna being

studied matches the predicted voltages exactly. The correction multiplier at this node is thus 1. If our model duplicated reality perfectly, we would expect to find an empirical map of factors in which every entry is 1. It is found that factors in our maps typically range from 0.6 to 1.2 with a strong distribution in the 0.85 to 1.10 range.

Interpolation between nodes of the empirical map becomes necessary when we seek a correction factor for points that do not coincide with the nodes of our map. The interpolation used is linear and is with respect to the eight nodes that form corners of a rectangular volume around the point. The interpolation corrected factor, *CF*, is given by

$$CF_{x,y,z} = \frac{\sum_{k=Z_L}^{Z_H}\sum_{j=Y_L}^{Y_H}\sum_{i=X_L}^{X_H}\frac{1}{d_{i,j,k}}CF_{i,j,k}}{\sum_{k=Z_L}^{Z_H}\sum_{j=Y_L}^{Y_H}\sum_{i=X_L}^{X_H}\frac{1}{d_{i,j,k}}} \qquad (3.9)$$

where,

X_L, Y_L, and Z_L are the coordinates of the closest nodes such that $X_{L\leq x}$, $Y_{L\leq y}$, and $Z_{L\leq z}$.

X_H, Y_H, and Z_H are the coordinates of the closest nodes such that $X_{H\geq x}$, $Y_{H\geq y}$, and $Z_{H\geq z}$.

with coordinates greater than *x*, *y*, *z*

$d_{i,j,k}$ is the distance from (x,y,z) to the node (X_i, Y_j, Z_k) given by the expression

$$d_{i,j,k} = \sqrt{(x-x_i)^2 + (y-y_j)^2 + (z-z_k)^2} \qquad (3.10)$$

3.4.1.2 Effect of the 27-Points

The graphs that appear in figures B.1 through B.8 of appendix B are the results of a straight line trajectory along the X-axis of the chute and parallel to it. Plots of the results with application of the 27 point corrections are shown in figure B.2 while figure B.1 shows the results when no corrections are used. In figures B.3-B.8, it is apparent that the corrected backward model predicted voltages shown match the measured voltages closer than do the purely theoretical predictions. In the case of figures B.5 and B.6, relative errors are decreased by up to 18% from 23% on the uncorrected theoretical model to 5% on the corrected model. Figure B.2 shows the predicted and actual x-trajectory of the tracking sphere using the 27-point corrections. Errors that appear at the midpoint of the trajectory in the uncorrected model (figure B.1) are diminished and the resulting curve of predicted x position is rendered smoother.

3.4.1.3 Limitations of the 27 Points

There are a number of limitations to the 27 point empirical mapping technique. For one thing, the portability of the 27-point space is justifiable only if the duplicated antennae are of identical geometry to the original. Also, it is unclear how points that fall outside of the space should be scaled. Of primary importance, however, is that the scaling factors are a function of position and not orientation. As shown in figure 3.7, the 27-point correction works well when the transmitter is oriented in a manner similar to the orientation used in developing the map. In other instances when this is not the case, the improvements have been marginal. In cases of very low antenna signals, the corrections have even deteriorated the results.

3.4.2 675 Point Corrections

To overcome the deficiencies of neglecting the transmitter orientation in the 27-point corrections, angles discretized by 45° with respect to two of the antenna axes and added to the map. The third axis is automatically covered because of the constraint on the three-dimensional angles:

$$\cos^2 \alpha_{ij} + \cos^2 \beta_{ij} + \cos^2 \gamma_{ij} = 1 \tag{3.11}$$

Thus, at every node point, the angles with respect to two axes are to be varied and readings taken to construct a new map. This map will have a total of 5×5 or 25 times as many point as the angle-neglecting map. The number of node points is still 27, but each of the nodes now have 25 different values depending on orientation. This gives a total of 25*27 or 675 points for the new map.

The 675-point map is a six-dimensional space in x, y, z, α, β and γ. Therefore, interpolation in the space is between $2^6 = 64$ nodes. The correction factor is given by

$$C.F_{\cdot x,y,z,\alpha,\beta,\gamma} = \frac{\sum_{k=Z_L}^{Z_H}\sum_{j=Y_L}^{Y_H}\sum_{i=X_L}^{X_H}\sum_{\alpha=A_L}^{A_H}\sum_{\beta=B_L}^{B_H}\sum_{\gamma=\Gamma_L}^{\Gamma_H}\frac{1}{d_{i,j,k,\alpha,\beta,\gamma}} C.F_{\cdot i,j,k,\alpha,\beta,\gamma}}{\sum_{k=Z_L}^{Z_H}\sum_{j=Y_L}^{Y_H}\sum_{i=X_L}^{X_H}\sum_{\alpha=A_L}^{A_H}\sum_{\beta=B_L}^{B_H}\sum_{\gamma=\Gamma_L}^{\Gamma_H}\frac{1}{d_{i,j,k,\alpha,\beta,\gamma}}} \tag{3.12}$$

Such an equation is computationally intensive and significantly increases computation time. This is undesirable given the number of evaluations needed to arrive at a solution:

(3.13)

(Number of Evaluations) = (Number of Iterations) * (Number of Antennae)

Further, it is difficult to extrapolate variables in this space because of the constraint that exists between the variables of orientation α, β and γ. In the 27-point space, extrapolation is between independent variables. It is trivial to find the eight nearest

nodes because they can be determined one at a time. This is not the case for the 675-point space. Suppose, for example, one wishes to find the nearest nodes to the point $\alpha = 55°$ $\beta = 65°$ and $\gamma = 45.4°$. If the space is discretized by $10°$, then the nearest high and low nodes to α are $60°$ and $50°$ respectively. Likewise the nearest high and low nodes to β are $70°$ and $60°$ and to γ are $50°$ and $40°$. However, when the low pair ($50°$, $60°$, $40°$) and the high pair ($60°$, $70°$, $50°$) are taken together or in combination, the three angles violate the angle constraint requiring that the square of their cosines sum to unity. Determination of the true nearest neighbors is complicated by this interdependence between variables. Methods to determine appropriate nearest nodes add to the already computational intensive effort, making this approach impractical.

3.4.3 Antenna Coupling

One phenomenon responsible for the introduction of systematic errors is the coupling that develops between adjacent antennae. When a signal is induced in any one antenna, that antenna behaves as a transmitter and induces signal in adjacent antennae. These antennae is turn induce signals onward to other antennae. In theory, the chain carries downward *ad infinitum* with each new transmitter signal weaker than the previous. In practice, though, the propagating signal strength drops so quickly from antenna to antenna that only the first transmission could cause an error of any significance. Here, we will consider the errors caused by antenna coupling.

3.4.3.1 Coupling Corrections

To avoid the complexities of theoretical formulations, an empirical approach to eliminated the antenna coupling is considered.

To correct the coupling between antennae, it is necessary to know how the signal strength in antenna i translates to a signal introduced in antenna j. As such, we

seek to find

$$\frac{\partial V_j}{\partial V_i}$$

for all i and j. For a system of k antennae, one can construct a *coupling matrix* of k^2 entries as shown below:

$$\begin{bmatrix} 1 & \frac{\partial V_1}{\partial V_2} & \frac{\partial V_1}{\partial V_3} & \cdots & \frac{\partial V_1}{\partial V_k} \\ \frac{\partial V_2}{\partial V_1} & 1 & \frac{\partial V_2}{\partial V_3} & \cdots & \frac{\partial V_2}{\partial V_k} \\ \frac{\partial V_3}{\partial V_1} & \frac{\partial V_3}{\partial V_2} & 1 & \cdots & \frac{\partial V_3}{\partial V_k} \\ & \vdots & \vdots & \vdots & \\ \frac{\partial V_k}{\partial V_1} & \frac{\partial V_k}{\partial V_2} & \frac{\partial V_k}{\partial V_3} & \cdots & 1 \end{bmatrix}$$

Elements on the diagonal of this matrix are unity by definition:

$$\frac{\partial V_i}{\partial V_i} \equiv 1 \qquad (3.14)$$

In the ideal case, non-diagonal elements would be zero, representing no effect on antenna j by the signal in antenna i. For a transmitting antenna signal level of 1.00mV, typical coupling signal levels are shown in the coupling matrix of Appendix C. Induced signals as high as 6.8% of the transmitting antenna signal are observed.

Unlike 27-point and 675-point corrections, the corrections for antenna-antenna decoupling are implemented against the data from the data acquisition system as opposed to the model predicted voltages. Here, it is assumed that errors are in the data and not in the theory. Thus, corrected voltages from the data acquisition are given by

$$\{V_c\} = \{V_{DAQ}\} - [C - I]\{V_{DAQ}\} \tag{3.15}$$

If there are k antennae in the system, then, V_C is a k-vector whose entries are the couple-corrected data acquisition voltage readings; V_{DAQ} is a k-vector whose elements are the background corrected data from the data acquisition system; **C** is the evaluated coupling matrix; **I** is the identity matrix, and $\mathbf{I} = \mathbf{I}_k$.

3.4.3.2 Evaluating [C - I]

The matrix **[C - I]** is given by the coupling matrix of section 3.4.3.1 less the diagonal elements:

$$[\mathbf{C}-\mathbf{I}] = \begin{bmatrix} 0 & \frac{\partial V_1}{\partial V_2} & \frac{\partial V_1}{\partial V_3} & \cdots & \frac{\partial V_1}{\partial V_k} \\ \frac{\partial V_2}{\partial V_1} & 0 & \frac{\partial V_2}{\partial V_3} & \cdots & \frac{\partial V_2}{\partial V_k} \\ \frac{\partial V_3}{\partial V_1} & \frac{\partial V_3}{\partial V_2} & 0 & \cdots & \frac{\partial V_3}{\partial V_k} \\ & \vdots & \vdots & \vdots & \\ \frac{\partial V_k}{\partial V_1} & \frac{\partial V_k}{\partial V_2} & \frac{\partial V_k}{\partial V_3} & \cdots & 0 \end{bmatrix} = \mathbf{C'} \tag{3.16}$$

We shall call this composite matrix **C'** and we seek to evaluate it by empirically determining expressions for each of its elements.

Consider antenna j of figure 3.8 subjected to coupling by the presence of a large signal in the adjacent antenna i.

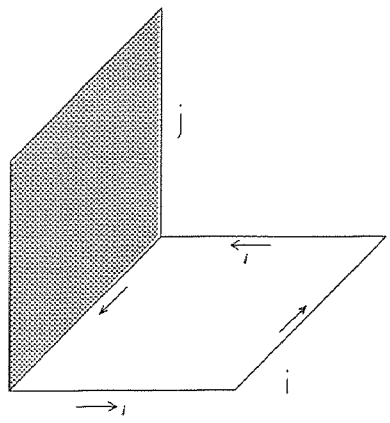

Figure 3.8 Antenna to Antenna signal Transfer: Antenna j is subjected to coupling from the large signal current *I* in antenna i.

It has been found empirically that the coupling in antenna *j* is dependent positively on the signal levels of adjacent antenna *i* and negatively so on the signal level in antenna *j* itself. In other words, when the signals in antenna *j* are low, this antenna is highly susceptible to coupling from antenna *i*. When the signals in *j* are stronger, this antenna becomes slightly affected by signals in *i*. Beyond a certain signal level in antenna *j*, that antenna becomes indifferent to the activities in antenna *i*. Figure 3.9 shows how the susceptibility of antenna *j* changes as the initial signal in *j* (plotted on the abscissa) is increased. Here, the ordinate is the change in the reading of antenna *j* , ΔV_j that occurs from a given fixed and large change in antenna *i*. Signal levels are controlled through a Marconi Instruments radio communications test set (see Appendix F) and monitored through the data acquisition system. The effects on the antenna can be seen from the graph to be highest when the signal in receiver *j* is null. Coupling effects decay exponentially from a maximum value when the initial reading in antenna *j* (Vo_j) is zero to zero when Vo_j is large. An exponential decay curve has been approximated and superimposed on the graph in figure 3.9:

$$f(V_0) = Ae^{-kV_0} \qquad (3.17)$$

$$A = \frac{\Delta V_j}{\Delta V_i} \tag{3.18}$$

k is a constant characterizing the rate of decay. Once determined, k should carry from antenna to antenna.

Thus, entries in **C'** are of the form

$$\frac{\Delta V_j}{\Delta V_i} e^{-kV_o}$$

ΔV_i is the magnitude of the signal forced into antenna i and ΔV_j is the response in

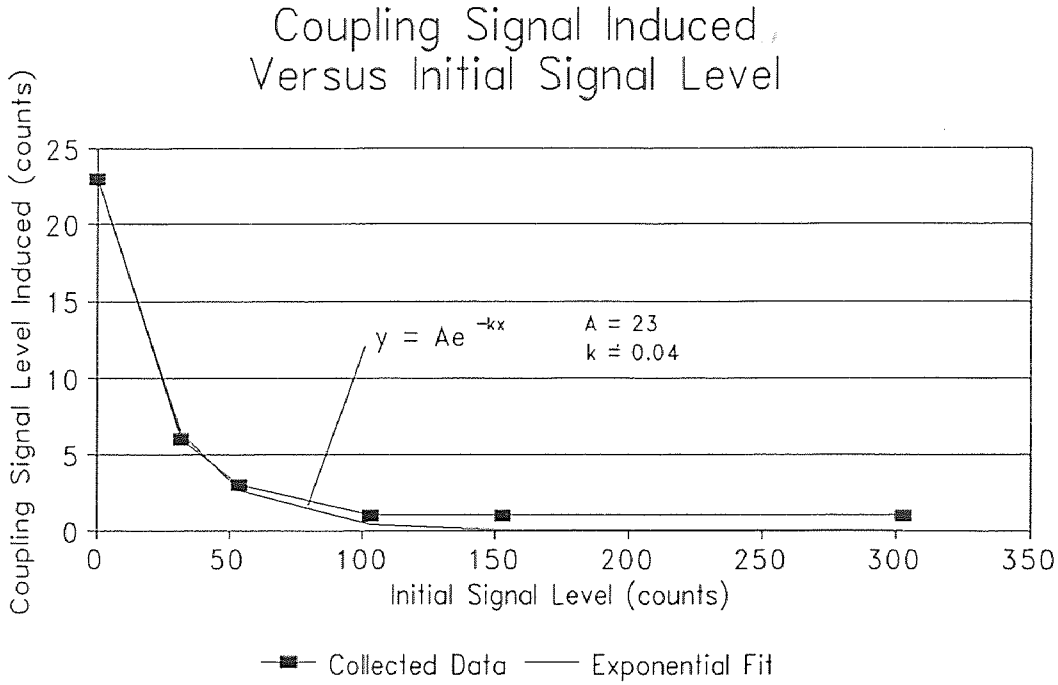

Figure 3.9 The susceptibility of an antenna to coupling from an adjacent antenna drops off exponentially as the signal level in that antenna increases.

antenna j. The constants in this expression can be evaluated by constructing plots like figure 3.9 for each antenna. k can be evaluated by considering any two points on the graph and fitting an exponential decay. In this example, k computed to be approximately 0.04.

3.4.3.3 Effects and Limitations of Antenna Decoupling Corrections

The antenna coupling phenomenon is a noteworthy effect that exists between antennae in the tessellation. It has been shown that the errors that stem from this effect are very systematic. In the case shown, the magnitude of the error is seen to depend on the magnitude of the signals in neighboring antennae. What is not apparent is the sign or direction of this error. While the model we are using is sign-independent (i.e. only the magnitude of the antennae signals interest us), the coupling antennae signals are not. The claim that there exists 180° of symmetry about the coil transmitter is valid insofar as we speak of magnitude. In actuality, there is a 180° phase shift in the induced currents when the transmitter is rotated through an angle of 180° about an axis perpendicular to its axis of symmetry. The currents that these loops pass on to neighboring antennae will also be shifted. Hence, coupling signals can have the effect of either adding or subtracting to the magnitude of the signal level. Because the entire tracking system and electronics are set up to exploit the 180° transmitter symmetry, it is not possible to know if coupling signals should be added or subtracted. In controlled cases, antenna pairs decoupled for a given transmitter orientation have improved model-reality agreement at that orientation. At instances where transmitter orientation is not strictly monitored or multiple antennae of high signals are present, the technique has failed to improve the agreement between model and reality.

Chapter 4
Signal Processing and the Inverse Solution

Once the signal from the antennae have been collected, filtered, amplified and preprocessed to remove background noise, the process of translating these readings into position and orientation of the transmitter is begun. This process we shall call the *inverse solution* and the algorithm and procedures used to perform it comprises the *backward model*. Validation of the backward model and details of its content and methodology may be found in Ashok, 1992 [Ashok (1)].

The arguments in this chapter refer extensively to the data set RUN067. Details of this set are presented in Appendix D.

4.1 The Optimization Problem

The forward model predicts the voltage in antenna j caused by the presence of transmitter i as a function of the position. and orientation of i

$$V_{ij} = g_{ij}(x, y, z, \alpha, \beta, \gamma) = g_{ij}(x) \qquad (4.1)$$

Given x, y, z, α, β, and γ, it is possible to predict V_{ij} by simple substitution. The reverse does not, however, true because it is not simple to invert the $\vec{B}$ equation (equation (3.1)). Given V_{ij}, we seek to determine x.

If the collected data were perfect (that is, if they matched the model predictions perfectly), then the backward model would reduce to a system of 6 equations to be solved for the 6 variables x, y, z, α, β, and γ. However, because noise and theory-reality disagreement is inevitable, such exact solutions exist only in simulations. In reality, no exact solution exists and we resort to finding an optimal solution to an over-determined system of m equations in 6 unknowns, where, m is the number of antenna voltages to be matched, and $m>6$. We define the optimal solution

as the one that produces the minimum least-squares residual. The least squares problem reduces to the minimization of the total system residual vector **R**, given by

$$\mathbf{R} = \frac{1}{2}\sum_{i=1}^{m} r_i(x)^2 \tag{4.2}$$

where

$$r_i = \left(V_{\text{model}} - V_{\text{daq}}\right) \tag{4.3}$$

Here, V_{model} and V_{daq} are the model predicted and DAQ-collected voltages respectively. details of the optimization procedures are found in Dave [Dave *et al.*(2)]

Residual minimization is done using the Levenberg-Marquardt Algorithm (see Appendix F). The L-M Algorithm requires an initial guess to begin its work. The residual at this initial guess is evaluated and iterated to a minimum.

4.2 Initial Approximation

The efficiency of the L-M algorithm is dependent on the accuracy of the initial approximation. In certain cases, initial guesses that are too far from the correct solution causes the algorithm to converge to an incorrect local minimum. In other cases, initial guesses that are extremely erroneous lead to no convergence at all. On several occasions, the function's space that we wish to minimize is so non-linear and local minima are packed so closely around the global minimum that different initial guesses that are no more than 1 inch and 10° away from the correct solution converge to solutions other than the global minimum. Methods of selecting good initial guesses are thus very important to the success of the algorithm.

4.2.1 Use of Previous Point as Initial Guess

Because it is assumed that the data acquisition system will be collecting data at a speed high enough such that the linear and angular velocities of the tracking sphere will not change very much from reading to reading, the computed positions and orientations from the previous iterate can be used as initial guesses for the current iterate. This method of initial approximation works well when the speed of the data acquisition is high with respect to the speed of the particle, but becomes less viable as the speed of the particle increases with respect to the speed of the data acquisition system. For the data of RUN067 shown in figures D.3-D.8 of appendix D, the particle is displaced 1/2" between samples.

4.2.2 Use of Extrapolation for Initial Guess

To reduce the dependency of initial guesses on the speed of the data acquisition system, a technique of extrapolation is used to make initial guesses. Here, the last two points in the tracking sphere's history is examined and extrapolated to arrive at a new location where the sphere would be if its path were not disturbed. For example if the last two points are examined and it is found that the particle started at X=0.5" then proceeded to X=1.0", then the extrapolated guess for the location of the particle would be X=1.5". This technique has improved significantly the outcome of several runs. Figures D.3-D.8 are plot comparing the outcome of runs using the extrapolation technique to those that only use the previous-point technique (described in 4.2.1) as an initial guess. A clear improvement is visible from the two data sets. The linear extrapolation technique potentially has two disadvantages. First, is assumes a continuity in the particle's path that may not be typical of granular flows. In real flows, both the particle's linear and angular velocity can reverse in the flow. Second, the linear extrapolation technique has the tendency to aggravate situations where one data

point may be bad. Errors in the previous estimate are doubled in the extrapolated guess. One could overcome this by using more than one previous point in the extrapolation and fitting a higher-order curve or a best fit line to the data.

4.2.3 Use of Perturbations

To reduce the likelihood that errors amplified by the use of extrapolation are not totally unrecoverable, a technique of perturbation is used. Here, initial guesses are randomly incremented within an arbitrary limit which we shall call the *radius of perturbation* to search for alternative minima. Should one be found (as is almost always the case), a new perturbation is performed about this new minimum. The process is repeated any number of times and the minimum residual of all the perturbations is selected as the global solution. The perturbation method developed is similar but not identical to the multiple-initial-guess method common in numerical methods. That approach is confined to guessing around an initial guess. If the radius used to vary the initial guesses is small, then little chance exists that the numerical methods will converge to alternate minima. If the radius is large, then a good chance exists that we will converge to new minima, however, a large number of initial guesses are needed to explore the space where possible solutions exist. In our case, the number of initial guesses would have to grow as the sixth power of the radius to cover the space with equal efficiency. The perturbation technique attempts to overcome this by allowing us the chance of moving far away from local minima without the need for a large search radius. Results of the perturbation technique are similar to those of the linear extrapolation technique for RUN067 (Appendix D) and are shown in figures D.9-D.14. However, the limitations of the extrapolation technique are not present.

4.3 The Multiple Solutions Problem

In a perfect model-reality agreement situation, it is very unlikely that multiple solutions to an over-determined system of eleven equations in six unknowns can exist. Indeed simulations has proven time and time again that given perfect data, the inverse solution is always perfect [Ashok(1)], suggesting strongly that only unique solutions of position and orientation exist for a given set voltages. However, because the space is so non-linear, there are, packed around the unique true solution, several "good" solutions. The signal levels that correspond to these sub-optimal solutions can vary from the optimal solution by as little as 10% on the average. Because the disagreement between model and the collected data is typically no less than 10%, these sub-optimal solutions become important and introduce the possibility of multiple numeric solutions. The data set RUN067 shown in appendix D is typical of a multiple-solution occurrence described above. We shall refer to the data in this appendix throughout the remainder of this chapter for different analyses. Parts will be reproduced in the text for convenience of reference.

RUN067 is a straight line constant angle trajectory performed on a chute configured with thirteen antennae. Eleven of these are orthogonal to the axes of the chute. The other two are mounted at +45° and -45° with respect to the X-axis. Inspection of the resulting solution graphs (figures D.9-D.14) show that the *x*-computations are fairly good, but have a small discontinuity around the fourteenth data point. The same discontinuity appears more clearly in the Y-graph. Here, because the scaling is different, the error appears to be larger, but can be seen to be approximately 0.6". Examination of the Z-graph is shows clearly that something has gone wrong in the numerical solutions. The discontinuity at the thirteenth data point in the Z-graph is more than 2.0".

Figures D.15-D27 are plots of the signal levels in the thirteen antennae used in the run. Because the data was collected under controlled conditions (i.e., the transmitter is displaced by a fixed amount along a known trajectory), we know the exact solution and can thus predict, using the model, what the collected data should look like. This prediction is represented by the curve labeled "Expected Voltage". The actual background corrected data is also plotted and is labeled "Measured Voltage". The points labeled "Computed Voltage" in the figures is determined as follows. By applying the inverse solution method, a trajectory is computed using the measured voltage ("Measured Voltage"). This trajectory is then fed into the forward model to yield the computed antenna voltages. How well the measured voltages match the computed voltages is an indication of how well the inverse solution is working and at which points it is having trouble.

Figure D.11 shows that near data point #14, there is at least two inches of discrepancy from one data point to the next. One would expect that such a discrepancy would amount to large discontinuity in the "Computed Voltage" lines. Inspection of all thirteen voltage plots show that this is not the case. In fact, only the graphs of antennae 2, 4, 5 and 6 show even an indication of the discontinuity in the solution when their scales are reduced, and those indications are well within the range of acceptable errors. The conclusion is that given our range of acceptable errors, multiple-solutions is a reality to be dealt with. In what follows, we carefully examine the discrepancy near data point #14 and seek evidence for multiple solutions.

Data Point	RUN067 Antenna # 1	2	3	4	5	6	7	8	9	10	11	12	13
:	:	:	:	:	:	:	:	:	:	:	:	:	:
9	3	112	272	34	102	1	72	12	4	5	41	114	360
10	4	117	264	36	108	2	72	14	8	6	41	112	363
11	6	123	252	38	117	3	71	16	12	6	40	107	364
12	4	128	241	39	126	3	70	17	17	7	40	105	363
13	6	135	231	40	132.	3	69	19	24	8	39	101	363
14	6	142	223	43	136	5	67	20	26	9	37	100	364
15	7	149	215	44	140	5	66	22	29	10	37	99	364
16	8	158	206	48	144	5	63	24	34	11	35	97	362
17	9	166	195	50	151	7	61	24	36	13	33	96	359
:	:	:	:	:	:	:	:	:	:	:	:	:	:

Data Point	RUN067A Antenna # 1	2	3	4	5	6	7	8	9	10	11	12	13
:	:	:	:	:	:	:	:	:	:	:	:	:	:
6	6	107	277	30	102	3	59	10	4	3	60	93	401
7	7	112	268	32	109	3	57	11	7	3	59	91	393
8	7	117	258	34	114	3	56	12	8	4	57	89	383
9	8	122	248	36	119	4	54	12	12	4	55	88	374
10	9	127	236	37	124	4	53	14	14	5	52	87	361
11	9	133	227	39	128	5	51	14	16	5	50	85	353
12	10	141	217	41	132	6	49	15	20	6	49	84	345
13	11	147	206	43	135	6	47	16	22	7	47	82	337
14	12	154	196	44	138	7	44	17	25	8	45	82	329
:	:	:	:	:	:	:	:	:	:	:	:	:	:

Table 4.1 Partial Listing of RUN067 and RUN067A.

According to the inverse solution, at data point #14 of RUN067 (table 4.1), there exist two points that offer similar readings in all thirteen antennae. These points differ primarily in the computed z-coordinates. That is, the x, y, α, β, and γ values of these two points are not very different. z is the only variable that is increased by about 2 inches. To validate the solution, a new trajectory called RUN067A is performed. This trajectory is a repeat of RUN067 in all variables except in z, which is increased by two inches:

	Start	Finish
RUN067	x = 38	x = 18
	y = 0	y = 0
	z = 4	z = 11
	α = 51.0°	α = 51.0°
	β = 138.5°	β = 138.5°
	γ = 103°	γ = 103°
RUN067A		
	x = 38	x = 18
	y = 0	y = 0
	z = 6	z = 13
	α = 51.0°	α = 51.0°
	β = 138.5°	β = 138.5°
	γ = 103°	γ = 103°

We expect that at about the fourteenth data point of this new trajectory, we will see numbers comparable to those of RUN067. Table 4.1 is a partial listing of counts from RUN067 and RUN067A. Observe that the numbers of the twelfth data point of RUN067 resemble those of the tenth data point of RUN067A. Because all the antennae with high readings (Antennae 2, 3, 5, 12, and 13) have good model-reality agreement, the residuals of RUN067A indicate that position and orientation at this point is mathematically an acceptable solution to RUN067 albeit incorrect in actuality. It is conceivable from the data presented that small variations in x, y, z, α, β, and γ may indeed result in readings that may approximate even closer the readings of RUN067. Table 4.2 is an excerpt of the iterations and perturbations of RUN067 taken from appendix D. Computation of the fourteenth data point is shown. Five perturbations are performed at this data point, and perturbation number 4, having the

least residual is selected as the solution. The corresponding solution is

$x = 30.696"$ $y = 0.651"$ $z = 7.814"$

$\alpha = 48.487°$ $\beta = 135.173°$ $\gamma = 103.897°$

However, the known correct solution is

$x = 31.81$ $y = 0.0$ $z = 6.167$

$\alpha = 51.0°$ $\beta = 138.5°$ $\gamma = 103°$

which is most closely approximated by the results of perturbations number 1 and 5. The residual of perturbation 4 is 0.000081 compared to 0.000091 for perturbation 1 and 5. Given that the range of residuals from this single data set is 0.000081 to 0.001297 (perturbation 3), there exists no significant mathematical difference between these two residuals. Let us suppose that the speed of the data acquisition system is 1000 samples per second. From sample to sample then, only 1/1000 of a second will have elapsed. For the transmitter to have a displacement of 3.5" from data point #13 to #14 would imply a particle speed of 3500 inches/sec or 200 miles/hour. Because these speeds are impractical, methods are investigated to eliminate certain solutions altogether. Where the mathematics are inadequate, other approaches are considered.

4.3.1 Some Heuristics

Because we can reason that it will not be possible for the transmitter to be displaced very far from sample to sample from the data acquisition system, it is possible to add a "penalty" to the residual of these perturbations that converge very far from the previous iterate. The weight and method of implementation of these penalties are such that the probability of very distant successive iterates are reduced but not eliminated.

Data point # 14
==========

Perturbation 1
Initial Approximation: X = 32.013209 Y = -0.107699 Z = 5.411770 A = 50.229541 B = 136.041906 G = 105.629581
Initial residual: 0.000106
Converges to: X = 31.567366 Y = -0.086868 Z = 5.557476 A = 49.868630 B = 135.734270 G = 105.537119
Final Residual: 0.000091

Perturbation 2
Initial Approximation: X = 31.890262 Y = 1.380257 Z = 5.013749 A = 40.118694 B = 105.281081 G = 136.191617
Initial residual: 0.017551
Converges to: X = 33.870811 Y = -1.187400 Z = 3.569387 A = 49.658942 B = 126.484192 G = 118.653984
Final Residual: 0.000584

Perturbation 3
Initial Approximation: X = 33.571246 Y = 0.949469 Z = 7.211216 A = 79.373913 B = 129.852437 G = 88.461850
Initial residual: 0.055477
Converges to: X = 36.807691 Y = -7.192644 Z = 14.675249 A = 57.705294 B = 147.508680 G = 86.159879
Final Residual: 0.001297

Perturbation 4
Initial Approximation: X = 32.734133 Y = 1.223507 Z = 5.134473 A = 43.744925 B = 116.633165 G = 115.248771
Initial residual: 0.009541
Converges to: X = 31.217467 Y = 0.198597 Z = 6.397609 A = 49.384315 B = 135.565205 G = 104.929628
Final Residual: 0.000090

Perturbation 5
Initial Approximation: X = 31.857681 Y = 1.959145 Z = 5.220781 A = 32.253626 B = 155.662207 G = 104.896225
Initial residual: 0.061150
Converges to: X = 31.575464 Y = -0.093179 Z = 5.537932 A = 49.880818 B = 135.739017 G = 105.551227
Final Residual: 0.000091

Using perturbation #4
Initial Approximation: X = 32.734133 Y = 1.223507 Z = 5.134473 A = 43.744925 B = 116.633165 G = 115.248771
Initial residual: 0.009541
Converges to: X = 30.685827 Y = 0.651336 Z = 7.813586 A = 48.486932 B = 135.173213 G = 103.897066
Residual Vector = {-0.000027 0.000015 -0.000009 0.000006 -0.000005 -0.000030 -0.000036 0.000016 -0.000005 -0.000045
0.000020 0.000024 -0.000000 0.000000 0.000000 0.000000}
Final residual: 0.000081
Stopping Criterion: 1
Number of function evaluations = 92

Table 4.2 Excerpt of iterations and perturbation of RUN067 showing the solution at the fourteenth data point.

4.3.1.1 Residual Add-Ons

Two factors F1 and F2 are added to the residual such that the residual grows in slow proportion with the distance from the solutions between consecutive iterates. A residual add-on is computed as follows:

$$\text{residual add-on} = \sqrt{\Delta x^2 + \Delta y^2 + \Delta z^2} * F1 + \sqrt{\Delta \alpha^2 + \Delta \beta^2 + \Delta \gamma^2} * F2 \qquad (4.4)$$

where,

$\Delta x, \Delta y, \Delta z, \Delta\alpha, \Delta\beta$ and $\Delta\gamma$ are the changes in x, y, z, α, β, and γ from iteration to iteration

F1 is a factor restricting translation and

F2 is a factor restricting rotations.

If F2 is set to zero, then no restrictions are imposed on how much the tracking sphere can rotate from iteration to iteration. Conversely, large values of F1 and F2 mean that the residual add-on will grow quickly as the distance between consecutive iterates grows. If these numbers are too large, then there will be a tendency to adversely bias the convergence of the inverse solution. This is not the aim. Rather, we aim to select values of F1 and F2 that are just large enough to raise the residual of points more that 1 inch away to a level where they become less likely to be selected over nearby points with slightly higher but comparable residuals. Null values of F1 and F2 are equivalent to no add-ons to the residual. Graphs with various values of F1 and F2 are presented in figures D.28-D.33 of appendix D. If F1 = F2 = 0, then no restrictions are placed either on translations or rotations and the graphs are equivalent to those of figures D.9-D.14.

In figures D.28-D.30, a slight restriction is imposed on translation, but none on rotations. It is observed that the graph is markedly improved at the vicinity of previous trouble but is unaffected in areas near the front and back edges where translations and rotations between iterates are small. A small discontinuity in the plots still appears around the eighteenth to nineteenth data points. This discontinuity is reduced further in figures D.31-D.33 where the restriction on translation is increased to F1 = $3.5e^{-5}$ and no restriction is imposed on rotation (F2=0).

In all the cases above, the x, y, α, β, and γ graphs were as good or better than those of RUN067 done with no restrictions on displacements.

4.3.1.2 Residual Conditioning

Comparable residuals between point on RUN067 and RUN067A stem from the fact that antennae with large signal levels have good agreement. Antennae with lower signals are outweighed and thus contribute little to the residual. Because the emphasis placed on matching larger signals does not lead to unique solutions, a focus is placed on the antennae with lower signal levels. Here, the relative errors between the model and collected data is examined. This error is typically large for antennae with low readings and small for antennae with large readings. Thus, to identify antennae with low readings and whose model-reality correspondence is poor, the relative errors are analyzed. Two constants S and T are introduced into the individual components of the residual as follows. If the relative error between the model and collected data is larger that T, then the contribution to the residual is increased by a factor of S:

$$\text{if} \quad \frac{Model_i - DAQ_i}{Model_i} > T$$

$$\text{then,} \quad res_i = res_i * S \tag{4.5}$$

where,

$Model_i$ is the model predicted voltage for antenna *i*,

DAQ_i is the measured voltage from antenna *i*,

res_i is the *i*th component of the residual and is given by equation (4.3).

Several values of T and S were used in experimentations. The results of these experiments are stated here qualitatively for the sake of brevity. Values of T=15% and S=3.0 are found to produce the best results. In every case, solution plots in X, Y and Z became much less smoother, though equally accurate, compared to plots without these correction terms. Improvements do appear in the areas of trouble (around data

point #14 in RUN067). However, these improvements come only with a compromise in other parts of the plot that have deteriorated.

4.3.2 Residual Manipulations

One way to overcome the limitations introduced by simply selecting the lowest residual is to change the way by which the residual is computed. Currently, this is done by the Euclidean norm or L_2 norm:

$$R = \sqrt{\sum r_i^2} \tag{4.6}$$

where,

R is the total residual and

r_i are the components of R given by

$$r_i = \left(V_{\text{model}} - V_{\text{daq}}\right) \tag{4.3}$$

This norm, as any other, has advantages and disadvantages. It finds its advantage in its ability to weigh a large range of numbers equally, even if the numbers being normalized differ from one another by several orders of magnitudes. The Euclidean norm has the disadvantage of masking trends that may exist in the components of the residual. For example, for the three residual vectors shown below, the Euclidean norm yields the same result:

$$\begin{aligned}
&\bar{r} = \{20,20,20,20\} && L_2 = \sqrt{\sum r_i^2} = \sqrt{20^2+20^2+20^2+20^2} = 40 \\
&\bar{r} = \{20,-20,20,-20\} && L_2 = \sqrt{\sum r_i^2} = \sqrt{20^2+(-20)^2+20^2+(-20)^2} = 40 \\
&\bar{r} = \{40,0,0,0\} && L_2 = \sqrt{\sum r_i^2} = \sqrt{40^2+0^2+0^2+0^2} = 40
\end{aligned} \tag{4.7}$$

It is unclear which of the above residual vectors is the better solution. Alternate methods of examining the residuals are thus in order.

The infinity norm (L_∞) applied to the set above yields

$$\begin{aligned} \bar{r} &= \{20,20,20,20\} & L_\infty &= \max|\bar{r}| = \{|20|,|20|,|20|,|20|\} = 20 \\ \bar{r} &= \{20,-20,20,-20\} & L_\infty &= \max|\bar{r}| = \{|20|,|-20|,|20|,|-20|\} = 20 \\ \bar{r} &= \{40,0,0,0\} & L_\infty &= \max|\bar{r}| = \{|40|,|0|,|0|,|0|\} = 40 \end{aligned} \tag{4.8}$$

The unity norm (L_1) norm yields

$$\begin{aligned} \bar{r} &= \{20,20,20,20\} & L_1 &= \sum|r_i| = 20+20+20+20 = 80 \\ \bar{r} &= \{20,-20,20,-20\} & L_1 &= \sum|r_i| = 20+20+20+20 = 80 \\ \bar{r} &= \{40,0,0,0\} & L_1 &= \sum|r_i| = 40+0+0+0 = 40 \end{aligned} \tag{4.9}$$

These norms have been used instead of the Euclidean norm and have produced mixed results. Combinations of the norms have also been done, though an exhaustive study remains to be done. For example, the L_∞ or the L_1 norm could be computed and incorporated as one component of the Euclidean norm. Such combinations have been successful in the past, but their success is realized only with some hind-sight of what the solution should be. Development of an "intelligent" algorithm to determine which norm or combination of norms is optimal given the data set is non-trivial and beyond the scope of this document.

Chapter 5
Experimental Results: A Case for Multiple Transmitters

5.1 Experimental Results of Controlled Trajectories

Several runs were taken in the development of this tracking technique. The results of some of these trajectories are presented in Appendix E. All data in this appendix is collected through the single 2.04 MHz transmitter described in section 2.2.2.

5.1.1 Fixed-Angle Runs

Figures E.1-E.12 are the results of three typical fixed-angle runs. The coordinate systems used on these runs are not necessarily those depicted in Figure D.1 of appendix D. This is not, however, important to our arguments. What we seek to point out is the dependence of the final solution on the course of the trajectory. Note the relationship that exists between the quality of the solution in a given direction and the angle of the transmitter with that direction. In every case, it can be argued that when the axis of the transmitter is at a small angle ($< 45°$) with a principle direction (X, Y or Z), the result in that direction is generally good. In the case of RUN068 (figures E.5-E.7), agreement in the X-direction surpasses that in the Z direction considerably. Of no coincidence, this is reflected in the angle that the transmitter makes with the axes:

$$\alpha = 48° \qquad \beta = 136° \qquad \gamma = 77°$$

Because the symmetry, $\beta=136°$ is equivalent to $\beta=44°$. We expect that if the angle with a principle axis is zero, we should get excellent results along that direction, while compromising the quality of the solution in other directions.

5.1.2 Simulated Roll

While small angles in a given direction usually leads to improved solutions in that direction, it is not impossible to obtain good results in the other directions. This is particularly true when the large angles are temporary. Such is expected to be the case in a true granular flow. Figures E.13-E.18 are the solution of a "simulated roll". By this we mean that the transmitter is rotated and translated by a prescribed amount in a prescribed direction between each data point. Thus, transmitter-receiver orthogonalities are transient; they never occur in consecutive data points. Witness the surprisingly high quality of the solution given that four orthogonalities (two with X and two with Y) occur in the course of the run.

5.2 Multiple Transmitters

It can be concluded from the arguments of the previous section that good solutions in a given direction are usually the result of good (small) transmitter angle in that direction. Extrapolation techniques to overcome transient orthogonalities and near-orthogonal situations as well as techniques to reduce random and systematic noises to a level low enough to eliminate multiple solutions when such incidents do occur have proven inadequate to consistently produce acceptable results. We conclude that the best way to overcome the orthogonality problem is to prevent these occurrences altogether. Two methods of doing just that suggest themselves. The first method is through the addition of more receiver antennae in orientations not coincident with principle axes. For example, one could equip the chute with antennae mounted at 45° and 135° with each principle axes. This requires that the number of antennae around the flow area be doubled. Such a setup has been attempted. Antenna #12 and #13 or RUN067 (see figure D.26 and D.27 of appendix D) are a typical 45°-135° pair. Surprisingly, the addition of these antennae improved but did not rid the final solution

of discontinuities despite the accuracy of the voltage plots. Because an orthogonality in one direction means that a minimum of 45° exists with the corresponding slanted antenna, a multitude of slanted antennae inclined at several different angles would be necessary such that at least three angles are below 45°. This increase in the number of antennae increases the number of components in the residual vector, thereby decreasing the weight of individual components. The results is that only a marginal improvement arises from the addition of more receiver antennae. In cases where slanted antennae were implemented, it is found that the improvements in the results usually did not warrant the electronic and computational efforts expended.

The alternative is to increasing the number of receivers in the system is to increase the number of transmitters. If three orthogonal transmitters of differing frequencies could be packaged in the tracking sphere, then a transmitter-receiver orthogonality could never occur. In such a case, the largest angle that could ever exist between a give direction and axes of the transmitter is 54.7°. Even a two-transmitter system would drastically reduce the likelihood of orthogonalities.

One other limitation of the single transmitter system is depicted in figure 5.1. Because of the symmetry in the transmitter's output, there exists one axis about which the transmitter can rotate undetected. This axis is the axis coincident with the axis of the transmitter.

Several practical considerations need to be made before such systems are developed. The difficulties of packaging a single transmitter described in section 2.2.2 are further complicated when we speak of multiple transmitters. Also, the mutual effect of two transmitters in close proximity needs to be considered. Other matters requiring

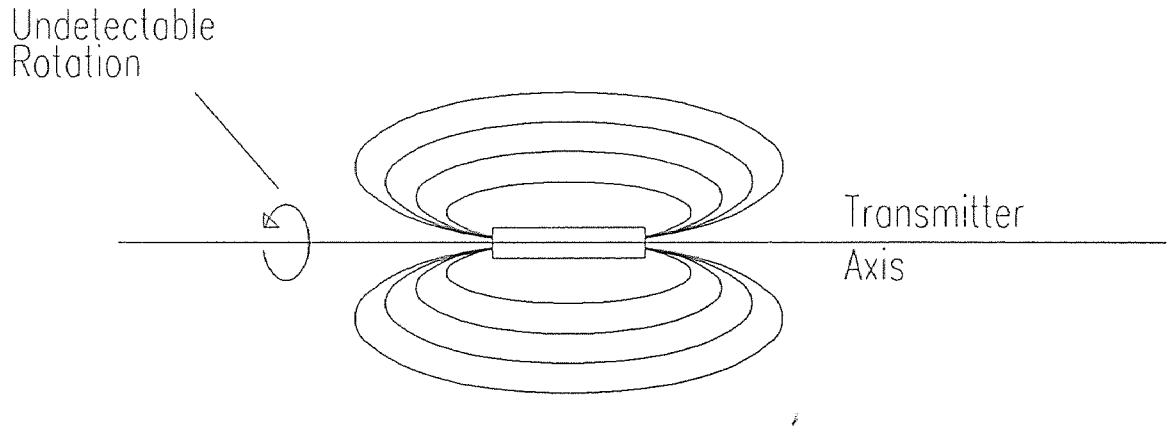

Figure 5.1. The need for multiple transmitters: a rotation about the transmitter's axis as shown in not detectable given the symmetry of the transmitting source. The rotation shown would not change the signal level in any receiving antenna, no matter what the orientation of the antenna with respect to the transmitter

attention include

- Power requirements for multiple transmitters
- Geometry of multiple transmitters
- Further reduction of circuitry to allow for new circuits
- Frequency of other transmitters
- Receiver circuitry

A two-transmitter system is already near completion. Figure 5.2 illustrates the geometry of the second transmitter operating at 3.65 MHz. The 2.04 MHz transmitter ferrite core mounts directly inside the 3.65 MHz air core as shown in figure 5.3. Results of the two-transmitter system are not yet available.

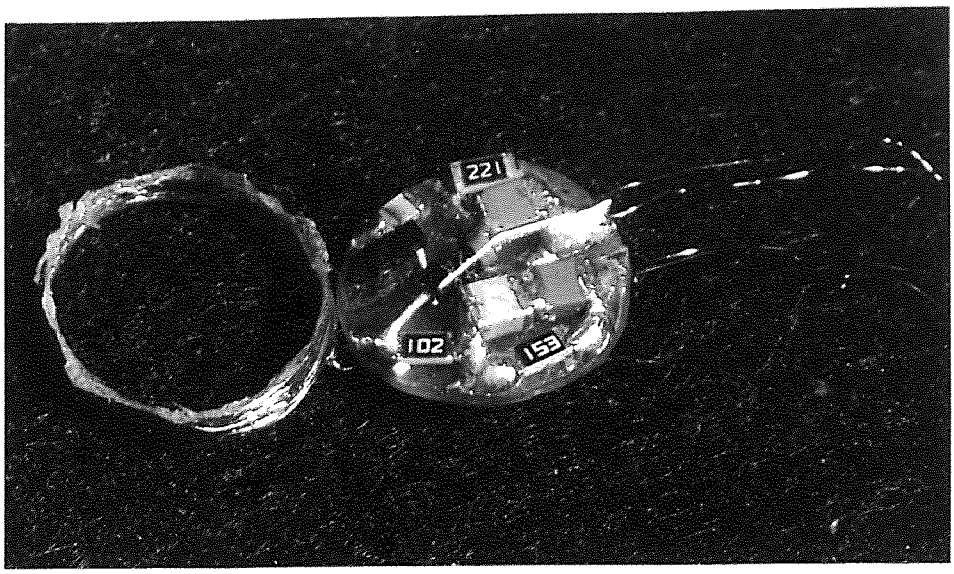

Figure 5.2 The 3.65 MHz Transmitter. The air-core coil on the left mounts directly beneath the circuit board shown on the right

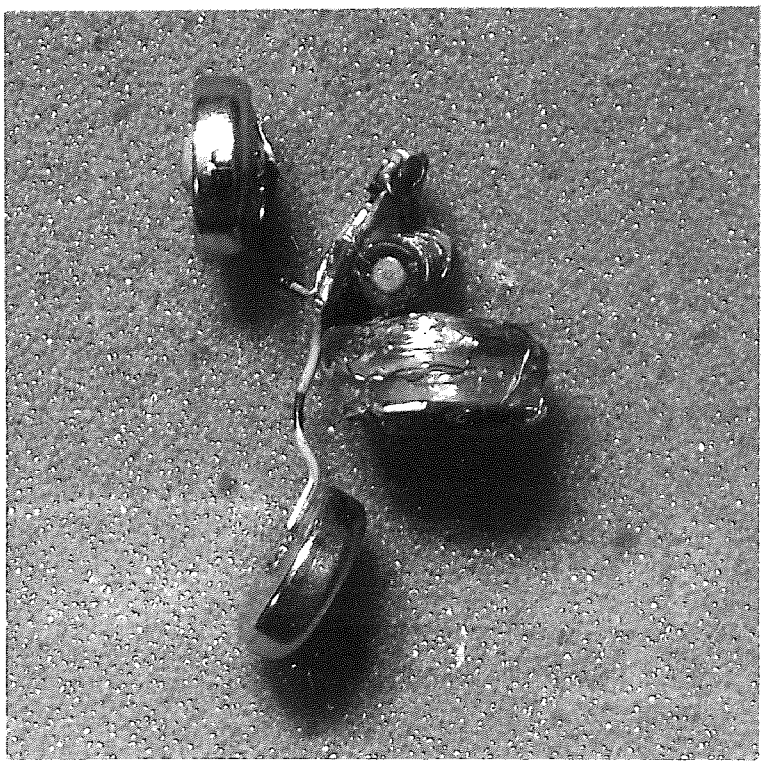

Figure 5.3 Two-Transmitter Assembly. The ferrite coil of the 2.04 MHz transmitter mounts directly inside the 3.65 MHz air coil.

Chapter 6
Summary and Conclusion

6.1 Summary of Progress

To date, most steps needed to successfully implement the proposed tracking system have been taken. A summary of these steps follows.

A miniature high-power electronic radio transmitter has been built. This transmitter has been packaged within a case machined from a 1-inch acrylic sphere. A "radio-transparent" chute instrumented with rectangular loop receiver antennae has been built. Receiver boards, which include amplifiers, band-pass filters and balance demodulators have been designed and built to monitor the signals in the antennae. A PC-based data acquisition system is in place to digitize and store data collected from the output of the receiver boards. Once collected, a method has been established to calibrate the data in order to reverse the gains and loses in the process of data acquisition. The results of this is a set of data indicative of the voltage in the respective antennae. A mathematical model capable of predicting voltage levels in a rectangular loop antenna given the position and orientation of the tracer particle has been derived. Numerical techniques for obtaining the inverse solution have been established. In the present study, efforts are steered toward the improvement of the inverse solution by two primary methods. The first method used attempts to improve the inverse solution by reducing model-reality discrepancy in the forward solution. Here again, two approaches are considered. The first approach assumes that the collected data is free of systematic errors and that model-reality discrepancies arise from inadequacies in the voltage model that may have come up as a result of simplifications, invalid assumptions or the neglecting of higher-order terms. An attempt to correct model-reality discrepancy is implemented using a two-part model. The "first" part of the model is the theoretical model of section 3.1. The "second" part

is an empirical map of scaling factors as outlined is sections (3.4.1 and 3.4.2). Results of a simplified two-part model are promising (sections 3.4.1.2) but methods of building a complete map are still under investigation.

The second approach to reducing model-reality discrepancy assumes that the theoretical model is accurate in predicting voltage induced in the receiving antennae. Errors, it is assumed, stem from magnetic coupling between antennae. The nature of this coupling has been studied and found to be complex. Further study is in progress.

The second method used to increase the quality of the inverse solutions is based on altering the numerical methods. Techniques of initial approximation including the use of extrapolations and perturbations (section 4.2) are considered. Such techniques have greatly increased the robustness of the numerical methods.

We consider the computed inverse solution to be the correct solution when the numerical method converges to the solution that is the global minimum. This is the solution with the least squares residual. Because of noise, model-reality discrepancies and the non-linear nature of the model formulation, a multitude of local minima surround this global minimum. Heuristic approaches are considered to reduce the likelihood that the numerical techniques will converge to one such local minimum. These are implemented in the form of the residual add-ons and manipulations described in section 4.3

Experimental results show that the tracking system being developed works consistently and predictably but is slightly outside the acceptable levels of accuracy.

6.2 Direction for Future Work

A lot of work remains to be done to perfect the proposed tracking system. Issues to be resolved can be categorized into three classes. The first class of issues deals with difficulties in data acquisition and the experimental setup. The second class of issues is related to the voltage model and the discrepancy that exists with measured antenna

voltages. The third class of issues deserving further attention deals with convergence issues in the inverse solution.

6.2.1 Data Acquisition and the Physical System

There are several aspects of the data acquisition process and the physical experimental setup that potentially weigh heavily in determining the quality and validity of the inverse solution. A few of these are outlined below:

6.2.1.1 Configuration of antennae

An exhaustive study on the optimal configuration of antennae, that is their size, shape and number can potentially boost the accuracy of the tracking system. Throughout this study, it has been observed that in a given data set, certain antennae have weighed heavily in determining the outcome of the inverse solution. On the other hand, in certain cases, the addition of experimental antennae mounted on 45° angles have had little effect on the convergence of the numerical methods in the inverse solution. It is found that the addition of such antennae increases the number of components in the vector of residuals, thereby decreasing the weight of any single antenna. The effect of antennae with high signal levels, which could potentially provide results of high accuracy become less pronounced. Likewise, the effects of antennae with low signals levels, which typically do not yield results of high accuracy are also diminished. The result is usually only a marginal increase in the overall accuracy of the inverse solution.

6.2.1.2 Methods of calibration

Current methods of calibrating the data acquisition system are based on trial and error and observation. It is known, however, that different means of calibrating the system can result in slightly different solutions. Present calibration techniques are "single-point" techniques. That is, the prediction of the model at a given point is compared

with the readings from the data acquisition system and an appropriate scaling factor is determined. This technique of calibration is subject to human errors and the ability to accurately position the tracer particle in a prescribed position. Small shifts in the plots of the model and reality, such as the one shown in figure 2.11, are, in part, caused by this method of calibration. Better methods of calibrating the system at multiple locations like the 27-point corrections can reduce this shift.

6.2.1.3 Antenna Coupling

Work is currently in progress to determine how antennae become coupled and how they can be uncoupled. Experiments show that the coupling between antennae is dependent on the proximity of the antenna and the orientation of the antennae with respect to each other. A means of configuring antennae to reduce coupling may increase the accuracy of tracking. Where such a configuration is inadequate, it may be possible to eliminate coupling effects by empirical means similar to those outlined in chapter 4.

6.2.1.4 Multiple-Transmitters

The orthogonality and near-orthogonal conditions described in section 2.2.3 have been a primary reason why the numerical methods have failed to converge to the correct solution. In section 5.2, it is concluded that one approach to resolve the problems of large transmitter-receiver angles is to package multiple transmitters in the tracking sphere. Efforts to achieve this end is well in progress.

6.2.1.5 Balancing of the Tracking Sphere

Mechanical balancing of the tracking sphere refers to the addition of non-metallic weights into the package to give the tracer particle the same mass as the other acrylic spheres in the mass. Also, the packaged transmitter should not have a "heavy" side

(section 2.2.2.). Efforts to mechanically balance the tracking sphere require the use of fairly sophisticated CAD/CAM packages capable of doing centroid and moment analyses of composite rigid bodies.

6.2.2 Model-Reality Agreement

In simulations, the inverse solution from the numerical methods always converges to an exact solution. That is, when the model matched reality perfectly, the results would always be perfect. Thus, it is possible to improve the inverse solutions by improving the agreement between the model and reality. A few methods of doing this are outlined in chapter 3. All techniques that can improve the model-reality correspondence can potentially eliminate many or all of the difficulties encountered in developing the tracking system. All such techniques are worthy of investigation.

6.2.3 Convergence Issues in the Inverse Solution

Convergence Issues in the numerical methods of the inverse solution can be categorized in two ways:

1. Convergence to the wrong solution. Because the formulation relating transmitter position and orientation to induced voltage is extremely non-linear, there exists a strong possibility that the numerical methods will converge to a local minimum rather than the global minimum. Methods to reduce the likelihood of such an occurrence are described in chapter 4. Other methods to increase the probability of convergence to the global solution are worthy of investigation.

2. Problems of multiple solutions. In the case where there exists several local minima, the inverse solution credited as the "correct" solution is the one that corresponds to the solution producing the minimum residual. Problems arise when two or more local minima produce residuals that differ only slightly. In such cases

of multiple solutions, heuristics have been used to select the better of the two solutions. Other methods of selecting solutions or alternate methods of computing the residual may be able to reduce or eliminate the difficulties of multiple solutions.

6.3 Conclusion

It should be pointed out that the areas worthy of investigation described in section 6.2 are not "independent". That is, the resolution of one or two of these difficulties may eliminate the need for the others. For example, if a means of greatly improving the model-reality correspondence is found, then it is likely that convergence issues in the numerical methods of the inverse solution will disappear. Likewise, it has been noticed that when there exist multiple-solutions, one of the local minima is usually the correct solution even though it may not be the least residual solution. If a technique based on heuristics or an analysis of the tracking particle's displacement history could be implemented such that the correct (not necessarily the least residual) local minimum would always be selected as the best solution, then it is possible that efforts to improve model-reality agreement as well as efforts to improve calibration and obtain optimal antenna configurations, may not be needed. In the case of multiple-transmitter, it is believed that many of the convergence issues in the inverse solution will become insignificant even with a two transmitter system.

In summary, through simulations and experimentation, the viability of the proposed tracking system has been substantiated. Presently, the system is working consistently and predictably but is slightly outside the acceptable limits of accuracy. It is the author's belief that further study into the areas outlined in the previous section will result in a robust and accurate tracking technique.

APPENDIX A
Chute Construction Diagrams

The figures in this appendix are the major construction diagrams for the chute. The radio-transparent structure is composed primarily of Extren 500, Extren 600 and acrylic and is fastened with nylon nuts and bolts.

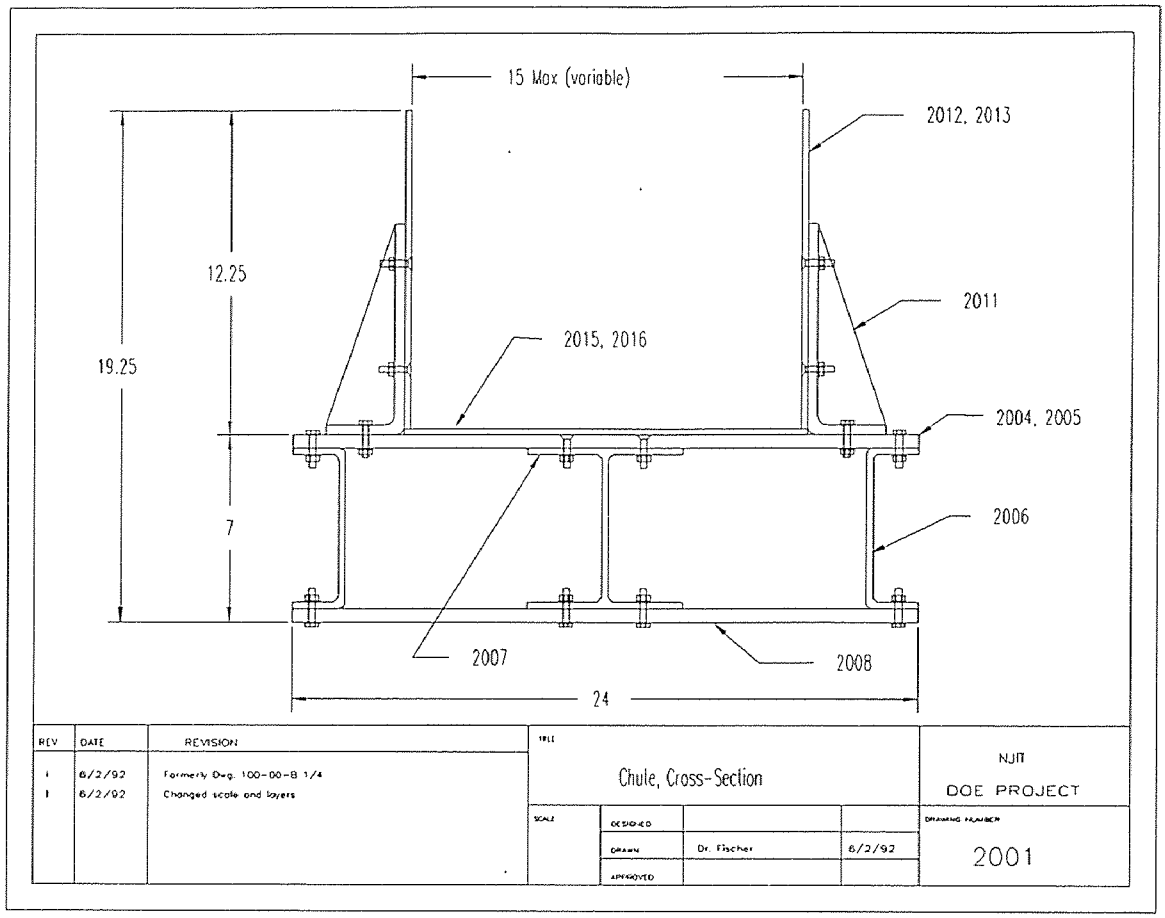

Figure A.1 Cross section of the chute showing a 15" x 12.25" flow space.

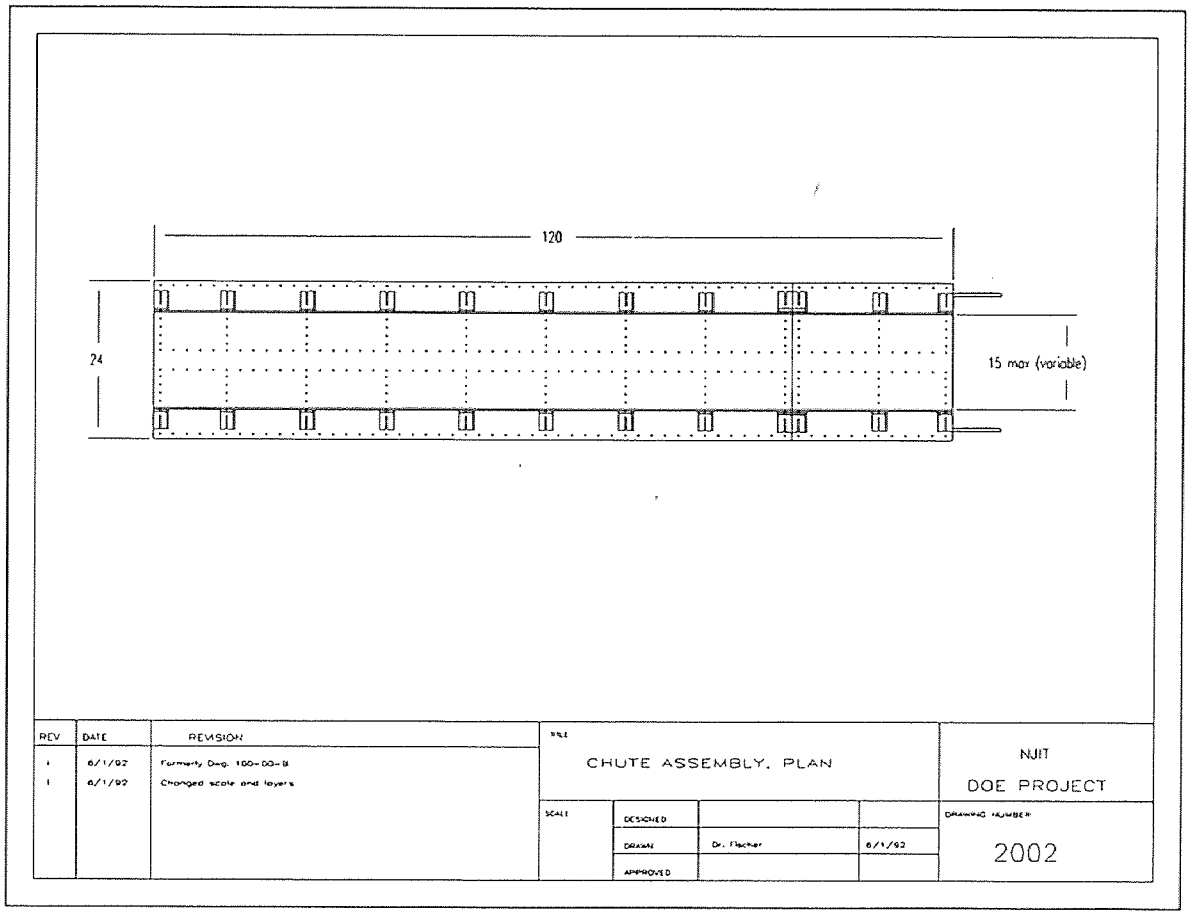

Figure A.2 Chute Assembly, plan view

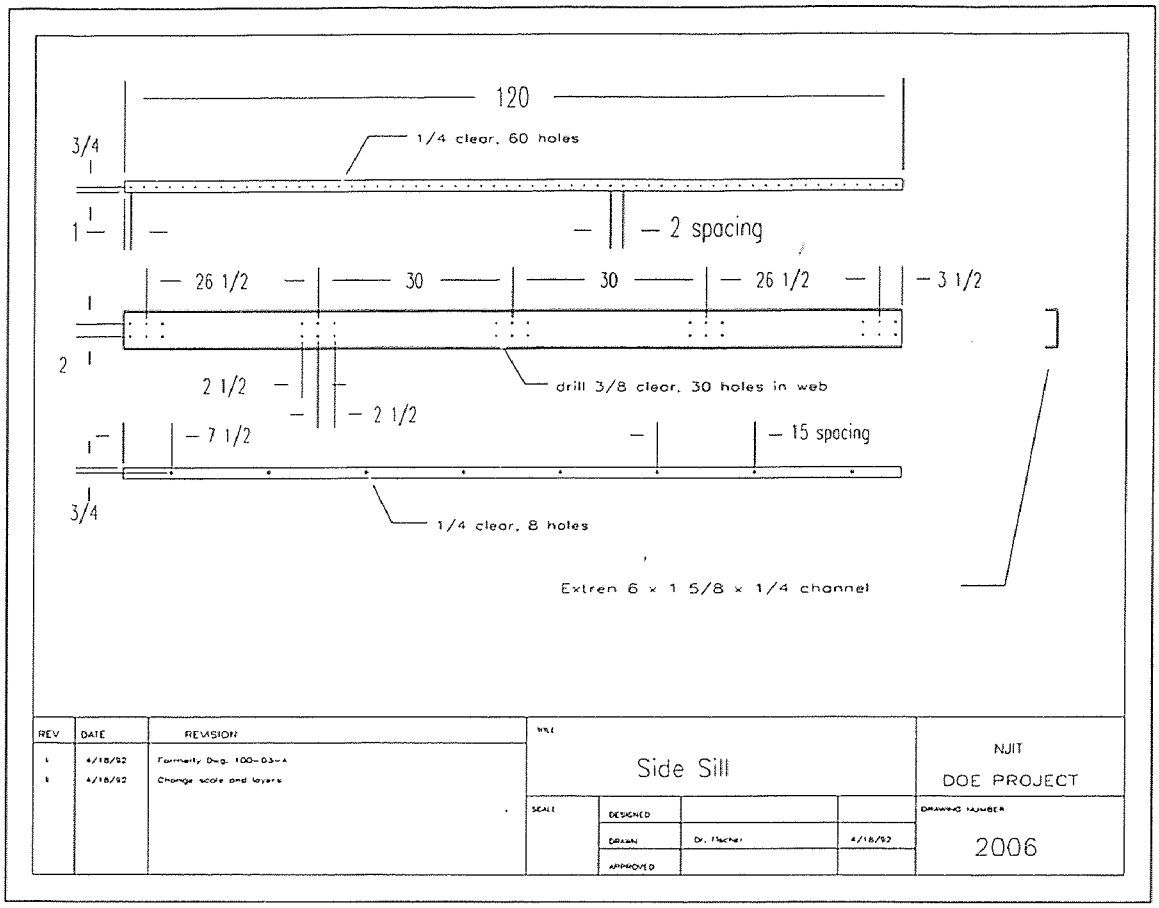

Figure A.3 Chute Side Sill

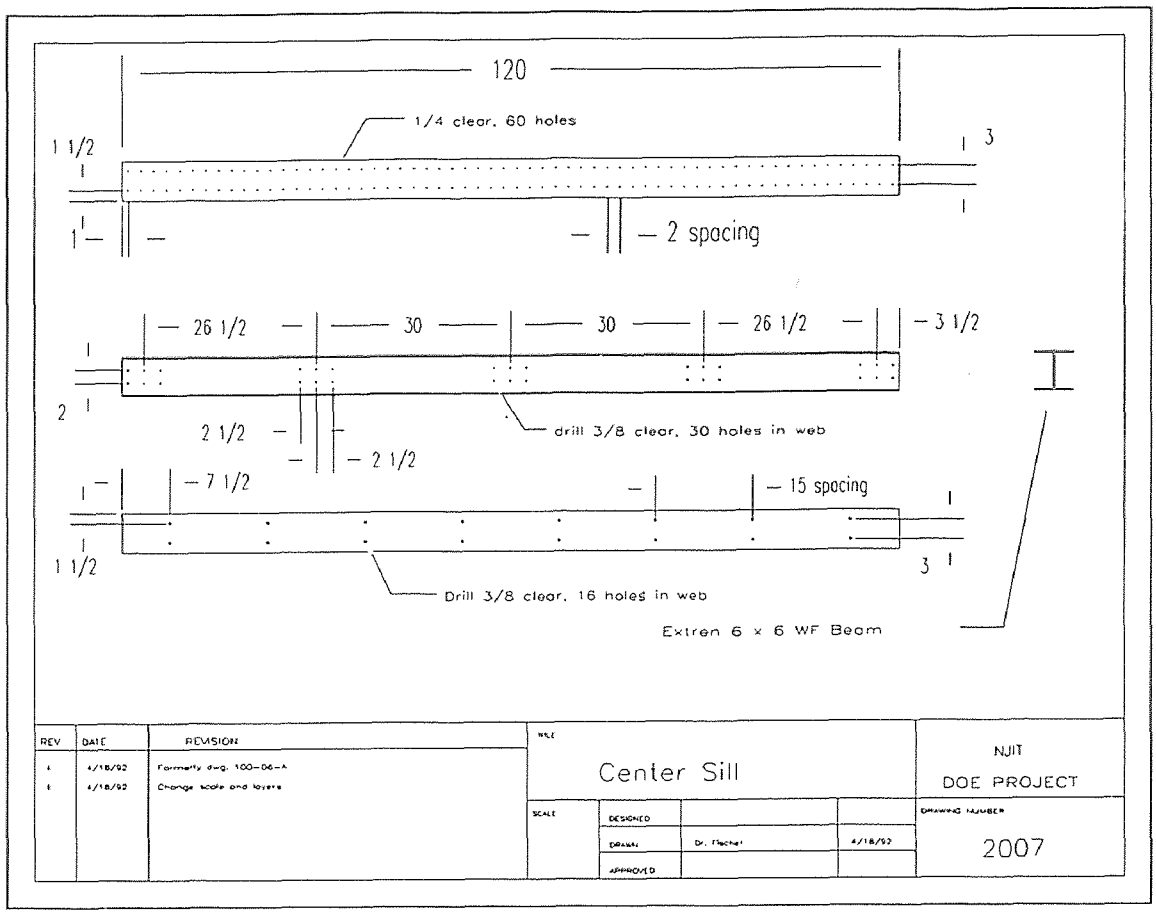

Figure A.4 Chute Center Sill

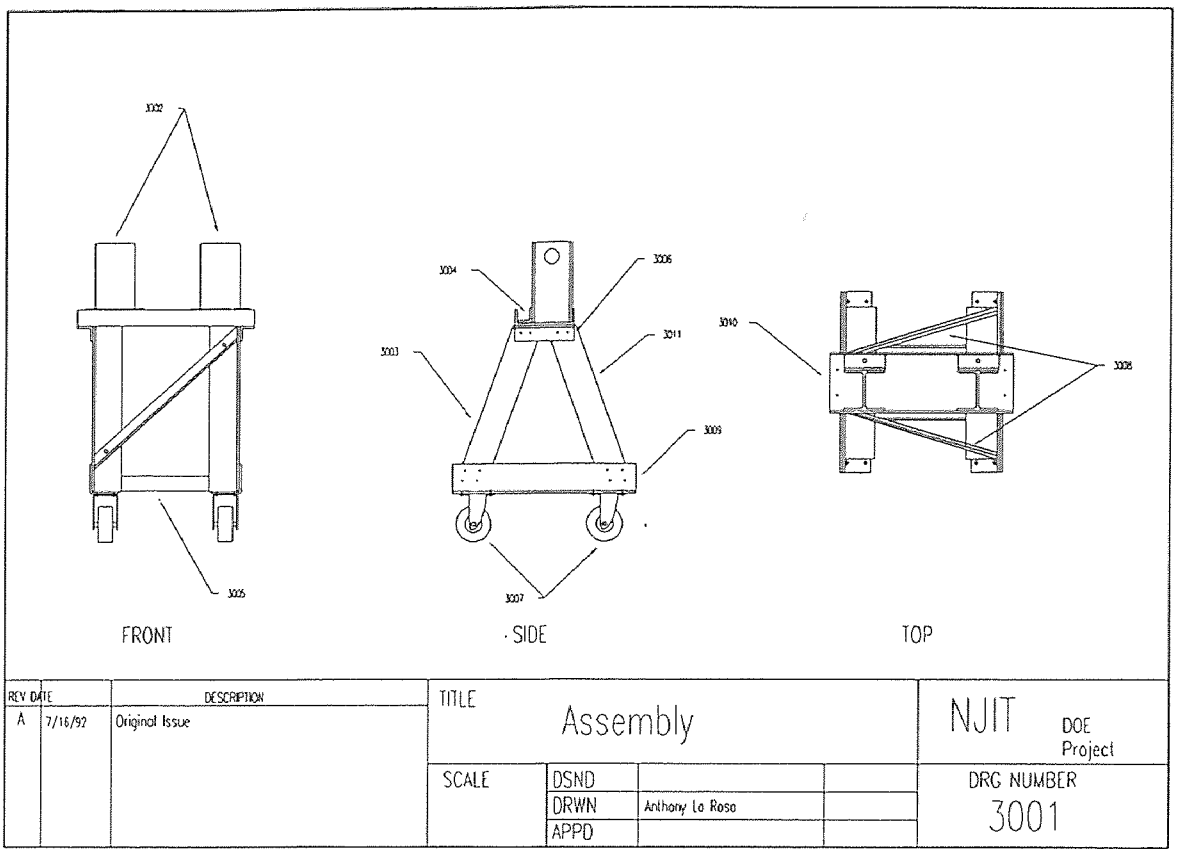

Figure A.5 Chute Base Support, assembly drawing

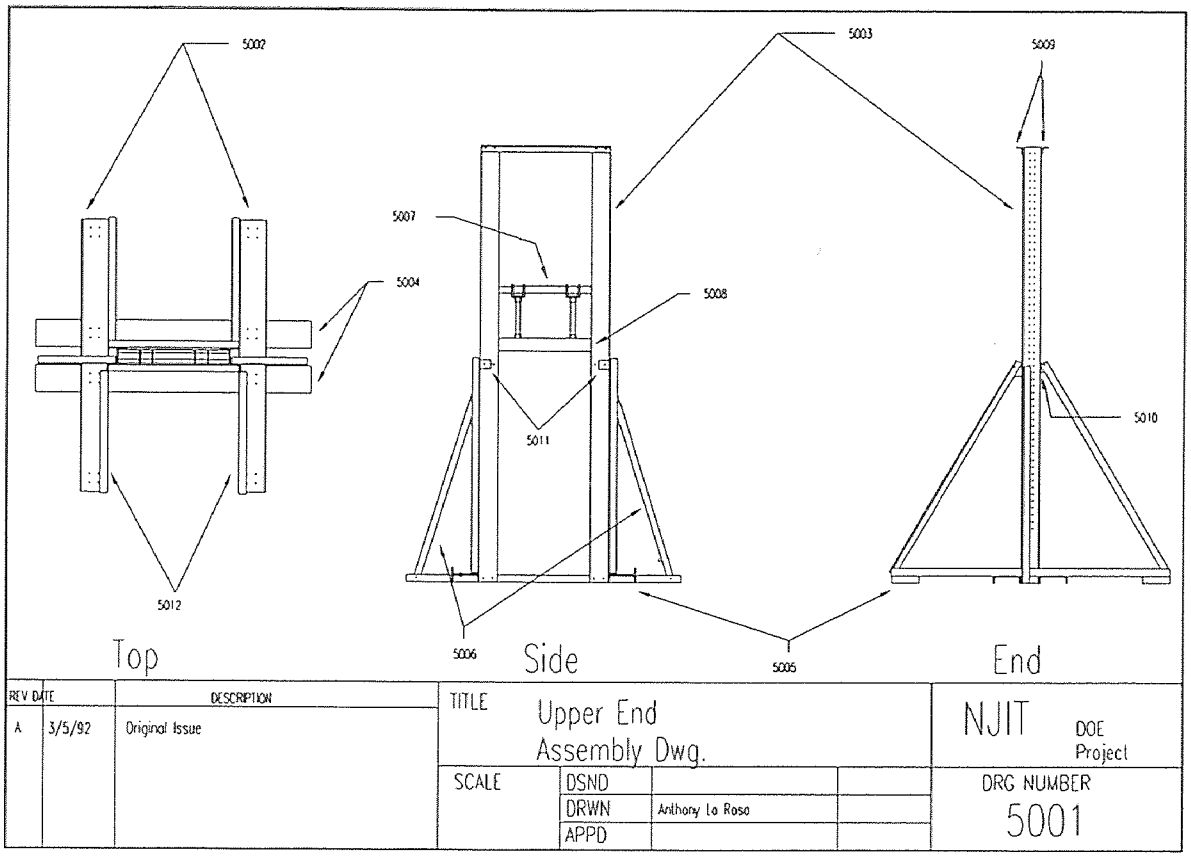

Figure A.6 Chute Upper End, assembly drawing

APPENDIX B
Effect of 27-Point Corrections

The data in this appendix pertain to a straight line trajectory along the X-direction. The axis of transmitter is parallel to the axis of the X-antenna. We expect that results in the Y and Z directions will be very poor. These results are omitted here. Antenna plots for three X-antennae are also presented. Again, readings in Y and Z antennae are expected to be overwhelmed with noise and interference.

The three antennae shown have axes in the X-direction and are located at X = 0", X = 20" and X = 40" respectively. Each antenna is square and has a 20" x 20" geometry. In figures B.1 and B.2 are the X-results from the inverse solution. Figure B.1 uses a purely theoretical voltage model in its computation. Figure B.2 uses the 27-point empirical extension added on to the theoretical model. Figures B.3 to B.8 are voltage plots showing model-reality plots. Each plot of reality and theoretical model is followed by a plot of reality and empirical-theoretical model. Antennae in the Y and Z directions have low signal levels and are thus of little interest to us.

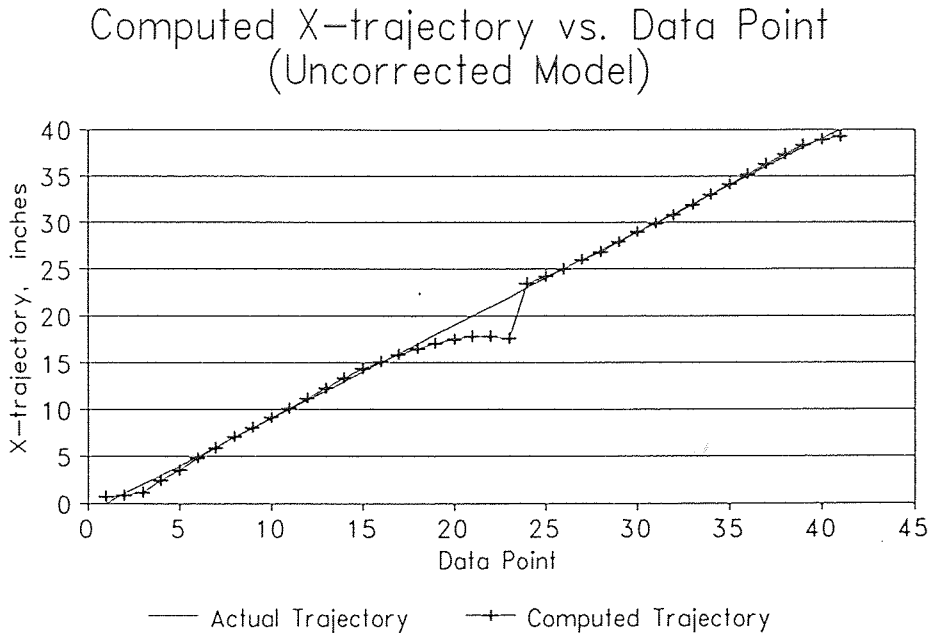

Figure B.1 Computed and actual X-displacement as X goes from 0 to 40 inches. The voltage model used carries no empirical modifications.

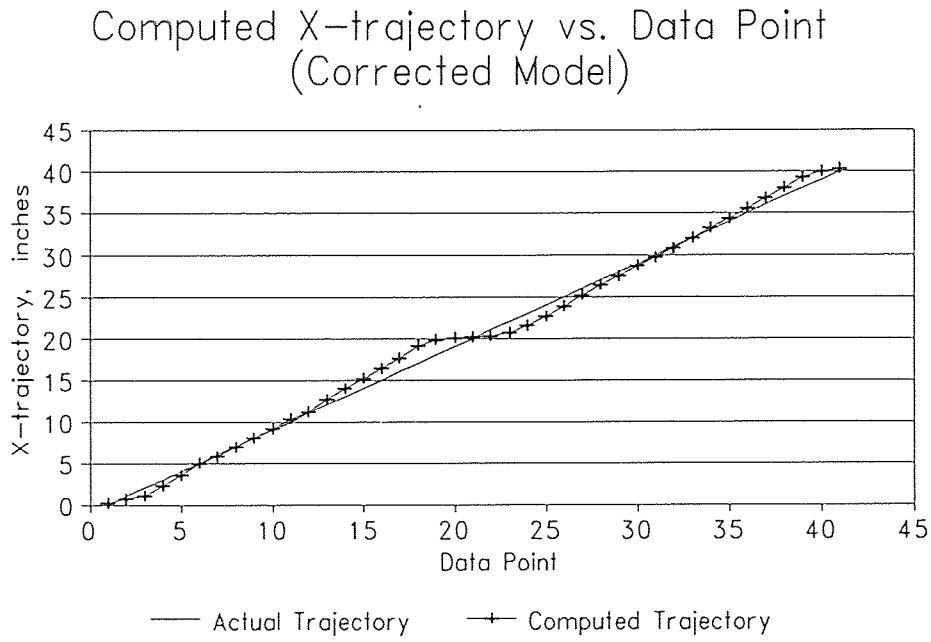

Figure B.2 Computed and actual X-displacement as X goes from 0 to 40 inches. The voltage model used is modified by the 27-point correction factors.

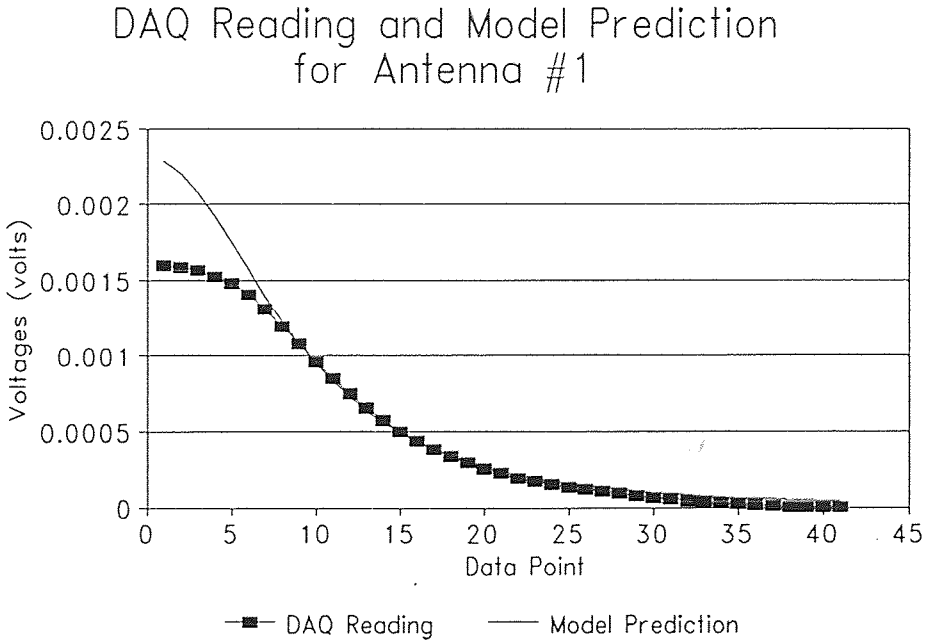

Figure B.3 Output of antenna #1 located at X=0"

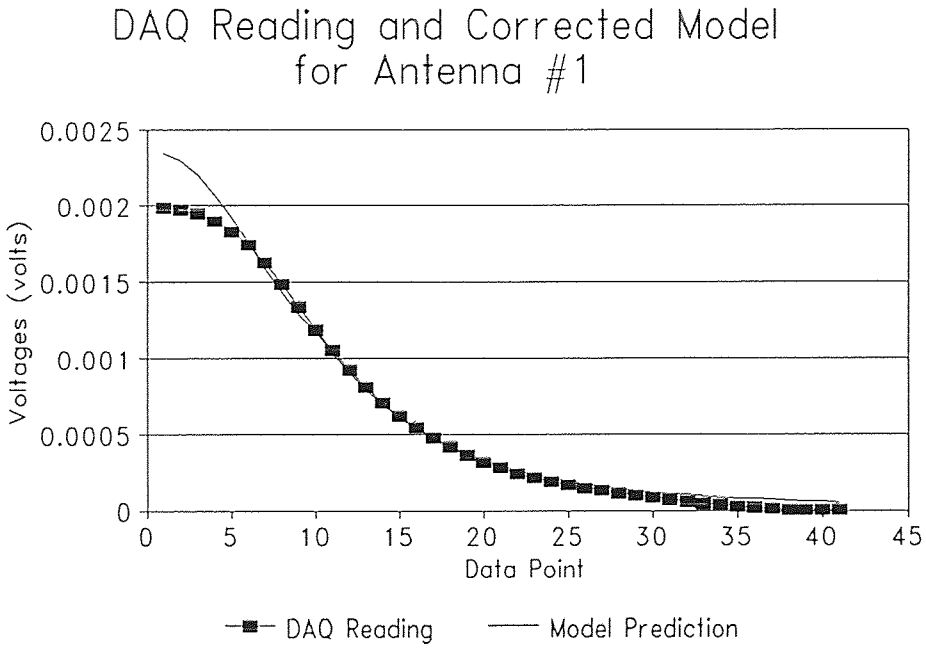

Figure B.4 Output of antenna #1 located at X=0"

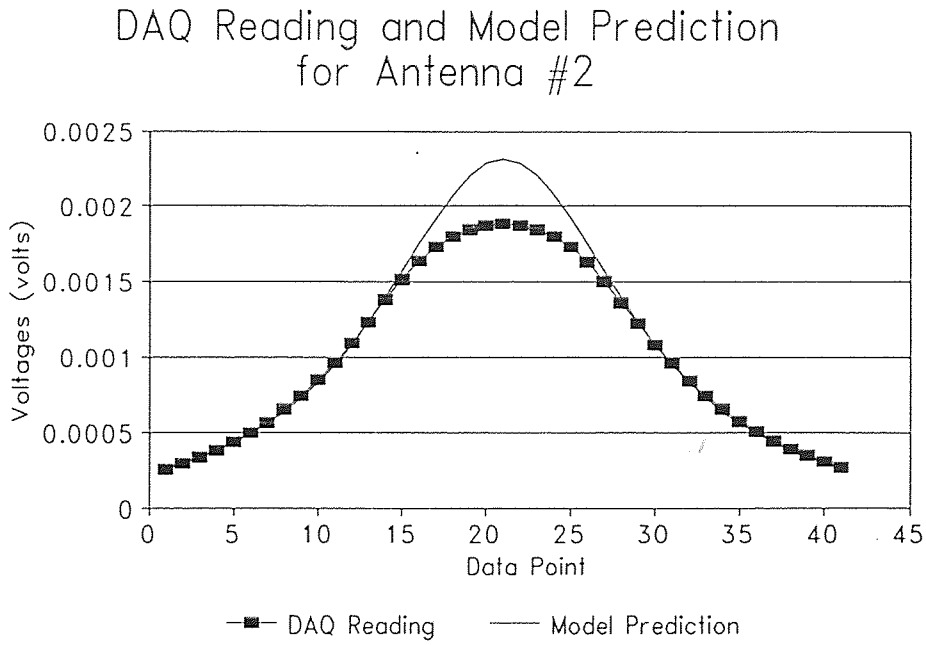

Figure B.5 Output of antenna #2 located at X=20"

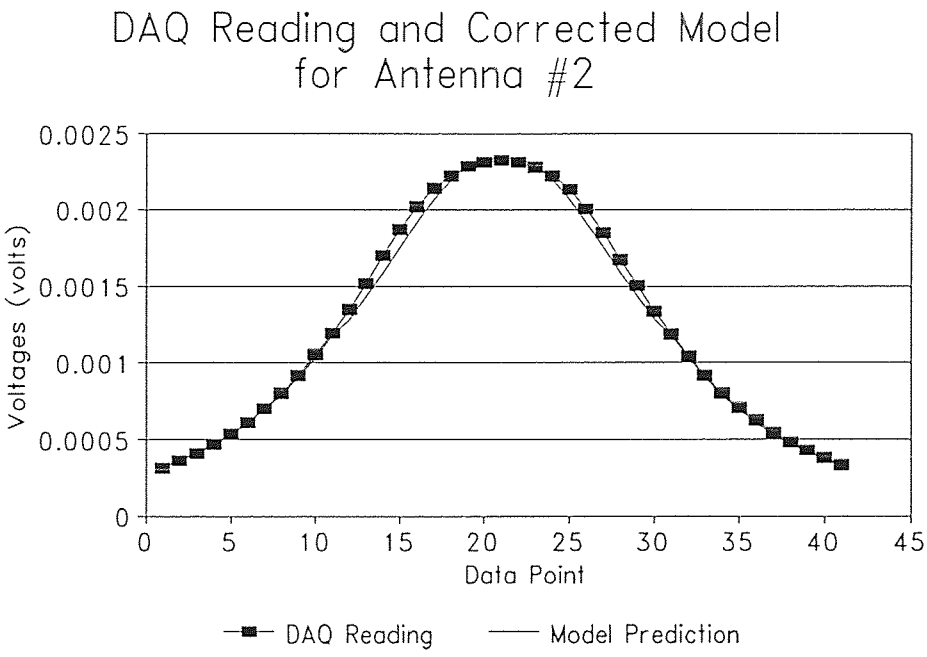

Figure B.6 Output of antenna #2 located at X=20"

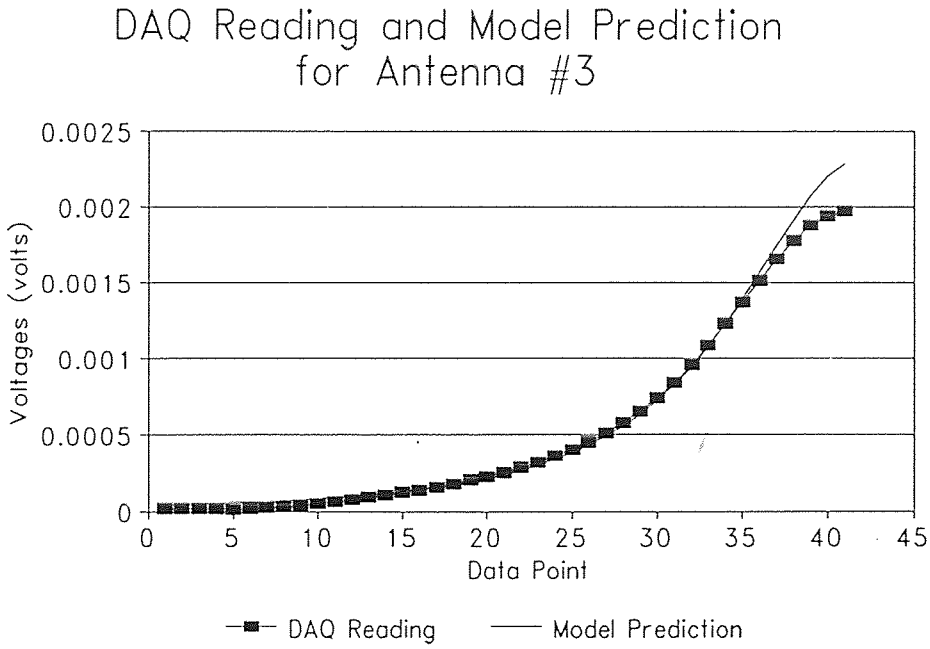

Figure B.7 Output of antenna #3 located at X=40"

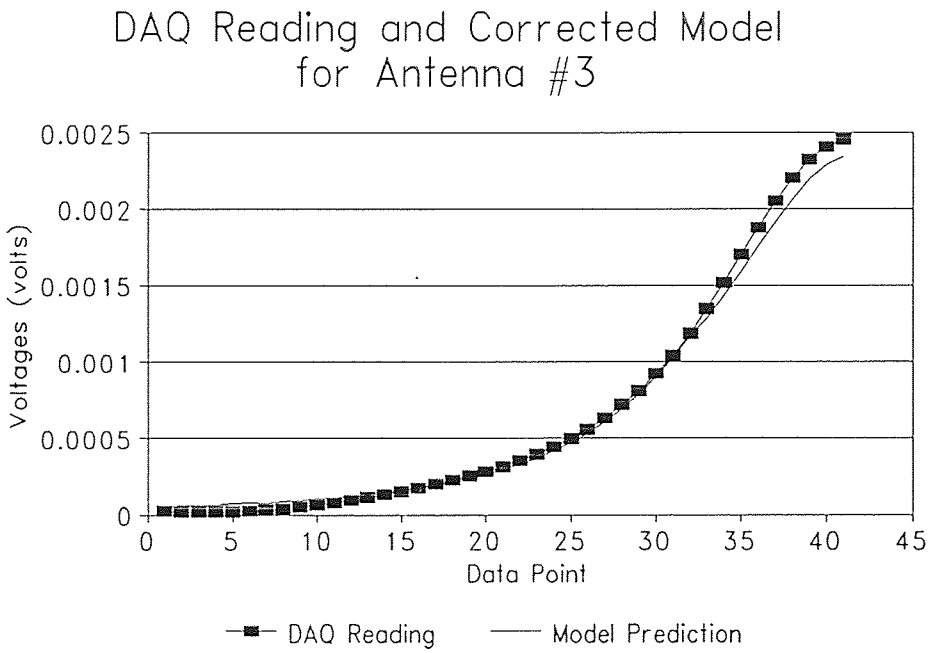

Figure B.8 Output of antenna #3 located at X=40"

The coupling matrix below is for an 11 antenna system. Columns of the coupling matrix are $\frac{\partial}{\partial V_i}$, where V_i is the voltage in antenna i causing coupling in other antennae. The rows of the coupling matrix are the V_j, the signals induced in antenna j by the presence of V_i. Thus, elements in the matrix are given by $\frac{\partial V_j}{\partial V_i}$. Elements on the diagonal are unity by definition.

1	0.0030211	0.00352467	0.00755287	0.00855992	0.0161128	-0.00352467	0.0176234	0.00201409	0.00453172	0.00050352
0.00796415	1	-0.00398208	0.0119462	0.0283723	0.0164261	0.0572423	0.0194126	0.0298656	0.00398208	0.0069686
0.00612814	-0.0038997	1	-0.00055710	0.0685237	-0.00222841	0.00724234	0.00222841	0.0518106	-0.00167131	0.016156
0.014176	0.0265801	-0	1	0.0318961	0.00826936	0.0200826	0.0135854	-0	0.00886002	-0.0011813
0.00724638	0.02657	0.026087	0.0188406	1	-0.00144928	-0.0067632	0.0014492	0.0400967	-0.0014492	0.0101449
0.0170704	0.00715859	-0	0.0132159	-0.0082599	1	0.0638767	0.0005506	0.00495595	0.00881057	0.0104626
0.00171821	0.0283505	0.0154639	0.00902062	-0.0073024	0.0154639	1	0.00042955	0.0274914	0.00042955	0.0064433
0.0483248	0.0405928	-0	0.00451031	0.00773196	0.0154639	0.0070876	1	0.0670104	0.00193299	-0
0.00257511	0.00515021	0.00944205	0.00472103	0.0141631	0.00557939	0.0111588	0.0081545	1	-0	-0.0012875
0.00814901	0.00232829	-0.00814901	0.0291036	-0.0104773	0.0349244	-0	-0	-0.00814901	1	0.00814901
-0.00813008	0.0433604	0.0243902	0.00722675	0.0271003	0.0108401	0.0569106	0.00090334	-0.00722675	0.00993678	1

Table C.1 Typical Coupling Matrix for an 11-antenna system.

APPENDIX D
RUN067 Data and Solution Using Perturbations

D.1 Overview

The materials in this appendix pertain to the data set RUN067. This data is the result to a straight-line, constant-angle trajectory. Antenna configuration and numbers are shown in figure D.1. An illustration of the particle's path is shown in figure D.2. A listing of the collected data is presented in Table D.1. Solution plots for x, y, z, α, β and γ using the previous-point and extrapolation techniques are shown in figures D.3-D.8. Solution plots for x, y, z, α, β and γ using the perturbation technique are shown in figures D.9-D.14. Voltage plots are shown in figures D.15-D.27. The first curve in the voltage plots is representative of the expected signal level given the exact trajectory. The second curve is the signal level as registered by the data acquisition system. The third curve is from the inverse solution.

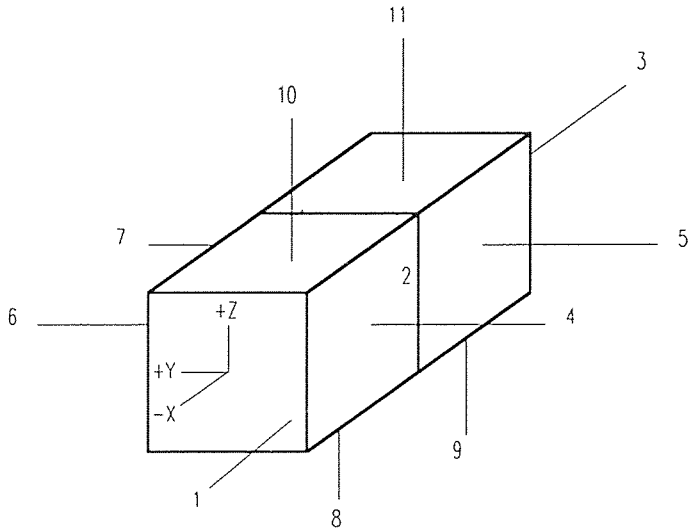

Figure D.1 Antenna configuration and numbers for the system used in RUN067.

The complete solution process including iterations and perturbations for RUN067 appears in Table D.2. For each data point, 5 perturbations are performed about the initial guess. Some of these points converge to different minima, resulting in different final residuals. A record of local minima and residuals is kept, and at the completion of all perturbations, the local minima producing the lowest residual is selected as the solution. The residual vector has 16 components. The first 13 components are a measure of model-reality voltage agreement:

$$r_i = (V_{\text{model}} - V_{\text{DAQ}}) \tag{D.1}$$

The 14th element is a constraint on α, β and γ:

$$(1.0 - \cos^2\alpha + \cos^2\beta + \cos^2\gamma)F = 0 \tag{D.2}$$

The magnitude of the constant F is varied to change the weight of this constraint. Typically, F is selected such that the constraint carries more weight than any voltage match, but is not so great that a large number of significant figures are required to satisfy the condition. The 15th ant 16th components are for constraints on the velocity of the tracking sphere as described in section 4.3.1.1. Component # 15 is for translational velocities while # 16 is for rotational velocities. In the case shown here, both F1 and F2 (see sec. 4.3.1.1) are set to zero. Hence, components 15 and 16 are null and contribute nothing to the residual. In figures D.28 to D.33, the results after varying F1 is shown. Varying F2 is of little consequence here because the trajectory is angle-invariant.

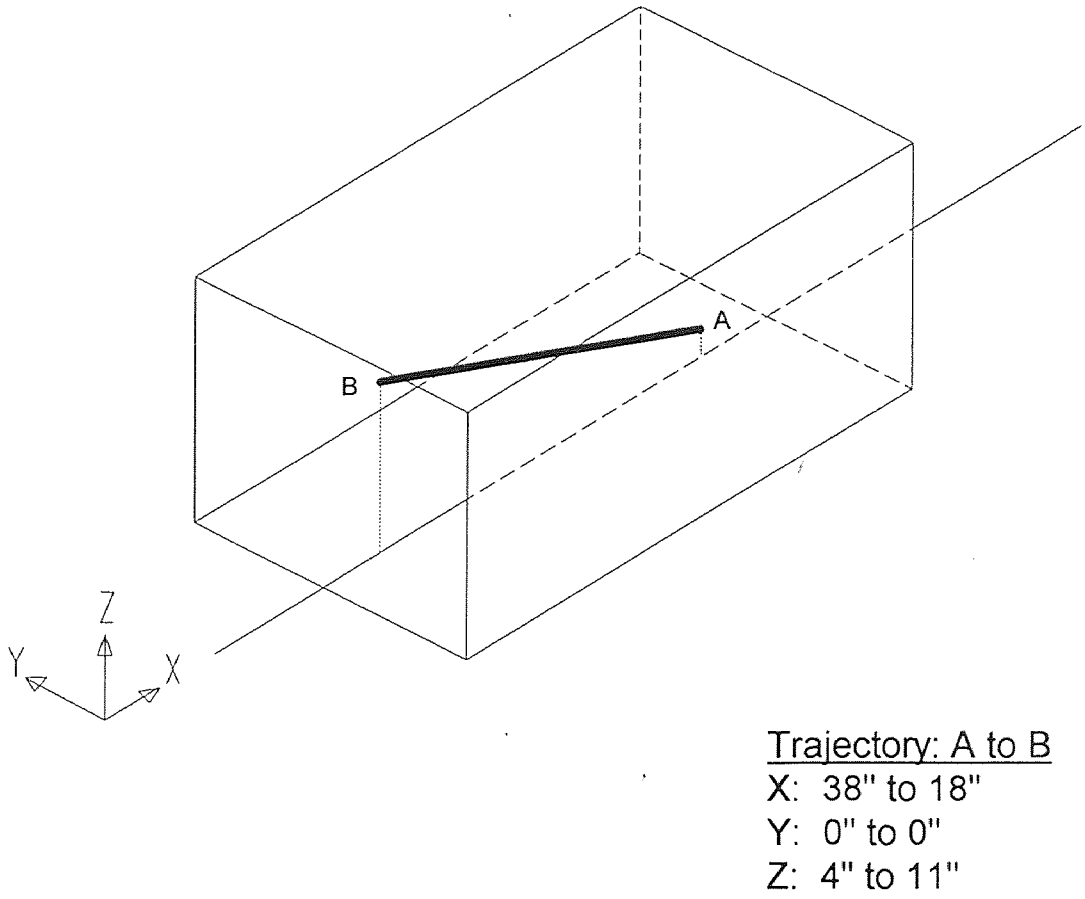

Figure D.2 Course of the controlled trajectory RUN067.

D.2 RUN067 Listing

Below is a listing of the data collected for RUN067. This data is typical of those from the data acquisition system. Each reading is repeated three times to reduce the chance of sporadic data. These readings are later averaged. The first readings in the file is the background reading. This is the data collected with the transmitter off and is representative of standing waves in the environment or noise in the amplification process. The background reading is followed by correlation points. For this run, 6 correlation points are taken. The remainder of the data are the actual readings as the tracking sphere is moved along the chute. 43 data points are taken here.

Data Point #	Antenna Readings — Antenna # 1	2	3	4	5	6	7	8	9	10	11	12	13
	# Name: RUN067												
	#												
	# 1 Background Reading												
1	-7	0	-15	-2	5	1	-5	-9	-4	-2	0	17	0
	-8	1	-16	-2	5	2	-6	-9	-4	-4	0	17	-1
	-7	1	-16	-3	5	1	-5	-9	-3	-2	0	16	-1
	# 6 Correlation Points												
1	26	287	255	72	7	22	-1	44	16	34	0	248	384
	27	286	254	71	7	22	-2	44	16	34	1	248	384
	27	287	255	71	6	22	-1	44	16	34	0	247	384
2	218	327	27	6	43	3	13	-1	45	7	22	121	162
	219	326	27	6	42	4	14	-1	46	7	21	120	163
	218	328	26	7	43	3	14	-1	45	7	22	121	163
3	-6	7	-9	13	224	6	88	-9	-3	-2	1	16	12
	-6	8	-8	14	223	6	88	-9	-2	-2	1	17	10
	-5	7	-8	14	224	6	88	-9	-3	-2	1	17	12
4	-3	7	-16	315	10	105	-3	-8	-3	-1	0	16	2
	-4	7	-15	315	9	106	-3	-8	-2	-1	-1	17	2
	-3	7	-16	315	9	105	-3	-7	-3	-1	0	17	3
5	-7	3	-12	-2	7	1	-3	8	167	7	104	300	468
	-7	3	-12	-2	7	1	-3	9	165	8	104	300	468
	-8	3	-12	-2	8	1	-2	9	166	7	105	299	468
6	-6	3	-16	8	4	4	-6	200	6	172	3	29	2
	-6	3	-15	7	5	4	-6	200	7	172	3	28	2
	-6	3	-16	9	4	4	-5	200	6	172	2	28	3
	# 43 Data Points												
1	-1	75	329	22	23	2	67	4	53	1	36	163	302
	-1	73	329	22	22	1	67	3	54	2	36	161	303
	0	74	329	22	23	0	66	3	54	2	35	162	302
2	1	78	324	23	34	2	68	5	46	2	37	155	314
	0	78	325	23	32	2	68	4	46	2	38	154	314
	0	78	325	23	34	1	69	4	46	1	37	154	313
3	-1	82	318	25	46	2	71	5	36	2	38	147	323
	1	82	317	25	46	1	70	6	36	2	39	147	323
	1	82	319	25	45	2	70	5	37	2	38	147	324
4	1	86	312	27	57	1	71	6	28	3	39	140	333
	-1	87	312	27	57	1	71	7	28	3	40	140	333
	1	86	311	26	56	2	72	6	28	3	40	139	333
5	2	91	306	27	66	1	73	7	20	3	40	134	341
	-1	91	306	27	66	2	73	8	21	3	39	135	342
	2	90	306	27	66	1	72	9	20	3	40	136	341
6	1	96	297	30	76	2	73	9	12	3	41	129	347
	3	96	297	29	76	3	73	9	13	3	41	129	348
	2	96	298	29	75	1	73	9	12	3	42	129	348
7	3	100	292	31	84	2	73	11	7	4	42	125	355
	3	100	292	31	83	1	73	10	7	3	42	126	354
	3	101	291	31	83	2	73	10	5	4	41	125	354
8	3	106	281	32	94	1	73	12	3	5	42	118	359

continues...

Table D.1 Collected data for RUN067 (counts)

...continued

	3	106	282	32	93	3	72	12	2	5	42	119	357
	3	105	282	32	92	2	73	11	3	5	40	119	359
9	3	112	272	34	102	2	72	13	4	5	41	115	359
	3	112	272	34	102	1	72	12	4	5	41	114	360
	3	111	272	34	102	2	72	13	5	5	41	115	360
10	4	117	264	36	108	2	72	14	8	6	41	112	363
	4	116	264	36	109	3	72	14	8	6	40	112	363
	4	116	264	35	108	2	71	14	8	6	41	112	362
11	6	123	252	38	117	3	71	16	12	6	40	107	364
	4	124	253	36	116	2	71	16	14	6	40	108	364
	5	123	252	37	117	2	71	15	14	7	40	107	365
12	4	128	241	39	126	3	70	17	17	7	40	105	363
	4	128	242	39	125	3	70	17	17	7	40	104	363
	4	128	241	39	125	2	70	18	18	7	40	104	363
13	6	135	231	40	132	3	69	19	24	8	39	101	363
	6	135	231	41	132	3	68	18	23	8	39	102	363
	6	135	231	41	132	3	68	18	22	8	39	101	362
14	6	142	223	43	136	5	67	20	26	9	37	100	364
	6	143	224	44	137	4	67	20	26	9	38	99	364
	6	142	223	44	136	4	67	20	26	9	38	101	363
15	7	149	215	44	140	5	66	22	29	10	37	99	364
	8	151	215	45	140	4	65	22	29	11	38	98	364
	8	150	215	45	140	5	65	21	29	10	36	99	364
16	8	158	206	48	144	5	63	24	34	11	35	97	362
	8	158	206	47	146	5	63	23	35	12	36	97	363
	9	158	206	47	144	5	63	23	33	11	36	97	362
17	9	166	195	50	151	7	61	24	36	13	33	96	359
	10	166	196	51	151	6	62	24	36	13	34	98	359
	9	166	195	50	150	7	61	24	36	13	34	96	359
18	9	173	185	53	157	8	59	26	39	14	33	95	351
	10	173	184	54	157	8	60	26	40	14	32	95	352
	10	174	185	53	157	8	60	26	39	14	33	95	352
19	11	182	175	55	161	9	57	28	43	16	32	93	349
	11	182	176	54	160	8	58	27	43	16	32	93	350
	11	182	176	55	161	9	57	28	43	16	32	93	351
20	11	192	169	58	163	11	55	28	46	18	30	93	348
	12	192	169	57	163	11	55	29	46	18	30	93	349
	12	192	168	56	163	10	55	29	46	18	31	94	349
21	14	202	160	59	166	11	53	31	48	19	28	95	342
	12	202	161	59	166	12	53	30	48	20	27	95	342
	13	201	160	59	167	12	53	31	47	19	27	95	343
22	14	211	152	61	170	14	51	32	50	22	25	95	336
	12	211	151	61	171	14	50	32	49	22	26	96	337
	13	211	152	61	170	14	51	32	50	22	26	95	336
23	15	222	144	64	173	15	48	32	51	25	25	96	331
	15	221	144	63	173	15	48	33	51	25	24	96	331
	15	222	145	64	172	15	48	33	52	25	25	94	332
24	15	232	136	66	176	17	46	34	52	28	22	97	324
	16	232	136	65	177	18	46	34	53	27	21	97	323
	15	232	136	65	177	17	46	34	54	27	23	96	324
25	16	243	128	67	180	20	44	35	54	31	19	99	318
	16	243	128	66	179	18	43	35	54	31	20	99	318
	17	243	127	67	179	19	43	35	55	30	20	99	317

continues...

Table D.1 (continued) Collected data for RUN067 (counts)

...continued

26	18	255	122	68	180	21	40	36	57	35	17	101	313
	18	255	123	67	180	22	39	36	56	34	17	102	314
	18	255	123	68	180	21	40	35	56	34	18	101	314
27	19	268	115	67	182	24	37	36	58	39	14	104	305
	20	268	116	68	181	24	37	37	59	39	14	104	306
	18	268	115	68	183	23	36	37	58	39	14	104	306
28	21	280	108	67	184	26	34	37	59	44	11	107	300
	21	279	109	68	184	25	34	38	59	43	11	107	299
	20	279	109	68	184	26	33	37	59	44	11	106	299
29	22	292	102	66	185	30	30	37	59	48	7	111	294
	22	292	103	67	184	29	31	37	60	50	8	111	294
	21	293	103	67	184	28	31	37	60	49	7	111	293
30	22	304	96	64	184	31	26	37	59	56	4	116	281
	22	305	95	64	186	31	27	36	59	56	4	115	282
	23	304	95	64	186	31	27	36	60	56	4	116	281
31	24	317	91	61	185	34	24	36	61	63	2	124	276
	24	316	91	61	184	34	24	37	60	63	3	124	276
	24	316	91	60	184	34	24	36	62	63	2	123	275
32	24	329	85	56	183	36	20	36	61	71	3	131	265
	25	329	84	56	184	37	20	36	61	71	3	131	266
	26	328	85	56	184	36	20	36	61	72	3	131	266
33	27	342	80	50	182	39	16	35	61	81	8	142	259
	26	341	81	50	181	40	16	34	62	82	7	140	260
	26	342	80	51	182	39	16	35	61	82	8	142	258
34	28	355	77	44	179	42	12	34	61	94	14	155	252
	28	354	77	44	179	42	12	34	62	93	13	154	252
	28	355	78	44	179	42	13	34	62	93	14	154	253
35	31	368	71	34	175	46	8	32	61	107	21	171	243
	30	367	72	35	174	46	8	33	61	107	21	171	243
	30	367	72	34	174	46	8	32	60	107	21	171	244
36	32	380	68	24	171	48	4	32	60	123	31	192	233
	32	380	68	24	170	48	3	31	60	123	30	192	235
	32	380	68	25	171	48	4	31	61	123	30	192	235
37	34	392	64	13	165	50	0	29	61	140	39	217	226
	34	392	65	13	164	50	0	29	60	140	39	217	224
	34	392	64	13	165	51	0	29	61	139	39	216	226
38	35	403	61	0	159	53	-4	27	59	159	51	249	216
	35	404	62	1	158	52	-4	28	61	159	52	249	216
	35	404	61	1	158	53	-4	27	60	160	51	249	216
39	38	412	58	5	151	55	-4	25	60	178	63	285	206
	37	413	58	6	152	54	-4	26	60	178	64	286	205
	38	412	58	5	151	54	-4	26	59	177	63	286	205
40	40	422	55	22	144	56	-1	23	61	199	75	327	195
	40	423	55	21	144	56	-2	24	60	198	75	326	195
	40	423	55	22	143	55	-1	23	61	199	76	327	195
41	40	429	53	36	135	56	2	21	60	215	86	366	186
	41	429	52	36	136	56	2	21	59	214	87	367	185
	42	429	53	35	135	57	2	21	59	215	87	367	185
42	44	435	50	51	126	57	4	19	59	229	98	404	175
	44	435	49	52	126	58	4	19	59	229	97	405	174
	43	436	49	52	126	57	4	19	59	229	98	404	174
43	46	439	47	67	117	56	6	17	56	237	106	428	163
	46	439	46	67	117	57	6	16	57	237	105	427	164
	46	440	47	67	117	57	6	16	57	238	106	427	164

Table D.1 (continued) Collected data for RUN067 (counts)

D.3 Effect of Initial Guess on Solution Trajectory

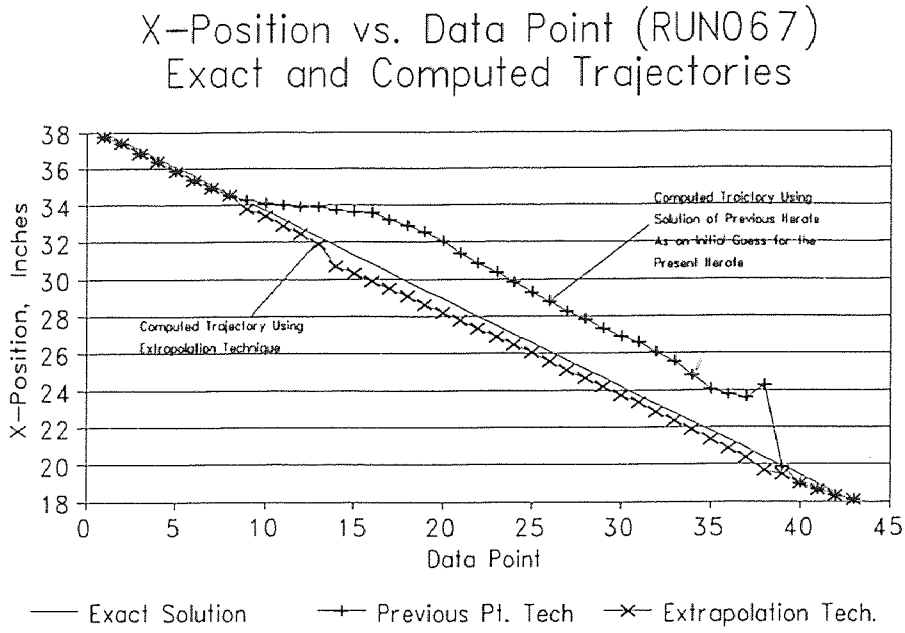

Figure D.3 X-Calculations using two techniques.

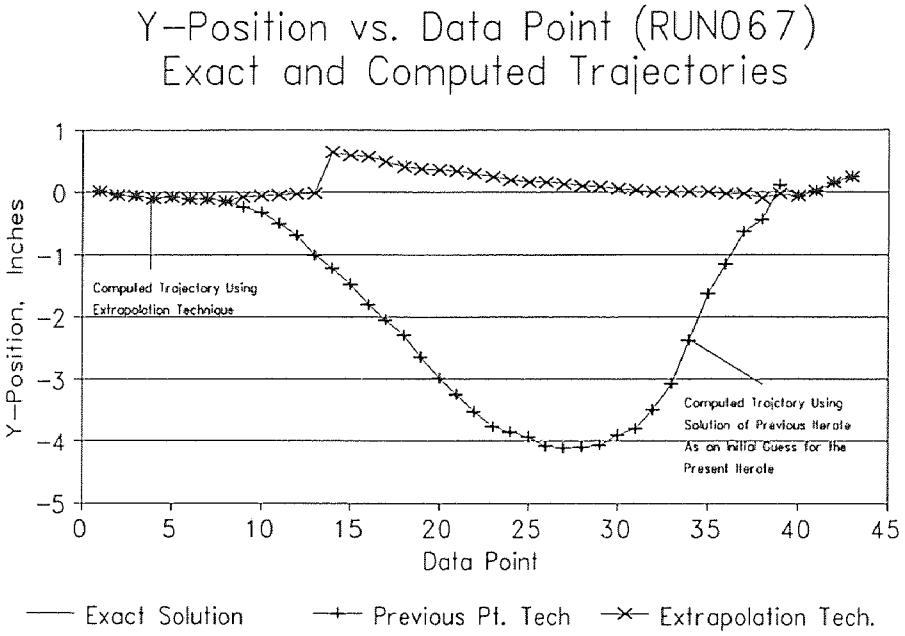

Figure D.4 Y-Calculations using two techniques.

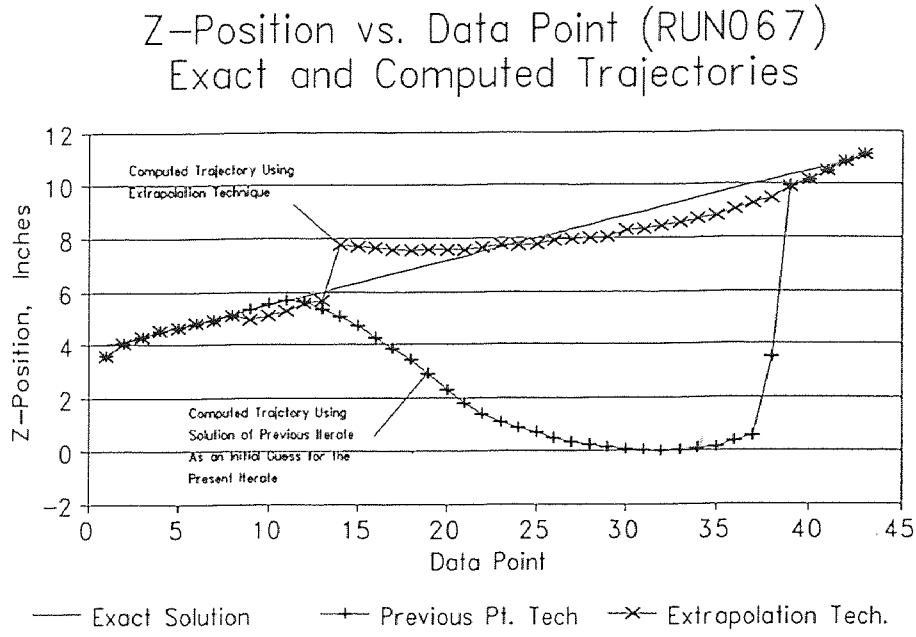

Figure D.5 Z-Calculations using two techniques.

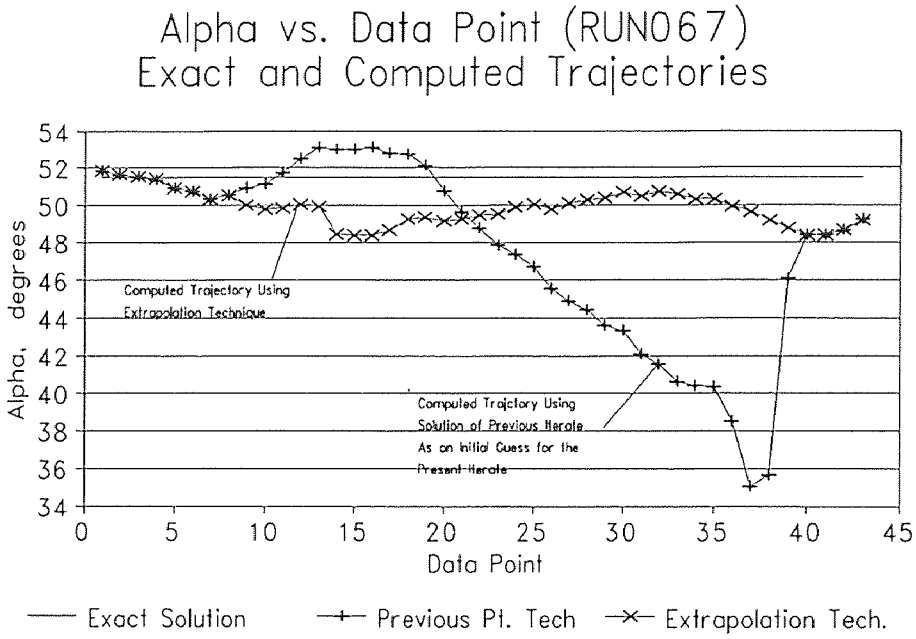

Figure D.6 Alpha-Calculations using two techniques.

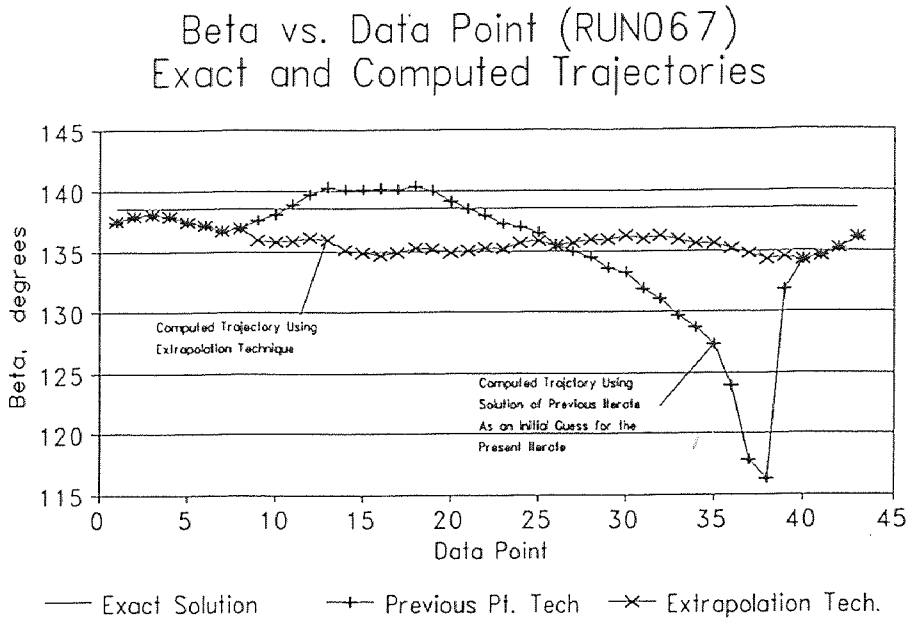

Figure D.7 Beta-Calculations using two techniques.

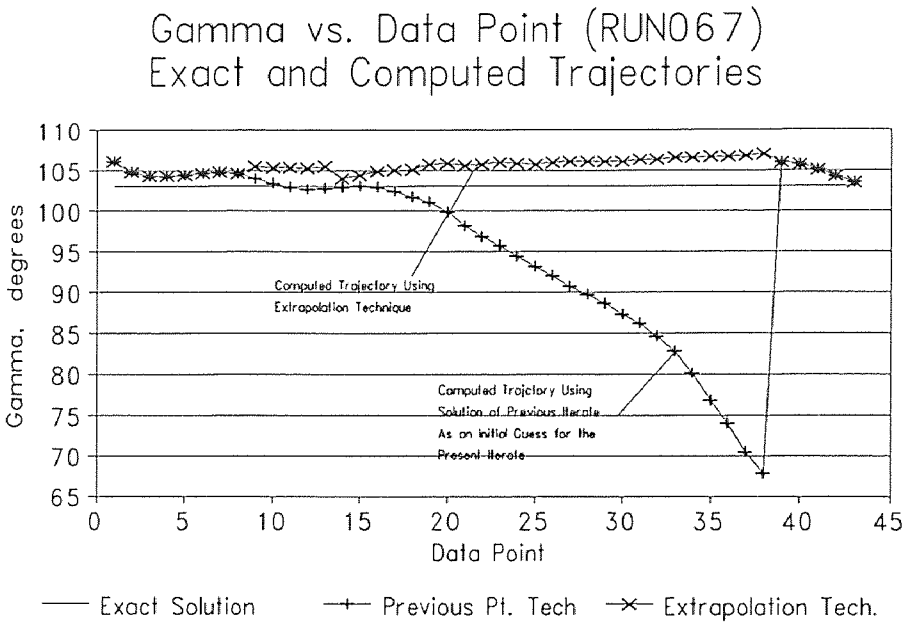

Figure D.8 Gamma-Calculations using two techniques.

D.4 Solution to RUN067 Using the Perturbation Technique

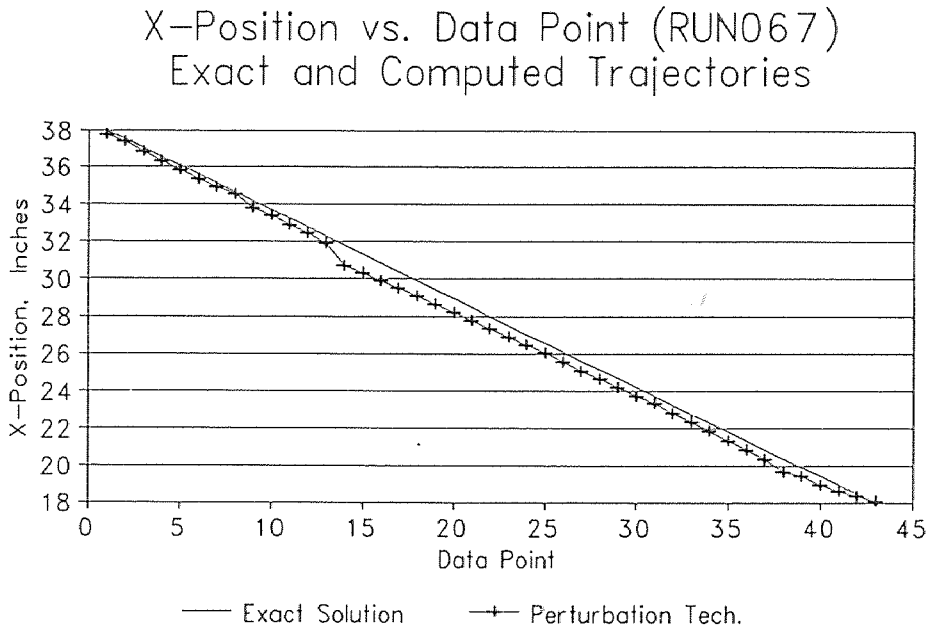

Figure D.9 X-Calculations using perturbation technique.

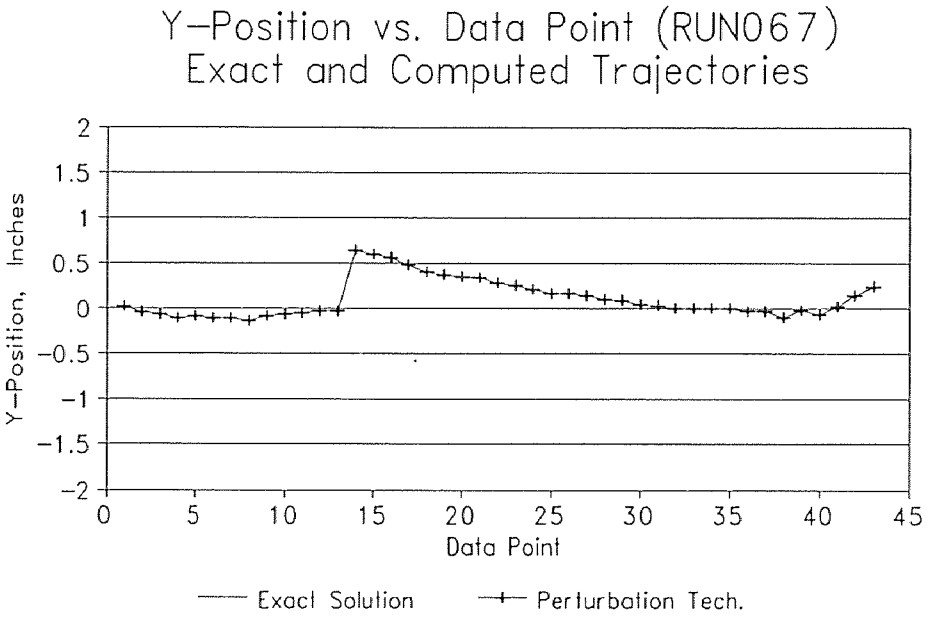

Figure D.10 Y-Calculations using perturbation technique.

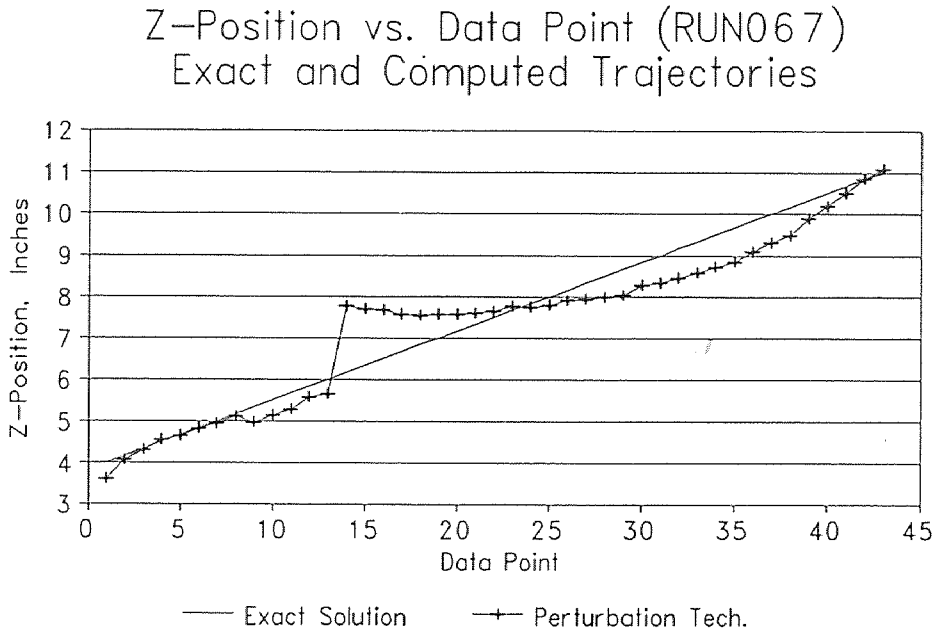

Figure D.11 Z-Calculations using perturbation technique.

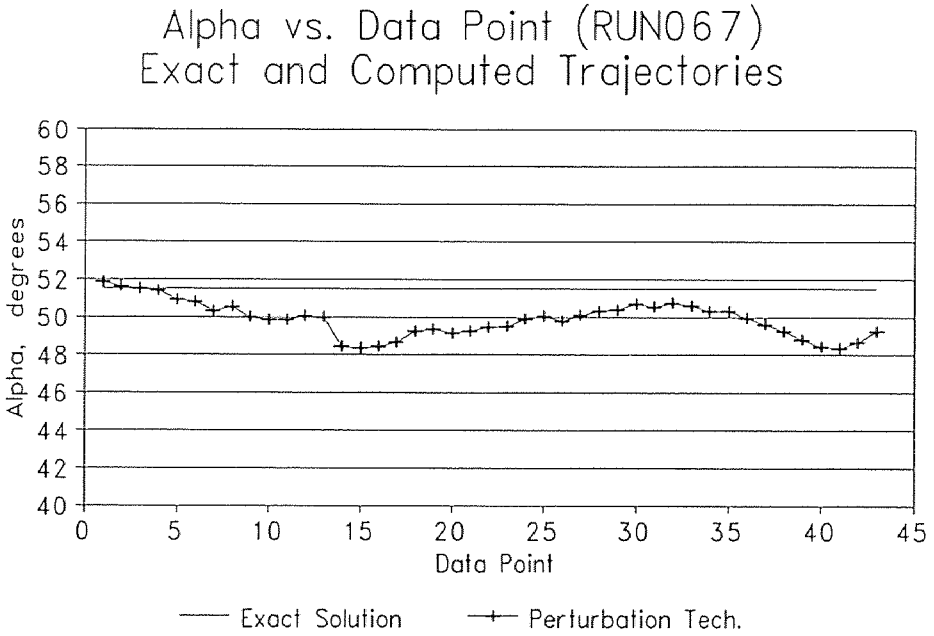

Figure D.12 Alpha-Calculations using perturbation technique.

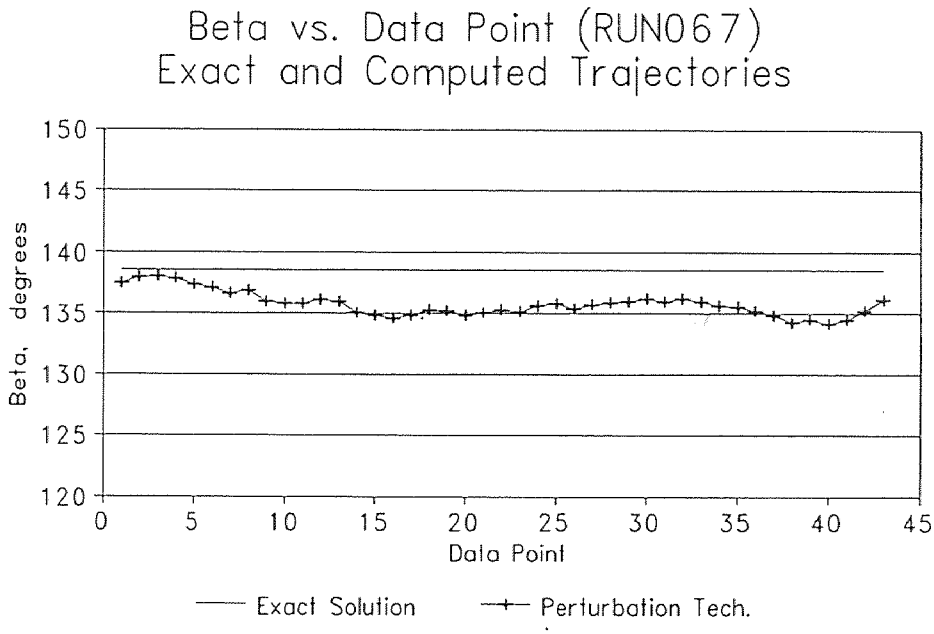

Figure D.13 Beta-Calculations using perturbation technique.

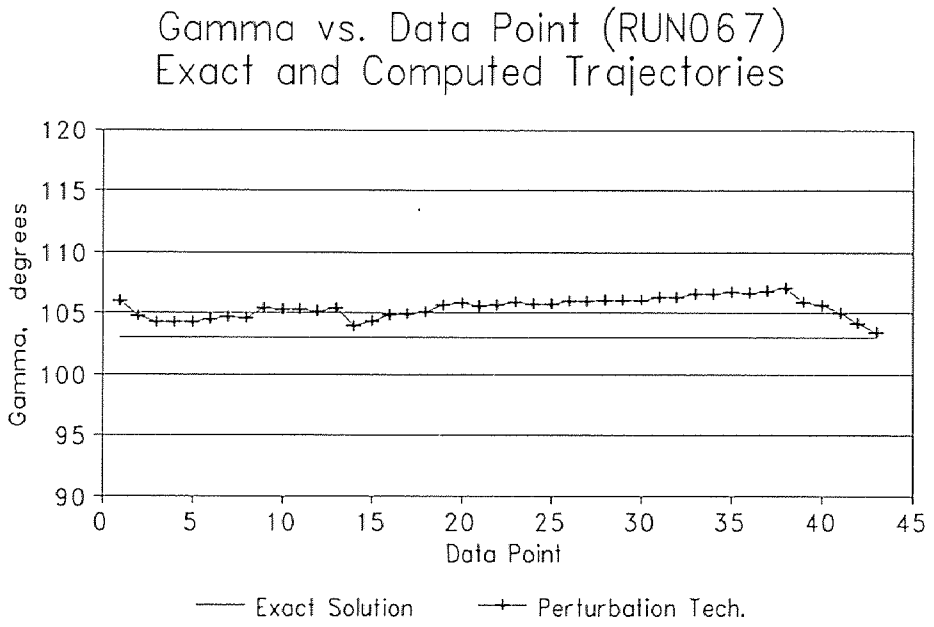

Figure D.14 Gamma-Calculations using perturbation technique.

D.5 RUN067 Solution Voltages

The data in Figures D.14 - D.26 are the voltage solutions for RUN067 using the perturbation technique. There are 13 graphs corresponding to the 13 antennae used in that sample. Each graph has 3 plots. The first plot, labeled "Expected Voltage" is the theoretical voltage that is induced in the receiving antenna given the position and orientation of the tracking sphere. The second plot, labeled " Measured Voltage" is the antenna signal strength as recorded by the data acquisition system. The third plot, labeled "Computed Voltage" is the resulting plots from the inverse solution. Refer to section 4.3.

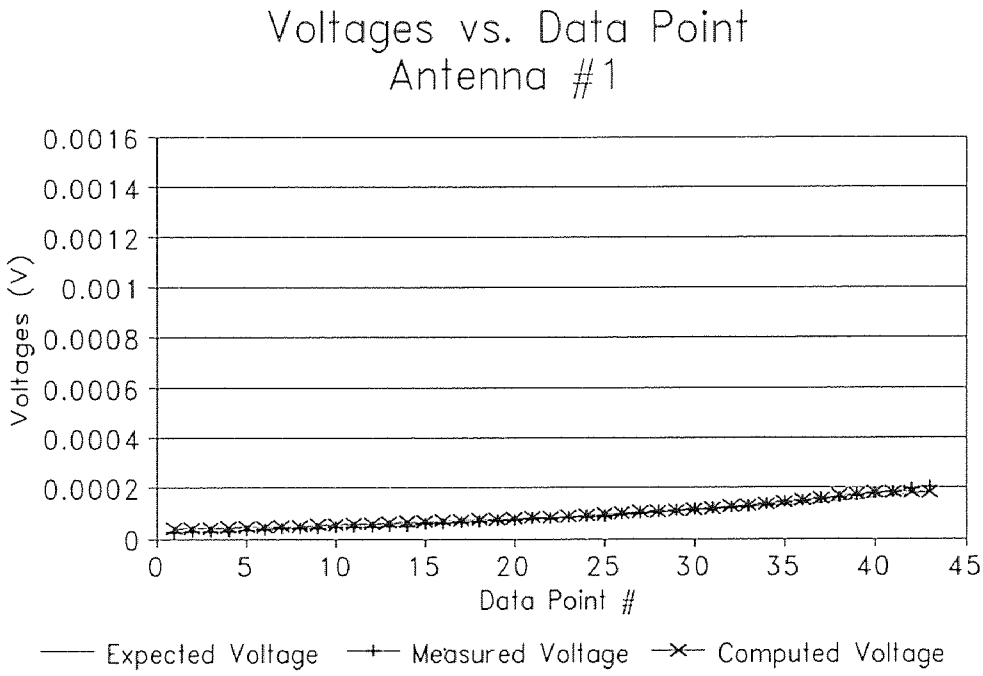

Figure D.15 Solution voltages for antenna #1

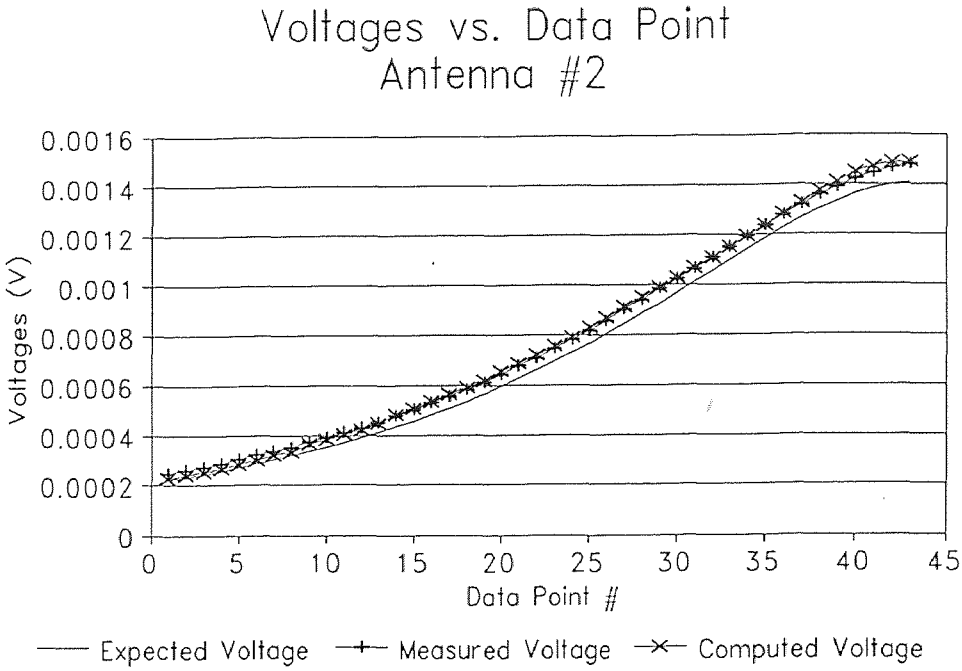

Figure D.16 Solution voltages for antenna #2

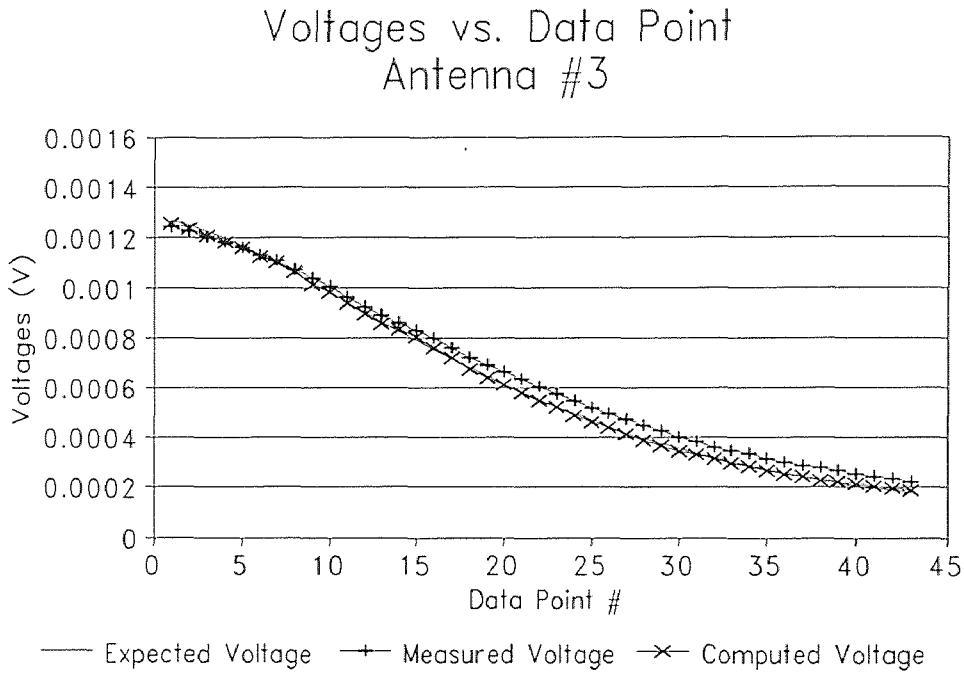

Figure D.17 Solutions voltages for antenna #3

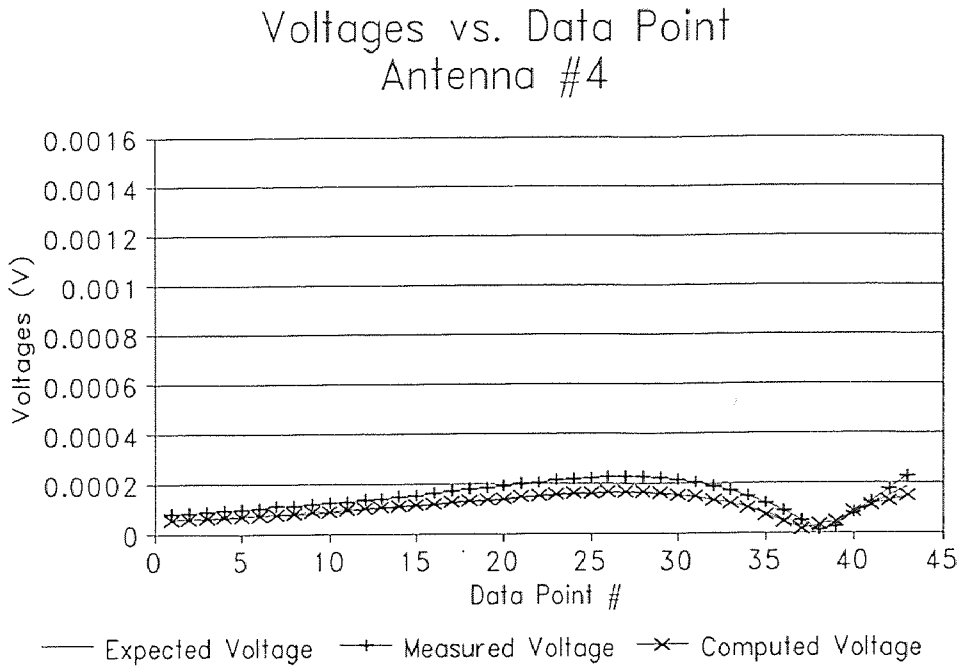

Figure D.18 Solution voltages for antenna #4

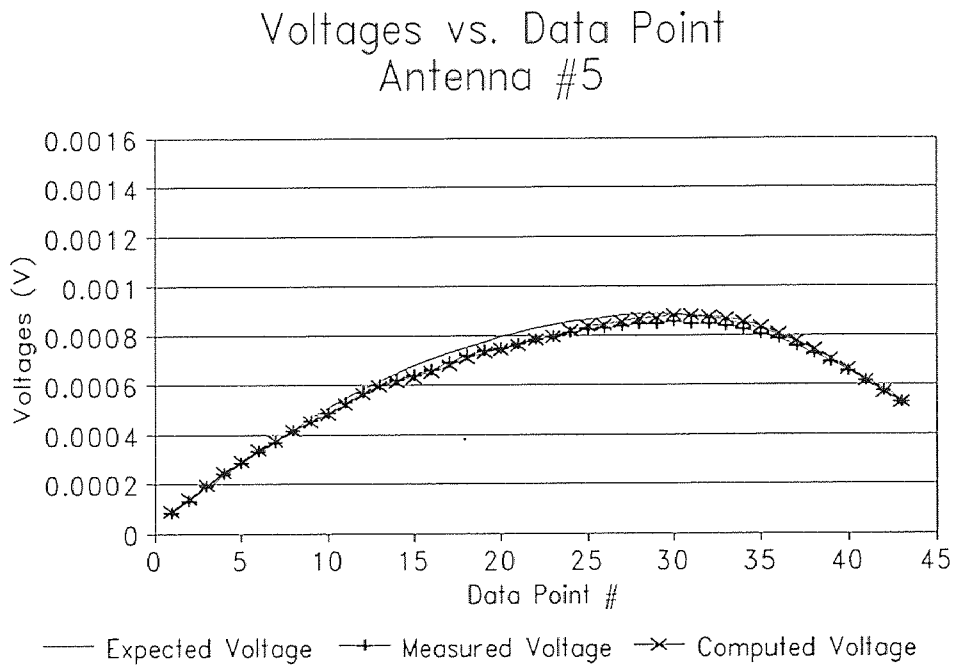

Figure D.19 Solution voltages for antenna #5

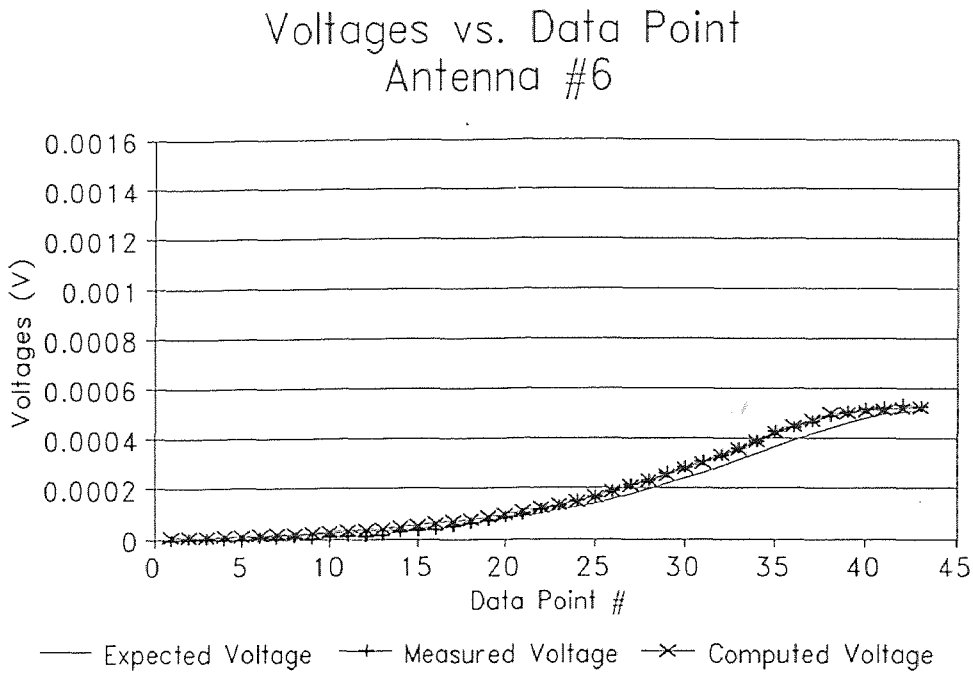

Figure D.20 Solution voltages for antenna #6

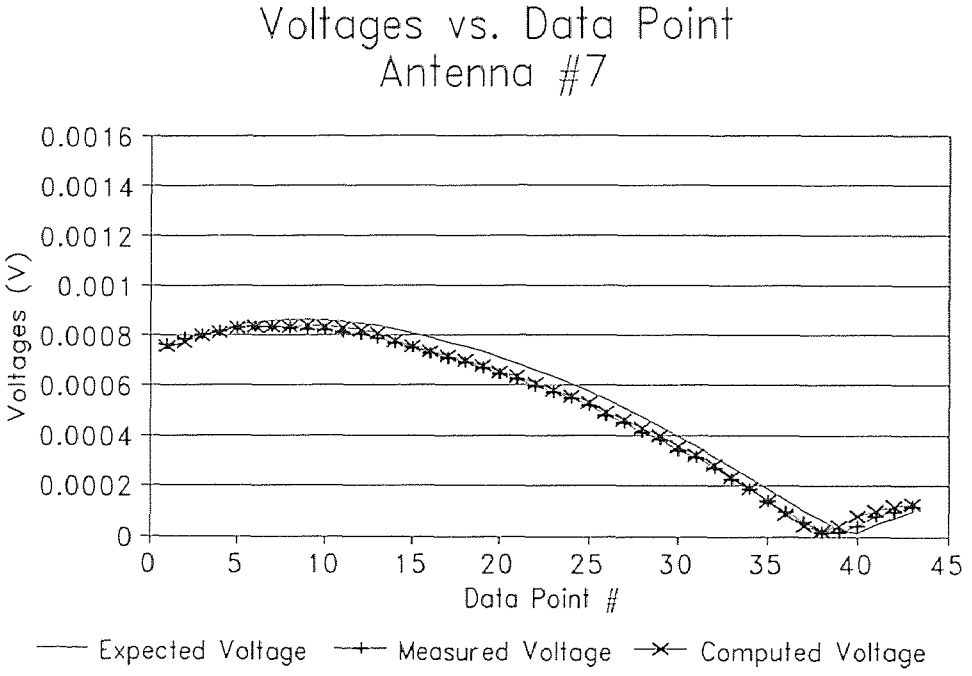

Figure D.21 Solution voltages for antenna #7

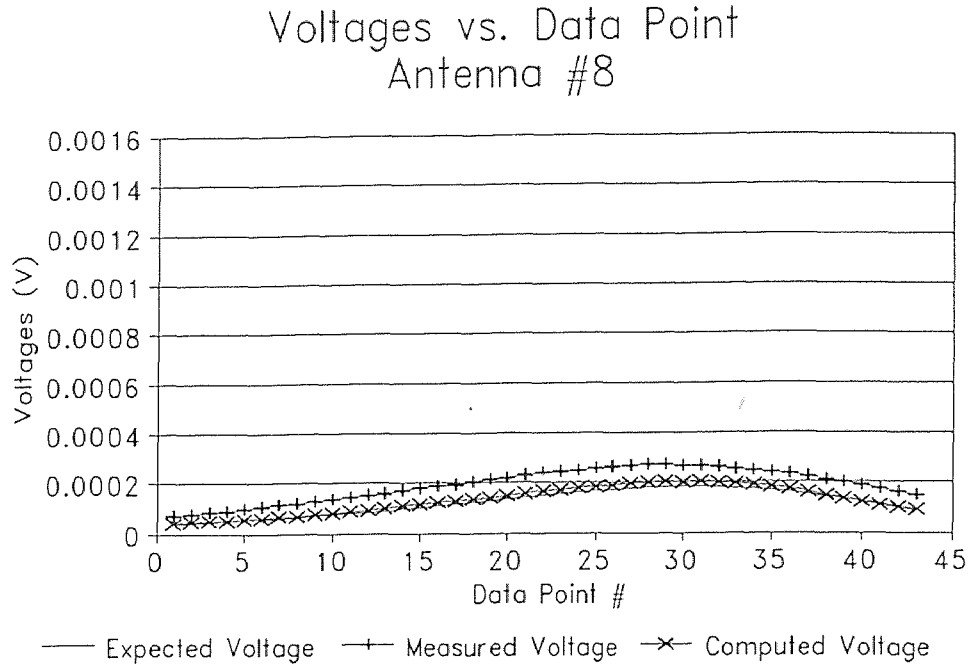

Figure D.22 Solution voltages for antenna #8

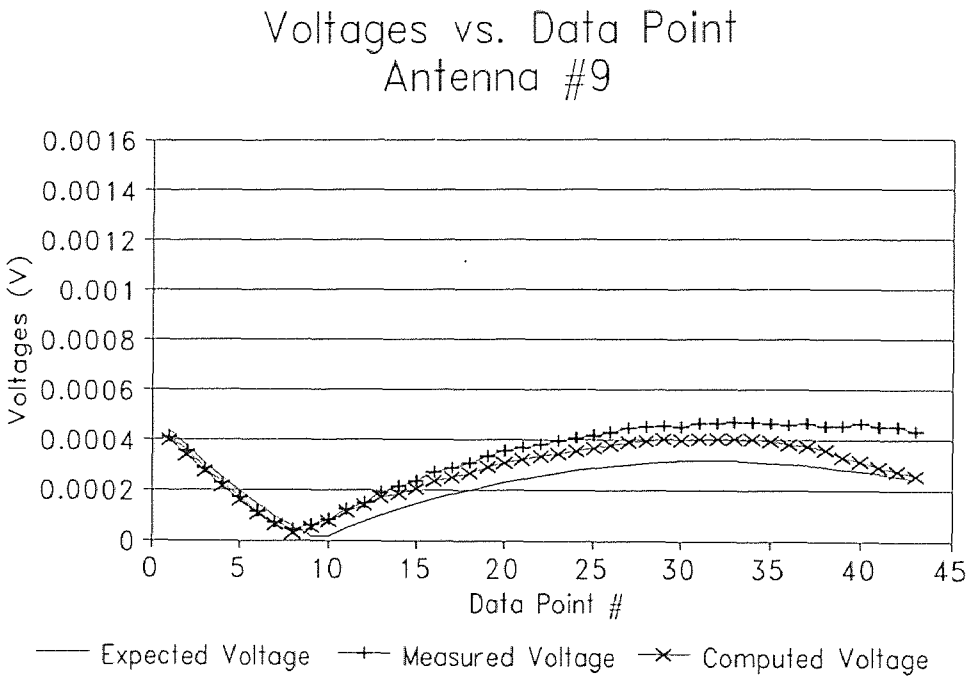

Figure D.23 Solution voltages for antenna #9

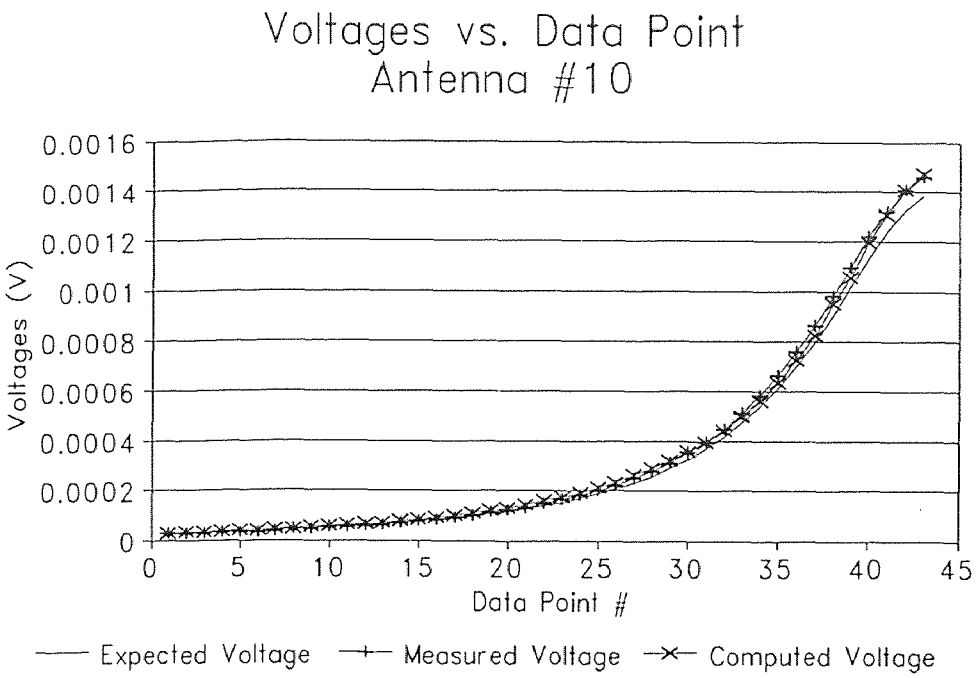

Figure D.24 Solution voltages for antenna #10

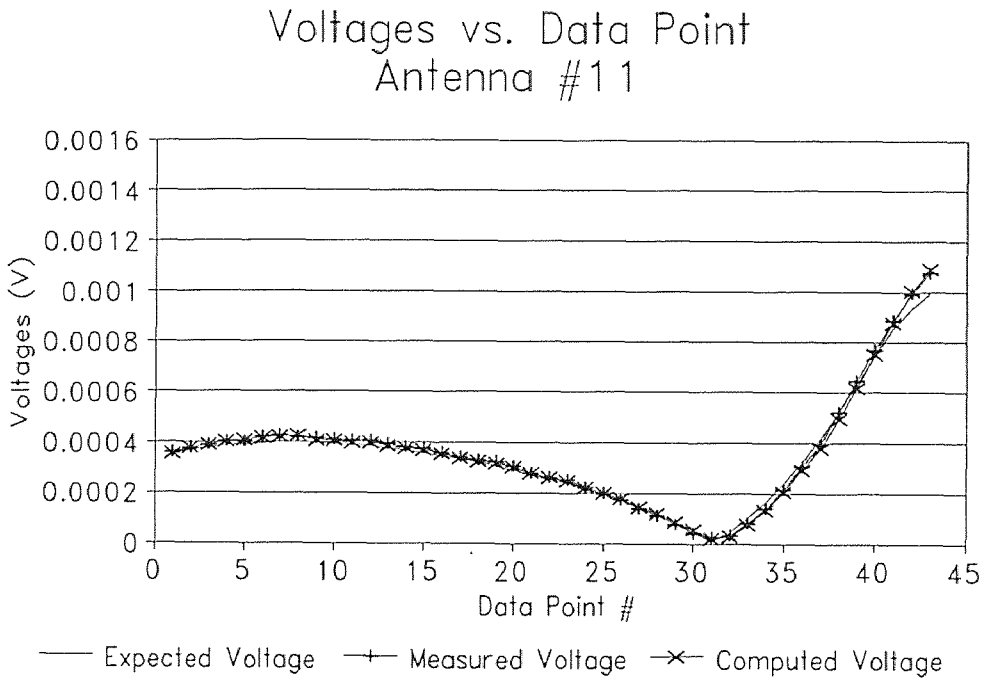

Figure D.25 Solution voltages for antenna #11

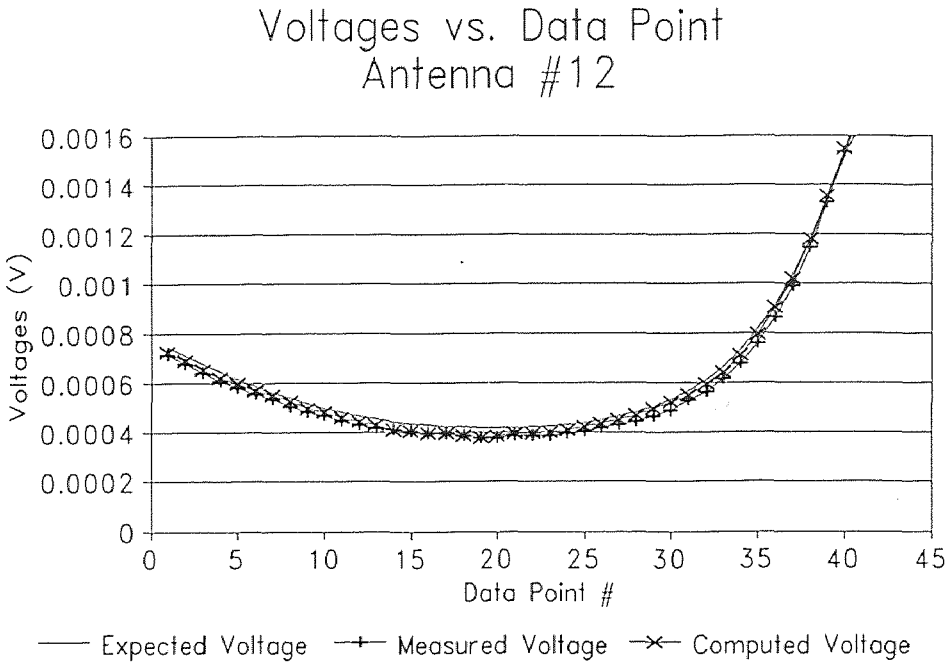

Figure D.26 Solution voltages for antenna #12

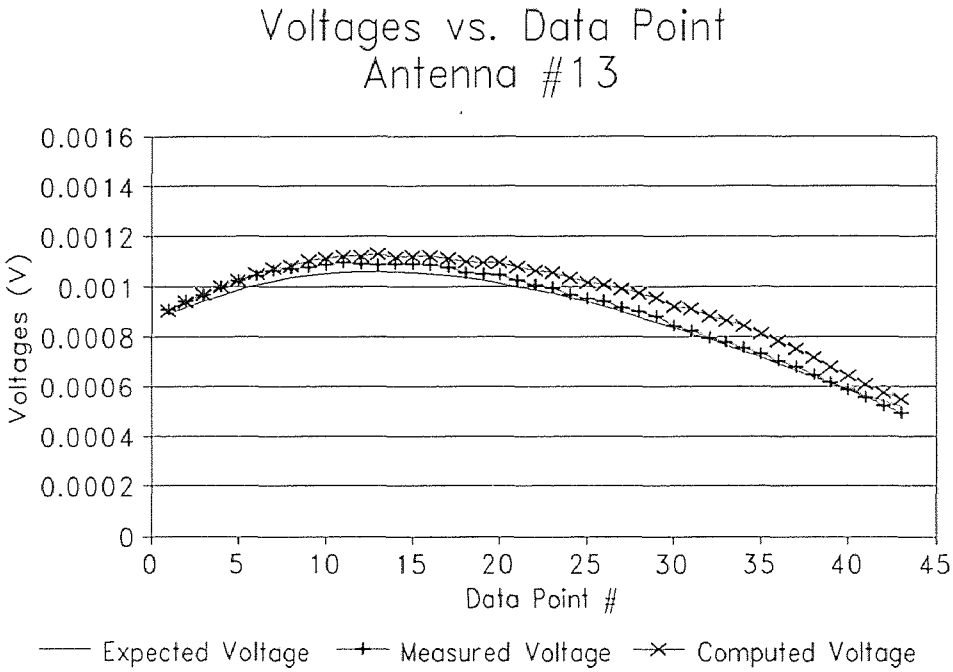

Figure D.27 Solution voltages for antenna #13

D.6 RUN067 Iterations Listing

Below is a complete listing of the iteration process that leads to the solution of RUN067. The perturbation technique is used. Refer to section 4.3.

Table D.2 Listing or Iterations and Perturbation for RUN067.

Data point # 1
==========

Perturbation 1
Initial Approximation: X = 38.000000 Y = 0.000000 Z = 4.000000 A = 51.500000 B = 138.500000 G = 103.122049
Initial residual: 0.000090
Converges to: X = 37.475848 Y = 0.040007 Z = 3.190097 A = 51.844294 B = 136.603410 G = 107.495125
Final Residual: 0.000039

Perturbation 2
Initial Approximation: X = 37.109071 Y = 1.444707 Z = 3.078077 A = 44.958586 B = 133.089761 G = 113.659891
Initial residual: 0.012852
Converges to: X = 37.481239 Y = 0.040757 Z = 3.200078 A = 51.847561 B = 136.622934 G = 107.464363
Final Residual: 0.000039

Perturbation 3
Initial Approximation: X = 39.373011 Y = 0.876455 Z = 2.432940 A = 60.421380 B = 138.969927 G = 95.917387
Initial residual: 0.017676
Converges to: X = 37.481204 Y = 0.040752 Z = 3.200015 A = 51.847533 B = 136.622811 G = 107.464526
Final Residual: 0.000039

Perturbation 4
Initial Approximation: X = 37.582902 Y = 1.461594 Z = 6.051216 A = 54.547552 B = 173.108729 G = 67.752055
Initial residual: 0.046547
Converges to: X = 38.317041 Y = 0.171232 Z = 7.409116 A = 51.574918 B = 140.822300 G = 83.482898
Final Residual: 0.000093

Perturbation 5
Initial Approximation: X = 38.243639 Y = 0.324112 Z = 2.991103 A = 81.907377 B = 129.744290 G = 83.137935
Initial residual: 0.055732
Converges to: X = 46.755265 Y = 2.745049 Z = 7.010665 A = -10.382015 B = 94.732984 G = 80.779125
Final Residual: 0.000608

Using perturbation #3
Initial Approximation: X = 39.373011 Y = 0.876455 Z = 2.432940 A = 60.421380 B = 138.969927 G = 95.917387
Initial residual: 0.017676
Converges to: X = 37.481204 Y = 0.040752 Z = 3.200015 A = 51.847533 B = 136.622811 G = 107.464526
Residual Vector = {0.000005 0.000015 0.000001 -0.000010 0.000002 -0.000007 -0.000015 0.000009 0.000003 -0.000026 0.000010 -0.000004 -0.000000 0.000000 0.000000 0.000000}
Final residual: 0.000039
Stopping Criterion: 1
Number of function evaluations = 36

Data point # 2
==========

Perturbation 1
Initial Approximation: X = 37.481204 Y = 0.040752 Z = 3.200015 A = 51.847533 B = 136.622811 G = 107.464526
Initial residual: 0.000105
Converges to: X = 37.165093 Y = -0.023633 Z = 3.684299 A = 51.565466 B = 137.129898 G = 106.051103
Final Residual: 0.000042

Perturbation 2
Initial Approximation: X = 39.198695 Y = 0.774030 Z = 2.602562 A = 45.042656 B = 158.913189 G = 120.518289
Initial residual: 0.062771
Converges to: X = 38.021220 Y = 0.775754 Z = 1.559449 A = 53.392852 B = 124.585079 G = 124.584519
Final Residual: 0.000076

Perturbation 3
Initial Approximation: X = 38.795424 Y = 1.049168 Z = 2.433927 A = 39.981745 B = 133.770419 G = 127.497941
Initial residual: 0.043629
Converges to: X = 38.028571 Y = 1.719538 Z = -0.517599 A = 55.275396 B = 113.217137 G = 136.171586
Final Residual: 0.000178

Perturbation 4
Initial Approximation: X = 36.579634 Y = 2.071584 Z = 2.800076 A = 58.474678 B = 118.053430 G = 129.543308
Initial residual: 0.010033
Converges to: X = 38.021129 Y = 0.775607 Z = 1.559577 A = 53.392387 B = 124.586510 G = 124.582608
Final Residual: 0.000076

Perturbation 5
Initial Approximation: X = 36.337045 Y = 0.510529 Z = 2.399798 A = 66.859020 B = 133.033944 G = 90.891531
Initial residual: 0.037968
Converges to: X = 37.165072 Y = -0.023636 Z = 3.684257 A = 51.565441 B = 137.129811 G = 106.051215
Final Residual: 0.000042

Using perturbation #5
Initial Approximation: X = 36.337045 Y = 0.510529 Z = 2.399798 A = 66.859020 B = 133.033944 G = 90.891531
Initial residual: 0.037968
Converges to: X = 37.165072 Y = -0.023636 Z = 3.684257 A = 51.565441 B = 137.129811 G = 106.051215
Residual Vector = {0.000005 0.000012 0.000002 -0.000015 0.000004 -0.000011 -0.000018 0.000010 0.000008 -0.000027 0.000004 -0.000004 -
0.000000 0.000000 0.000000 0.000000}
Final residual: 0.000042
Stopping Criterion: 1
Number of function evaluations = 43

Data point # 3
==========

Perturbation 1
Initial Approximation: X = 37.165072 Y = -0.023636 Z = 3.684257 A = 51.565441 B = 137.129811 G = 106.051215
Initial residual: 0.000119
Converges to: X = 36.668648 Y = -0.047103 Z = 3.997662 A = 51.358196 B = 137.356141 G = 105.227550
Final Residual: 0.000046

Perturbation 2
Initial Approximation: X = 36.806677 Y = 0.505444 Z = 2.295568 A = 63.717631 B = 106.859964 G = 90.826833
Initial residual: 0.071966
Converges to: X = -15.888624 Y = 105.991629 Z = -178.919390 A = 94.365455 B = 190.613072 G = 260.337615
Final Residual: 0.001956

Perturbation 3
Initial Approximation: X = 35.691521 Y = 0.936465 Z = 2.301715 A = 67.783250 B = 119.618120 G = 108.294507
Initial residual: 0.051431
Converges to: X = 34.368631 Y = 0.677076 Z = 1.573737 A = 44.606708 B = 128.707084 G = 108.633661
Final Residual: 0.000215

Perturbation 4
Initial Approximation: X = 39.121755 Y = 1.133139 Z = 3.453872 A = 77.365470 B = 142.235013 G = 138.838664
Initial residual: 0.023976
Converges to: X = 39.282400 Y = 8.592128 Z = 7.764423 A = 73.526276 B = 111.320100 G = 152.550212
Final Residual: 0.000415

Perturbation 5
Initial Approximation: X = 37.955142 Y = 0.517409 Z = 3.512415 A = 46.532542 B = 122.996688 G = 91.694727
Initial residual: 0.022941
Converges to: X = 39.964757 Y = 1.379384 Z = 5.318910 A = 50.103001 B = 134.815642 G = 107.661994
Final Residual: 0.000262

Using perturbation #1
Initial Approximation: X = 37.165072 Y = -0.023636 Z = 3.684257 A = 51.565441 B = 137.129811 G = 106.051215
Initial residual: 0.000119
Converges to: X = 36.668648 Y = -0.047103 Z = 3.997662 A = 51.358196 B = 137.356141 G = 105.227550
Residual Vector = {0.000003 0.000014 0.000002 -0.000014 0.000005 -0.000010 -0.000020 0.000011 0.000009 -0.000030 0.000006 -0.000003 -
0.000000 0.000000 0.000000 0.000000}
Final residual: 0.000046
Stopping Criterion: 1
Number of function evaluations = 29

Data point # 4
==========

Perturbation 1
Initial Approximation: X = 36.668648 Y = -0.047103 Z = 3.997662 A = 51.358196 B = 137.356141 G = 105.227550
Initial residual: 0.000109
Converges to: X = 36.218334 Y = -0.083403 Z = 4.277666 A = 51.167434 B = 137.310236 G = 104.948090
Final Residual: 0.000048

Perturbation 2
Initial Approximation: X = 36.112041 Y = 0.993055 Z = 3.576746 A = 55.094611 B = 160.524520 G = 137.590437
Initial residual: 0.076148
Converges to: X = 39.605505 Y = 8.247927 Z = 7.890088 A = 69.146446 B = 113.284559 G = 147.862498
Final Residual: 0.000489

Perturbation 3
Initial Approximation: X = 38.348674 Y = 0.829820 Z = 5.214604 A = 23.475013 B = 169.670529 G = 121.921922
Initial residual: 0.108881
Converges to: X = 34.230655 Y = 0.448672 Z = 2.338166 A = 45.837193 B = 130.150518 G = 108.361745
Final Residual: 0.000189

Perturbation 4
Initial Approximation: X = 35.180790 Y = 1.664432 Z = 2.277345 A = 61.310028 B = 118.708567 G = 96.279915
Initial residual: 0.052686
Converges to: X = 36.218334 Y = -0.083403 Z = 4.277666 A = 51.167434 B = 137.310237 G = 104.948088
Final Residual: 0.000048

Perturbation 5
Initial Approximation: X = 35.101503 Y = 1.056265 Z = 2.748259 A = 45.592518 B = 108.182613 G = 68.372031
Initial residual: 0.027760
Converges to: X = 38.468645 Y = 0.892052 Z = 9.640783 A = 50.267577 B = 133.288734 G = 69.575413
Final Residual: 0.000384

Using perturbation #1
Initial Approximation: X = 36.668648 Y = -0.047103 Z = 3.997662 A = 51.358196 B = 137.356141 G = 105.227550
Initial residual: 0.000109
Converges to: X = 36.218334 Y = -0.083403 Z = 4.277666 A = 51.167434 B = 137.310236 G = 104.948090
Residual Vector = {-0.000002 0.000015 0.000001 -0.000015 0.000005 -0.000011 -0.000021 0.000007 0.000013 -0.000032 0.000000 -0.000000 -0.000000 0.000000 0.000000 0.000000 0.000000}
Final residual: 0.000048
Stopping Criterion: 1
Number of function evaluations = 29

Data point # 5
==========

Perturbation 1
Initial Approximation: X = 36.218334 Y = -0.083403 Z = 4.277666 A = 51.167434 B = 137.310236 G = 104.948090
Initial residual: 0.000098
Converges to: X = 35.716702 Y = -0.061861 Z = 4.420974 A = 50.674170 B = 136.917108 G = 104.765087
Final Residual: 0.000049

Perturbation 2
Initial Approximation: X = 34.377769 Y = 0.581834 Z = 3.620795 A = 66.708602 B = 139.662095 G = 119.483150
Initial residual: 0.002193
Converges to: X = 39.566994 Y = 5.707361 Z = 8.275620 A = 68.362145 B = 126.156165 G = 135.930994
Final Residual: 0.000591

Perturbation 3
Initial Approximation: X = 37.750739 Y = 1.049137 Z = 4.233376 A = 62.109720 B = 132.812433 G = 119.782143
Initial residual: 0.007279
Converges to: X = 34.244575 Y = 0.347327 Z = 2.998091 A = 47.023262 B = 131.550423 G = 107.985781
Final Residual: 0.000150

Perturbation 4
Initial Approximation: X = 35.130177 Y = 0.803318 Z = 3.867005 A = 23.872344 B = 135.802979 G = 91.992564
Initial residual: 0.035157
Converges to: X = 34.245164 Y = 0.347081 Z = 2.997889 A = 47.029416 B = 131.555577 G = 107.987582
Final Residual: 0.000150

Perturbation 5
Initial Approximation: X = 37.252708 Y = 1.590135 Z = 2.865276 A = 64.236404 B = 137.617269 G = 128.575294
Initial residual: 0.012356
Converges to: X = 34.555634 Y = 0.241205 Z = 2.959989 A = 48.544718 B = 132.495417 G = 109.028817
Final Residual: 0.000182

Using perturbation #1
Initial Approximation: X = 36.218334 Y = -0.083403 Z = 4.277666 A = 51.167434 B = 137.310236 G = 104.948090
Initial residual: 0.000098
Converges to: X = 35.716702 Y = -0.061861 Z = 4.420974 A = 50.674170 B = 136.917108 G = 104.765087
Residual Vector = {-0.000004 0.000014 -0.000000 -0.000012 0.000009 -0.000011 -0.000026 0.000011 0.000014 -0.000030 0.000000 -0.000001 -0.000000 0.000000 0.000000 0.000000 0.000000}
Final residual: 0.000049
Stopping Criterion: 2
Number of function evaluations = 29

Data point # 6
==========

Perturbation 1
Initial Approximation: X = 35.716702 Y = -0.061861 Z = 4.420974 A = 50.674170 B = 136.917108 G = 104.765087
Initial residual: 0.000105
Converges to: X = 35.268141 Y = -0.082089 Z = 4.630406 A = 50.590972 B = 136.772620 G = 104.891581
Final Residual: 0.000052

Perturbation 2
Initial Approximation: X = 36.278215 Y = 1.689662 Z = 4.548290 A = 64.984458 B = 108.036329 G = 93.094944
Initial residual: 0.072245
Converges to: X = 36.246556 Y = -4.551166 Z = -6.548164 A = 91.964217 B = 164.911924 G = 104.969124
Final Residual: 0.001280

Perturbation 3
Initial Approximation: X = 35.107924 Y = 0.895694 Z = 4.703185 A = 62.865523 B = 113.066946 G = 109.630008
Initial residual: 0.052565
Converges to: X = 34.279091 Y = 0.180200 Z = 3.687986 A = 48.333283 B = 133.191956 G = 107.415701
Final Residual: 0.000115

Perturbation 4
Initial Approximation: X = 35.447468 Y = 0.682262 Z = 3.786572 A = 69.978660 B = 147.677143 G = 134.377267
Initial residual: 0.032058
Converges to: X = 39.939809 Y = 6.676893 Z = 8.922292 A = 67.240708 B = 125.249923 G = 135.999159
Final Residual: 0.000586

Perturbation 5
Initial Approximation: X = 35.305672 Y = 0.706197 Z = 4.890851 A = 13.177537 B = 160.534447 G = 89.719531
Initial residual: 0.083709
Converges to: X = 22.236821 Y = 0.056122 Z = 4.143176 A = 101.219680 B = 135.907379 G = 132.035667
Final Residual: 0.001373

Using perturbation #1
Initial Approximation: X = 35.716702 Y = -0.061861 Z = 4.420974 A = 50.674170 B = 136.917108 G = 104.765087
Initial residual: 0.000105
Converges to: X = 35.268141 Y = -0.082089 Z = 4.630406 A = 50.590972 B = 136.772620 G = 104.891581
Residual Vector = {-0.000006 0.000012 0.000000 -0.000014 0.000000 -0.000007 -0.000026 0.000014 0.000012 -0.000034 0.000009 0.000006 0.000000
0.000000 0.000000 0.000000}
Final residual: 0.000052
Stopping Criterion: 2
Number of function evaluations = 29

Data point # 7
==========

Perturbation 1
Initial Approximation: X = 35.268141 Y = -0.082089 Z = 4.630406 A = 50.590972 B = 136.772620 G = 104.891581
Initial residual: 0.000088
Converges to: X = 34.847595 Y = -0.083500 Z = 4.777967 A = 50.177102 B = 136.353388 G = 104.915771
Final Residual: 0.000056

Perturbation 2
Initial Approximation: X = 36.346384 Y = -0.120804 Z = 5.035561 A = 80.008988 B = 109.232567 G = 100.682378
Initial residual: 0.082714
Converges to: X = 44.660734 Y = -9.746835 Z = -3.112202 A = 77.596824 B = 145.612461 G = 121.497069
Final Residual: 0.001158

Perturbation 3
Initial Approximation: X = 34.019133 Y = 1.276694 Z = 6.125735 A = 58.393278 B = 117.038651 G = 107.007720
Initial residual: 0.043314
Converges to: X = 34.847595 Y = -0.083501 Z = 4.777964 A = 50.177105 B = 136.353387 G = 104.915779
Final Residual: 0.000056

Perturbation 4
Initial Approximation: X = 35.182704 Y = 0.101768 Z = 3.500607 A = 59.800031 B = 128.442824 G = 68.191059
Initial residual: 0.022292
Converges to: X = 37.392609 Y = 1.680255 Z = 13.041259 A = 57.904161 B = 129.160515 G = 55.602531
Final Residual: 0.000388

Perturbation 5
Initial Approximation: X = 33.866138 Y = 1.263452 Z = 6.161522 A = 26.375812 B = 169.408032 G = 91.767947
Initial residual: 0.076985
Converges to: X = 34.234309 Y = 0.084939 Z = 4.209655 A = 48.851425 B = 134.149660 G = 106.625043
Final Residual: 0.000087

Using perturbation #1
Initial Approximation: X = 35.268141 Y = -0.082089 Z = 4.630406 A = 50.590972 B = 136.772620 G = 104.891581
Initial residual: 0.000088
Converges to: X = 34.847595 Y = -0.083500 Z = 4.777967 A = 50.177102 B = 136.353388 G = 104.915771
Residual Vector = {-0.000010 0.000010 -0.000001 -0.000011 0.000001 -0.000005 -0.000029 0.000013 0.000012 -0.000036 0.000015 0.000008
0.000000 0.000000 0.000000 0.000000}
Final residual: 0.000056
Stopping Criterion: 2
Number of function evaluations = 29

Data point # 8
==========

Perturbation 1
Initial Approximation: X = 34.847595 Y = -0.083500 Z = 4.777967 A = 50.177102 B = 136.353388 G = 104.915771
Initial residual: 0.000098
Converges to: X = 34.473929 Y = -0.122405 Z = 4.982405 A = 50.444470 B = 136.677171 G = 104.793598
Final Residual: 0.000063

Perturbation 2
Initial Approximation: X = 35.950343 Y = 0.713743 Z = 3.648734 A = 37.636297 B = 124.914348 G = 79.546635
Initial residual: 0.001918
Converges to: X = 35.205755 Y = 0.482034 Z = 10.359570 A = 39.416397 B = 127.411761 G = 79.377653
Final Residual: 0.000695

Perturbation 3
Initial Approximation: X = 33.396374 Y = 1.123805 Z = 6.008480 A = 30.650881 B = 119.622154 G = 87.721093
Initial residual: 0.001609
Converges to: X = 33.066984 Y = 0.820215 Z = 8.964241 A = 46.935913 B = 135.951425 G = 97.526769
Final Residual: 0.000071

Perturbation 4
Initial Approximation: X = 35.162200 Y = 0.746282 Z = 4.230430 A = 87.904238 B = 117.625055 G = 93.312036
Initial residual: 0.078049
Converges to: X = 158.581119 Y = -17.557882 Z = 176.557303 A = 87.072453 B = 154.122405 G = 115.698796
Final Residual: 0.001941

Perturbation 5
Initial Approximation: X = 34.432221 Y = 1.368940 Z = 3.793115 A = 82.574201 B = 162.906552 G = 86.592209
Initial residual: 0.006775
Converges to: X = 34.312583 Y = 6.875066 Z = -0.542321 A = 88.243714 B = 168.519299 G = 78.586101
Final Residual: 0.000609

Using perturbation #1
Initial Approximation: X = 34.847595 Y = -0.083500 Z = 4.777967 A = 50.177102 B = 136.353388 G = 104.915771
Initial residual: 0.000098
Converges to: X = 34.473929 Y = -0.122405 Z = 4.982405 A = 50.444470 B = 136.677171 G = 104.793598
Residual Vector = {-0.000012 0.000011 -0.000001 -0.000017 0.000007 -0.000013 -0.000032 0.000007 0.000022 -0.000036 0.000014 0.000007 0.000000 0.000000 0.000000 0.000000}
Final residual: 0.000063
Stopping Criterion: 2
Number of function evaluations = 29

Data point # 9
==========

Perturbation 1
Initial Approximation: X = 34.473929 Y = -0.122405 Z = 4.982405 A = 50.444470 B = 136.677171 G = 104.793598
Initial residual: 0.000101
Converges to: X = 34.250097 Y = -0.212657 Z = 5.267357 A = 50.864261 B = 137.430168 G = 104.090935
Final Residual: 0.000082

Perturbation 2
Initial Approximation: X = 32.876044 Y = 1.471851 Z = 6.266812 A = 50.478408 B = 145.140038 G = 78.090278
Initial residual: 0.012125
Converges to: X = 36.847627 Y = -1.185873 Z = 13.670440 A = 47.687282 B = 126.737551 G = 63.891135
Final Residual: 0.000817

Perturbation 3
Initial Approximation: X = 34.049052 Y = 0.720811 Z = 4.197022 A = 55.503173 B = 152.037411 G = 114.756792
Initial residual: 0.027632
Converges to: X = 33.764518 Y = -0.069647 Z = 4.861186 A = 49.945599 B = 135.810953 G = 105.535633
Final Residual: 0.000069

Perturbation 4
Initial Approximation: X = 34.143097 Y = 1.104905 Z = 4.856800 A = 44.710517 B = 125.113518 G = 86.398462
Initial residual: 0.016035
Converges to: X = 34.250097 Y = -0.212657 Z = 5.267357 A = 50.864261 B = 137.430168 G = 104.090934
Final Residual: 0.000082

Perturbation 5
Initial Approximation: X = 34.038628 Y = 1.524103 Z = 4.953365 A = 18.555141 B = 169.819584 G = 107.082671
Initial residual: 0.095385
Converges to: X = 35.586282 Y = -0.775379 Z = 3.774010 A = 57.183435 B = 137.835406 G = 113.487862
Final Residual: 0.000341

Using perturbation #3
Initial Approximation: X = 34.049052 Y = 0.720811 Z = 4.197022 A = 55.503173 B = 152.037411 G = 114.756792
Initial residual: 0.027632
Converges to: X = 33.764518 Y = -0.069647 Z = 4.861186 A = 49.945599 B = 135.810953 G = 105.535633
Residual Vector = {-0.000028 0.000015 -0.000011 -0.000005 -0.000004 -0.000011 -0.000028 0.000014 0.000009 -0.000036 0.000022 0.000022 -0.000000 0.000000 0.000000 0.000000}
Final residual: 0.000069
Stopping Criterion: 1
Number of function evaluations = 36

Data point # 10
==========

Perturbation 1
Initial Approximation: X = 33.764518 Y = -0.069647 Z = 4.861186 A = 49.945599 B = 135.810953 G = 105.535633
Initial residual: 0.000089
Converges to: X = 33.389392 Y = -0.063440 Z = 5.014358 A = 49.808383 B = 135.723972 G = 105.441828
Final Residual: 0.000069

Perturbation 2
Initial Approximation: X = 33.142973 Y = 1.173207 Z = 4.153550 A = 60.337983 B = 162.343184 G = 116.642004
Initial residual: 0.035408
Converges to: X = 33.389368 Y = -0.063423 Z = 5.014428 A = 49.808339 B = 135.723976 G = 105.441732
Final Residual: 0.000069

Perturbation 3
Initial Approximation: X = 31.572614 Y = 1.356979 Z = 5.927553 A = 51.317481 B = 132.668645 G = 106.199869
Initial residual: 0.007224
Converges to: X = 33.389322 Y = -0.063392 Z = 5.014598 A = 49.808262 B = 135.724007 G = 105.441516
Final Residual: 0.000069

Perturbation 4
Initial Approximation: X = 34.814270 Y = 1.100721 Z = 4.620032 A = 18.785499 B = 157.446089 G = 89.424726
Initial residual: 0.074940
Converges to: X = 33.389554 Y = -0.063551 Z = 5.013787 A = 49.808665 B = 135.723884 G = 105.442568
Final Residual: 0.000069

Perturbation 5
Initial Approximation: X = 34.221089 Y = 0.080454 Z = 3.247552 A = 78.263701 B = 118.375962 G = 131.084489
Initial residual: 0.030115
Converges to: X = 36.197710 Y = 1.678933 Z = 7.323136 A = 69.067644 B = 143.137388 G = 118.810357
Final Residual: 0.000595

Using perturbation #1
Initial Approximation: X = 33.764518 Y = -0.069647 Z = 4.861186 A = 49.945599 B = 135.810953 G = 105.535633
Initial residual: 0.000089
Converges to: X = 33.389392 Y = -0.063440 Z = 5.014358 A = 49.808383 B = 135.723972 G = 105.441828
Residual Vector = {-0.000028 0.000013 -0.000010 -0.000005 -0.000004 -0.000010 -0.000030 0.000011 0.000010 -0.000038 0.000019 0.000023 -
0.000000 0.000000 0.000000 0.000000}
Final residual: 0.000069
Stopping Criterion: 1
Number of function evaluations = 29

Data point # 11
==========

Perturbation 1
Initial Approximation: X = 33.389392 Y = -0.063440 Z = 5.014358 A = 49.808383 B = 135.723972 G = 105.441828
Initial residual: 0.000108
Converges to: X = 32.897622 Y = -0.057870 Z = 5.170986 A = 49.911396 B = 135.796474 G = 105.498324
Final Residual: 0.000074

Perturbation 2
Initial Approximation: X = 33.096633 Y = 1.078201 Z = 5.734166 A = 65.627404 B = 160.494297 G = 107.267054
Initial residual: 0.014708
Converges to: X = 32.897638 Y = -0.057881 Z = 5.170940 A = 49.911423 B = 135.796474 G = 105.498378
Final Residual: 0.000074

Perturbation 3
Initial Approximation: X = 34.199294 Y = 1.273159 Z = 3.516282 A = 61.877890 B = 150.488093 G = 127.321154
Initial residual: 0.034720
Converges to: X = 35.270521 Y = 1.135324 Z = 6.781768 A = 67.693807 B = 142.455291 G = 118.472637
Final Residual: 0.000580

Perturbation 4
Initial Approximation: X = 31.685994 Y = 1.119820 Z = 3.864925 A = 50.628917 B = 145.849911 G = 102.521737
Initial residual: 0.013432
Converges to: X = 32.897673 Y = -0.057905 Z = 5.170842 A = 49.911484 B = 135.796476 G = 105.498492
Final Residual: 0.000074

Perturbation 5
Initial Approximation: X = 34.491246 Y = 1.037145 Z = 2.650819 A = 74.149924 B = 126.246185 G = 80.021378
Initial residual: 0.054595
Converges to: X = 32.897621 Y = -0.057869 Z = 5.170990 A = 49.911393 B = 135.796474 G = 105.498319
Final Residual: 0.000074

Using perturbation #4
Initial Approximation: X = 31.685994 Y = 1.119820 Z = 3.864925 A = 50.628917 B = 145.849911 G = 102.521737
Initial residual: 0.013432
Converges to: X = 32.897673 Y = -0.057905 Z = 5.170842 A = 49.911484 B = 135.796476 G = 105.498492
Residual Vector = {-0.000030 0.000011 -0.000009 -0.000008 -0.000003 -0.000011 -0.000032 0.000014 0.000012 -0.000038 0.000022 0.000026
0.000000 0.000000 0.000000 0.000000}
Final residual: 0.000074
Stopping Criterion: 1
Number of function evaluations = 43

Data point # 12
==========

Perturbation 1
Initial Approximation: X = 32.897673 Y = -0.057905 Z = 5.170842 A = 49.911484 B = 135.796476 G = 105.498492
Initial residual: 0.000107
Converges to: X = 32.469367 Y = -0.069411 Z = 5.414956 A = 50.201237 B = 136.139506 G = 105.386285
Final Residual: 0.000082

Perturbation 2
Initial Approximation: X = 31.698357 Y = 1.080274 Z = 5.581645 A = 15.689997 B = 121.666148 G = 88.394615
Initial residual: 0.020348
Converges to: X = 42.552403 Y = -12.171663 Z = 8.148381 A = 37.278929 B = 122.033777 G = 72.993095
Final Residual: 0.000814

Perturbation 3
Initial Approximation: X = 34.473717 Y = 0.713008 Z = 3.795671 A = 60.729919 B = 163.184588 G = 106.559836
Initial residual: 0.023665
Converges to: X = 32.469598 Y = -0.069574 Z = 5.414357 A = 50.201632 B = 136.139576 G = 105.386913
Final Residual: 0.000082

Perturbation 4
Initial Approximation: X = 34.761909 Y = 0.732407 Z = 5.552633 A = 50.426846 B = 127.379339 G = 114.323346
Initial residual: 0.005617
Converges to: X = 32.469166 Y = -0.069269 Z = 5.415477 A = 50.200893 B = 136.139444 G = 105.385739
Final Residual: 0.000082

Perturbation 5
Initial Approximation: X = 31.542571 Y = 0.960324 Z = 2.815461 A = 36.381705 B = 137.285172 G = 107.860880
Initial residual: 0.028211
Converges to: X = 32.469711 Y = -0.069654 Z = 5.414064 A = 50.201826 B = 136.139611 G = 105.387220
Final Residual: 0.000082

Using perturbation #3
Initial Approximation: X = 34.473717 Y = 0.713008 Z = 3.795671 A = 60.729919 B = 163.184588 G = 106.559836
Initial residual: 0.023665
Converges to: X = 32.469598 Y = -0.069574 Z = 5.414357 A = 50.201632 B = 136.139576 G = 105.386913
Residual Vector = {-0.000032 0.000016 -0.000008 -0.000007 -0.000007 -0.000016 -0.000036 0.000014 0.000010 -0.000040 0.000022 0.000032
0.000000 0.000000 0.000000 0.000000}
Final residual: 0.000082
Stopping Criterion: 1
Number of function evaluations = 57

Data point # 13
==========

Perturbation 1
Initial Approximation: X = 32.469598 Y = -0.069574 Z = 5.414357 A = 50.201632 B = 136.139576 G = 105.386913
Initial residual: 0.000114
Converges to: X = 32.013209 Y = -0.107699 Z = 5.411770 A = 50.229541 B = 136.041906 G = 105.629581
Final Residual: 0.000088

Perturbation 2
Initial Approximation: X = 34.170640 Y = 1.609376 Z = 5.262448 A = 33.078144 B = 157.639752 G = 126.722555
Initial residual: 0.091501
Converges to: X = 32.013309 Y = -0.107772 Z = 5.411514 A = 50.229700 B = 136.041951 G = 105.629796
Final Residual: 0.000088

Perturbation 3
Initial Approximation: X = 32.290979 Y = 1.128041 Z = 5.873549 A = 33.289142 B = 134.704886 G = 70.881465
Initial residual: 0.030115
Converges to: X = 36.500872 Y = -5.232040 Z = 14.127563 A = 51.062986 B = 135.717512 G = 72.234131
Final Residual: 0.000802

Perturbation 4
Initial Approximation: X = 34.058977 Y = -0.329744 Z = 4.926636 A = 74.258890 B = 134.597978 G = 121.863126
Initial residual: 0.015491
Converges to: X = 33.871999 Y = 0.510741 Z = 6.189309 A = 65.970164 B = 141.713021 G = 117.839172
Final Residual: 0.000553

Perturbation 5
Initial Approximation: X = 34.032077 Y = 0.880014 Z = 3.952650 A = 65.664971 B = 137.016098 G = 119.263837
Initial residual: 0.005646
Converges to: X = 33.882645 Y = 0.506140 Z = 6.179267 A = 65.978531 B = 141.700291 G = 117.861728
Final Residual: 0.000553

Using perturbation #1
Initial Approximation: X = 32.469598 Y = -0.069574 Z = 5.414357 A = 50.201632 B = 136.139576 G = 105.386913
Initial residual: 0.000114
Converges to: X = 32.013209 Y = -0.107699 Z = 5.411770 A = 50.229541 B = 136.041906 G = 105.629581
Residual Vector = {-0.000038 0.000010 -0.000010 -0.000006 -0.000008 -0.000022 -0.000034 0.000013 0.000010 -0.000040 0.000024 0.000038
0.000000 0.000000 0.000000 0.000000}
Final residual: 0.000088
Stopping Criterion: 1
Number of function evaluations = 36

Data point # 14
==========

Perturbation 1
Initial Approximation: X = 32.013209 Y = -0.107699 Z = 5.411770 A = 50.229541 B = 136.041906 G = 105.629581
Initial residual: 0.000106
Converges to: X = 31.567366 Y = -0.086868 Z = 5.557476 A = 49.868630 B = 135.734270 G = 105.537119
Final Residual: 0.000091

Perturbation 2
Initial Approximation: X = 31.890262 Y = 1.380257 Z = 5.013749 A = 40.118694 B = 105.281081 G = 136.191617
Initial residual: 0.017551
Converges to: X = 33.870811 Y = -1.187400 Z = 3.569387 A = 49.658942 B = 126.484192 G = 118.653984
Final Residual: 0.000584

Perturbation 3
Initial Approximation: X = 33.571246 Y = 0.949469 Z = 7.211216 A = 79.373913 B = 129.852437 G = 88.461850
Initial residual: 0.055477
Converges to: X = 36.807691 Y = -7.192644 Z = 14.675249 A = 57.705294 B = 147.508680 G = 86.159879
Final Residual: 0.001297

Perturbation 4
Initial Approximation: X = 32.734133 Y = 1.223507 Z = 5.134473 A = 43.744925 B = 116.633165 G = 115.248771
Initial residual: 0.009541
Converges to: X = 31.217467 Y = 0.198597 Z = 6.397609 A = 49.384315 B = 135.565205 G = 104.929628
Final Residual: 0.000090

Perturbation 5
Initial Approximation: X = 31.857681 Y = 1.959145 Z = 5.220781 A = 32.253626 B = 155.662207 G = 104.896225
Initial residual: 0.061150
Converges to: X = 31.575464 Y = -0.093179 Z = 5.537932 A = 49.880818 B = 135.739017 G = 105.551227
Final Residual: 0.000091

Using perturbation #4
Initial Approximation: X = 32.734133 Y = 1.223507 Z = 5.134473 A = 43.744925 B = 116.633165 G = 115.248771
Initial residual: 0.009541
Converges to: X = 30.685827 Y = 0.651336 Z = 7.813586 A = 48.486932 B = 135.173213 G = 103.897066
Residual Vector = {-0.000027 0.000015 -0.000009 0.000006 -0.000005 -0.000030 -0.000036 0.000016 -0.000005 -0.000045 0.000020 0.000024 -0.000000 0.000000 0.000000 0.000000}
Final residual: 0.000081
Stopping Criterion: 1
Number of function evaluations = 92

Data point # 15
==========

Perturbation 1
Initial Approximation: X = 30.685827 Y = 0.651336 Z = 7.813586 A = 48.486932 B = 135.173213 G = 103.897066
Initial residual: 0.000099
Converges to: X = 30.358927 Y = 0.594910 Z = 7.743632 A = 48.435673 B = 134.911409 G = 104.342836
Final Residual: 0.000082

Perturbation 2
Initial Approximation: X = 31.495608 Y = 2.279076 Z = 6.244488 A = 5.449682 B = 129.399815 G = 80.922522
Initial residual: 0.041894
Converges to: X = 33.912584 Y = -5.183422 Z = 13.557586 A = 99.558605 B = 170.731946 G = 92.068718
Final Residual: 0.001095

Perturbation 3
Initial Approximation: X = 29.764101 Y = 2.611793 Z = 8.506663 A = 70.180969 B = 161.563509 G = 105.345193
Initial residual: 0.008540
Converges to: X = 28.984207 Y = 2.657358 Z = 10.149550 A = 59.497159 B = 140.739239 G = 112.208641
Final Residual: 0.000482

Perturbation 4
Initial Approximation: X = 30.915194 Y = 2.699895 Z = 8.878138 A = 13.156284 B = 127.076410 G = 108.394089
Initial residual: 0.041131
Converges to: X = 28.922721 Y = 2.598270 Z = 10.090583 A = 59.347663 B = 140.504044 G = 112.350801
Final Residual: 0.000482

Perturbation 5
Initial Approximation: X = 29.681208 Y = 0.668730 Z = 8.770771 A = 29.748387 B = 146.350577 G = 95.816120
Initial residual: 0.045706
Converges to: X = 30.358871 Y = 0.594962 Z = 7.743755 A = 48.435588 B = 134.911356 G = 104.342769
Final Residual: 0.000082

Using perturbation #1
Initial Approximation: X = 30.685827 Y = 0.651336 Z = 7.813586 A = 48.486932 B = 135.173213 G = 103.897066
Initial residual: 0.000099
Converges to: X = 30.358927 Y = 0.594910 Z = 7.743632 A = 48.435673 B = 134.911409 G = 104.342836
Residual Vector = {-0.000028 0.000010 -0.000008 0.000002 -0.000006 -0.000030 -0.000039 0.000014 -0.000003 -0.000044 0.000022 0.000027 -0.000000 0.000000 0.000000 0.000000}
Final residual: 0.000082
Stopping Criterion: 3
Number of function evaluations = 36

Data point # 16
==========

Perturbation 1
Initial Approximation: X = 30.358927 Y = 0.594910 Z = 7.743632 A = 48.435673 B = 134.911409 G = 104.342836
Initial residual: 0.000116
Converges to: X = 29.920381 Y = 0.563124 Z = 7.722089 A = 48.465388 B = 134.702400 G = 104.832097
Final Residual: 0.000095

Perturbation 2
Initial Approximation: X = 32.394277 Y = 1.579433 Z = 9.955299 A = 72.752838 B = 134.198809 G = 83.429380
Initial residual: 0.041313
Converges to: X = 27.141212 Y = 3.738833 Z = 10.450107 A = 44.759809 B = 133.868177 G = 97.167422
Final Residual: 0.000458

Perturbation 3
Initial Approximation: X = 29.011392 Y = 0.176144 Z = 8.773039 A = 21.388998 B = 96.879366 G = 111.142707
Initial residual: 0.001536
Converges to: X = 32.071366 Y = -9.585694 Z = 11.590443 A = 8.845134 B = 98.185098 G = 94.533229
Final Residual: 0.000873

Perturbation 4
Initial Approximation: X = 31.456081 Y = 0.173623 Z = 7.221543 A = 25.640610 B = 130.554762 G = 106.155038
Initial residual: 0.031296
Converges to: X = 29.920254 Y = 0.563244 Z = 7.722277 A = 48.465255 B = 134.702296 G = 104.832042
Final Residual: 0.000095

Perturbation 5
Initial Approximation: X = 30.539882 Y = 2.117751 Z = 5.830805 A = 11.967674 B = 147.974567 G = 78.874168
Initial residual: 0.071314
Converges to: X = 34.243027 Y = -15.001191 Z = 13.571390 A = 97.978146 B = 187.861763 G = 88.133151
Final Residual: 0.000819

Using perturbation #1
Initial Approximation: X = 30.358927 Y = 0.594910 Z = 7.743632 A = 48.435673 B = 134.911409 G = 104.342836
Initial residual: 0.000116
Converges to: X = 29.920381 Y = 0.563124 Z = 7.722089 A = 48.465388 B = 134.702400 G = 104.832097
Residual Vector = {-0.000035 0.000010 -0.000010 0.000003 -0.000005 -0.000038 -0.000041 0.000016 -0.000003 -0.000047 0.000026 0.000033 -0.000000 0.000000 0.000000 0.000000}
Final residual: 0.000095
Stopping Criterion: 1
Number of function evaluations = 36

Data point # 17
==========

Perturbation 1
Initial Approximation: X = 29.920381 Y = 0.563124 Z = 7.722089 A = 48.465388 B = 134.702400 G = 104.832097
Initial residual: 0.000114
Converges to: X = 29.542003 Y = 0.464155 Z = 7.637686 A = 48.705968 B = 134.910523 G = 104.893771
Final Residual: 0.000092

Perturbation 2
Initial Approximation: X = 31.338139 Y = 0.761704 Z = 6.026905 A = 21.199953 B = 158.854545 G = 95.045900
Initial residual: 0.074689
Converges to: X = 36.529689 Y = -5.336388 Z = 13.479173 A = 53.227863 B = 133.090724 G = 65.130249
Final Residual: 0.000807

Perturbation 3
Initial Approximation: X = 30.956071 Y = 0.276540 Z = 9.345094 A = 39.547045 B = 116.031468 G = 104.953700
Initial residual: 0.014633
Converges to: X = 29.541909 Y = 0.464244 Z = 7.637877 A = 48.705863 B = 134.910449 G = 104.893711
Final Residual: 0.000092

Perturbation 4
Initial Approximation: X = 31.470591 Y = 0.831862 Z = 7.093911 A = 49.529936 B = 169.064684 G = 121.793065
Initial residual: 0.066291
Converges to: X = 29.541237 Y = 0.464873 Z = 7.639814 A = 48.704825 B = 134.909812 G = 104.892901
Final Residual: 0.000092

Perturbation 5
Initial Approximation: X = 28.970643 Y = 2.490204 Z = 7.349961 A = 31.351931 B = 147.132010 G = 102.108697
Initial residual: 0.047882
Converges to: X = 29.542022 Y = 0.464138 Z = 7.637641 A = 48.705993 B = 134.910539 G = 104.893788
Final Residual: 0.000092

Using perturbation #5
Initial Approximation: X = 28.970643 Y = 2.490204 Z = 7.349961 A = 31.351931 B = 147.132010 G = 102.108697
Initial residual: 0.047882
Converges to: X = 29.542022 Y = 0.464138 Z = 7.637641 A = 48.705993 B = 134.910539 G = 104.893788
Residual Vector = {-0.000037 0.000009 -0.000010 0.000003 -0.000003 -0.000035 -0.000038 0.000015 0.000000 -0.000052 0.000018 0.000032 -0.000000 0.000000 0.000000 0.000000}
Final residual: 0.000092
Stopping Criterion: 1
Number of function evaluations = 36

Data point # 18
==========

Perturbation 1
Initial Approximation: X = 29.542022 Y = 0.464138 Z = 7.637641 A = 48.705993 B = 134.910539 G = 104.893788
Initial residual: 0.000125
Converges to: X = 29.139873 Y = 0.375497 Z = 7.624506 A = 49.281172 B = 135.381205 G = 105.091741
Final Residual: 0.000104

Perturbation 2
Initial Approximation: X = 31.166139 Y = 1.425915 Z = 8.399163 A = 45.390265 B = 102.036892 G = 128.376300
Initial residual: 0.007899
Converges to: X = 27.421234 Y = 1.808173 Z = 9.457793 A = 59.846954 B = 139.559581 G = 114.231503
Final Residual: 0.000485

Perturbation 3
Initial Approximation: X = 31.107908 Y = 1.156919 Z = 8.788539 A = 79.371570 B = 116.956802 G = 84.361354
Initial residual: 0.075095
Converges to: X = 34.606216 Y = -16.894132 Z = 8.125974 A = 47.183484 B = 133.512739 G = 255.344149
Final Residual: 0.001034

Perturbation 4
Initial Approximation: X = 30.021906 Y = 1.941021 Z = 6.385301 A = 13.813349 B = 98.929805 G = 67.453004
Initial residual: 0.011532
Converges to: X = 33.512076 Y = -1.454402 Z = 16.697233 A = 16.277728 B = 95.241318 G = 74.630681
Final Residual: 0.001260

Perturbation 5
Initial Approximation: X = 30.703879 Y = 1.424360 Z = 6.021668 A = 30.845673 B = 141.551019 G = 102.001673
Initial residual: 0.039376
Converges to: X = 29.939320 Y = -0.309491 Z = 5.490056 A = 50.174363 B = 136.064244 G = 105.481232
Final Residual: 0.000117

Using perturbation #1
Initial Approximation: X = 29.542022 Y = 0.464138 Z = 7.637641 A = 48.705993 B = 134.910539 G = 104.893788
Initial residual: 0.000125
Converges to: X = 29.139873 Y = 0.375497 Z = 7.624506 A = 49.281172 B = 135.381205 G = 105.091741
Residual Vector = {-0.000042 0.000009 -0.000008 0.000003 -0.000006 -0.000041 -0.000043 0.000017 0.000000 -0.000056 0.000013 0.000040 -
0.000000 0.000000 0.000000 0.000000}
Final residual: 0.000104
Stopping Criterion: 1
Number of function evaluations = 29

Data point # 19
==========

Perturbation 1
Initial Approximation: X = 29.139873 Y = 0.375497 Z = 7.624506 A = 49.281172 B = 135.381205 G = 105.091741
Initial residual: 0.000125
Converges to: X = 28.724219 Y = 0.332444 Z = 7.649836 A = 49.395790 B = 135.240224 G = 105.590055
Final Residual: 0.000107

Perturbation 2
Initial Approximation: X = 28.191905 Y = 0.876015 Z = 6.148831 A = 26.080328 B = 164.584755 G = 140.854835
Initial residual: 0.133763
Converges to: X = 27.007337 Y = 1.596521 Z = 9.275433 A = 59.900087 B = 139.077033 G = 114.923050
Final Residual: 0.000478

Perturbation 3
Initial Approximation: X = 30.626427 Y = 1.612934 Z = 6.363988 A = 58.139972 B = 107.630123 G = 126.521341
Initial residual: 0.027563
Converges to: X = 28.724208 Y = 0.332455 Z = 7.650068 A = 49.395650 B = 135.240141 G = 105.589943
Final Residual: 0.000107

Perturbation 4
Initial Approximation: X = 30.573207 Y = 0.905877 Z = 6.132101 A = 72.934410 B = 146.193159 G = 96.472796
Initial residual: 0.021094
Converges to: X = 34.721278 Y = -6.957283 Z = -1.028409 A = 55.478164 B = 141.156228 G = 105.595412
Final Residual: 0.000799

Perturbation 5
Initial Approximation: X = 27.472566 Y = 2.287878 Z = 9.918193 A = 69.053057 B = 120.793757 G = 104.751753
Initial residual: 0.054532
Converges to: X = 26.995767 Y = 1.601700 Z = 9.274389 A = 59.907530 B = 139.074395 G = 114.934834
Final Residual: 0.000478

Using perturbation #1
Initial Approximation: X = 29.139873 Y = 0.375497 Z = 7.624506 A = 49.281172 B = 135.381205 G = 105.091741
Initial residual: 0.000125
Converges to: X = 28.724219 Y = 0.332444 Z = 7.649836 A = 49.395790 B = 135.240224 G = 105.590055
Residual Vector = {-0.000044 0.000007 -0.000006 0.000002 -0.000008 -0.000044 -0.000045 0.000014 0.000001 -0.000056 0.000015 0.000044 -
0.000000 0.000000 0.000000 0.000000}
Final residual: 0.000107
Stopping Criterion: 1
Number of function evaluations = 36

Data point # 20
==========

Perturbation 1
Initial Approximation: X = 28.724219 Y = 0.332444 Z = 7.649836 A = 49.395790 B = 135.240224 G = 105.590055
Initial residual: 0.000126
Converges to: X = 28.305640 Y = 0.315588 Z = 7.673011 A = 49.148168 B = 134.876773 G = 105.817578
Final Residual: 0.000109

Perturbation 2
Initial Approximation: X = 27.394774 Y = 1.422468 Z = 6.769254 A = 78.139009 B = 135.002128 G = 78.719008
Initial residual: 0.041966
Converges to: X = 41.254458 Y = -5.146055 Z = -0.852346 A = 68.774845 B = 158.122802 G = 83.615410
Final Residual: 0.001422

Perturbation 3
Initial Approximation: X = 28.887127 Y = 1.273514 Z = 5.525826 A = 38.516345 B = 140.025736 G = 97.364398
Initial residual: 0.021598
Converges to: X = 29.363495 Y = -0.615569 Z = 4.817605 A = 50.106052 B = 135.968238 G = 105.536812
Final Residual: 0.000130

Perturbation 4
Initial Approximation: X = 30.045758 Y = 1.563487 Z = 6.886181 A = 51.332488 B = 115.198840 G = 94.482169
Initial residual: 0.042230
Converges to: X = 28.305470 Y = 0.315746 Z = 7.673221 A = 49.148150 B = 134.876729 G = 105.817628
Final Residual: 0.000109

Perturbation 5
Initial Approximation: X = 29.932080 Y = 1.065151 Z = 9.302002 A = 53.814654 B = 143.861131 G = 107.993065
Initial residual: 0.009629
Converges to: X = 28.305286 Y = 0.315918 Z = 7.673496 A = 49.148097 B = 134.876660 G = 105.817660
Final Residual: 0.000109

Using perturbation #1
Initial Approximation: X = 28.724219 Y = 0.332444 Z = 7.649836 A = 49.395790 B = 135.240224 G = 105.590055
Initial residual: 0.000126
Converges to: X = 28.305640 Y = 0.315588 Z = 7.673011 A = 49.148168 B = 134.876773 G = 105.817578
Residual Vector = {-0.000046 0.000007 -0.000004 0.000003 -0.000008 -0.000045 -0.000043 0.000014 0.000002 -0.000058 0.000007 0.000047 -0.000000 0.000000 0.000000 0.000000}
Final residual: 0.000109
Stopping Criterion: 1
Number of function evaluations = 36

Data point # 21
==========

Perturbation 1
Initial Approximation: X = 28.305640 Y = 0.315588 Z = 7.673011 A = 49.148168 B = 134.876773 G = 105.817578
Initial residual: 0.000132
Converges to: X = 27.879039 Y = 0.292610 Z = 7.709786 A = 49.197567 B = 135.052583 G = 105.573857
Final Residual: 0.000114

Perturbation 2
Initial Approximation: X = 28.708958 Y = 0.480957 Z = 9.790016 A = 33.857805 B = 109.717572 G = 130.502715
Initial residual: 0.022562
Converges to: X = 26.105512 Y = 1.279373 Z = 9.015067 A = 60.389568 B = 138.663975 G = 115.994669
Final Residual: 0.000502

Perturbation 3
Initial Approximation: X = 29.690090 Y = 0.909190 Z = 7.896584 A = 36.155984 B = 111.259719 G = 97.374752
Initial residual: 0.020026
Converges to: X = 27.878881 Y = 0.292749 Z = 7.709961 A = 49.197596 B = 135.052570 G = 105.573935
Final Residual: 0.000114

Perturbation 4
Initial Approximation: X = 27.117995 Y = 0.824243 Z = 8.784265 A = 42.386857 B = 156.272700 G = 110.790398
Initial residual: 0.050963
Converges to: X = 27.878884 Y = 0.292746 Z = 7.709950 A = 49.197601 B = 135.052574 G = 105.573936
Final Residual: 0.000114

Perturbation 5
Initial Approximation: X = 26.992657 Y = 1.262300 Z = 6.780406 A = 30.258641 B = 119.960468 G = 98.411583
Initial residual: 0.001846
Converges to: X = 27.879025 Y = 0.292634 Z = 7.709947 A = 49.197467 B = 135.052508 G = 105.573807
Final Residual: 0.000114

Using perturbation #1
Initial Approximation: X = 28.305640 Y = 0.315588 Z = 7.673011 A = 49.148168 B = 134.876773 G = 105.817578
Initial residual: 0.000132
Converges to: X = 27.879039 Y = 0.292610 Z = 7.709786 A = 49.197567 B = 135.052583 G = 105.573857
Residual Vector = {-0.000048 0.000005 -0.000002 0.000003 -0.000004 -0.000046 -0.000047 0.000020 0.000005 -0.000059 0.000009 0.000049 0.000000 0.000000 0.000000 0.000000}
Final residual: 0.000114
Stopping Criterion: 1
Number of function evaluations = 36

Data point # 22
==========

Perturbation 1
Initial Approximation: X = 27.879039 Y = 0.292610 Z = 7.709786 A = 49.197567 B = 135.052583 G = 105.573857
Initial residual: 0.000135
Converges to: X = 27.445396 Y = 0.239184 Z = 7.772042 A = 49.397853 B = 135.214385 G = 105.643752
Final Residual: 0.000117

Perturbation 2
Initial Approximation: X = 27.785004 Y = 1.404402 Z = 8.794286 A = 62.486318 B = 112.117191 G = 100.117102
Initial residual: 0.061402
Converges to: X = 27.445269 Y = 0.239294 Z = 7.772172 A = 49.397912 B = 135.214399 G = 105.643837
Final Residual: 0.000117

Perturbation 3
Initial Approximation: X = 26.805470 Y = 0.250952 Z = 7.733973 A = 22.669263 B = 117.672443 G = 110.634920
Initial residual: 0.019149
Converges to: X = 27.445330 Y = 0.239242 Z = 7.772120 A = 49.397875 B = 135.214386 G = 105.643793
Final Residual: 0.000117

Perturbation 4
Initial Approximation: X = 29.144387 Y = 2.112584 Z = 6.683702 A = 40.925067 B = 117.872456 G = 98.449627
Initial residual: 0.018907
Converges to: X = 27.445268 Y = 0.239293 Z = 7.772156 A = 49.397925 B = 135.214409 G = 105.643843
Final Residual: 0.000117

Perturbation 5
Initial Approximation: X = 26.162639 Y = 0.673287 Z = 8.411428 A = 16.994206 B = 134.787329 G = 117.142297
Initial residual: 0.061904
Converges to: X = 25.714305 Y = 1.018340 Z = 8.831496 A = 60.853872 B = 138.625437 G = 116.543084
Final Residual: 0.000508

Using perturbation #1
Initial Approximation: X = 27.879039 Y = 0.292610 Z = 7.709786 A = 49.197567 B = 135.052583 G = 105.573857
Initial residual: 0.000135
Converges to: X = 27.445396 Y = 0.239184 Z = 7.772042 A = 49.397853 B = 135.214385 G = 105.643752
Residual Vector = {-0.000049 0.000008 0.000001 0.000005 -0.000005 -0.000047 -0.000048 0.000018 0.000006 -0.000060 -0.000001 0.000052
0.000000 0.000000 0.000000 0.000000}
Final residual: 0.000117
Stopping Criterion: 1
Number of function evaluations = 36

Data point # 23
==========

Perturbation 1
Initial Approximation: X = 27.445396 Y = 0.239184 Z = 7.772042 A = 49.397853 B = 135.214385 G = 105.643752
Initial residual: 0.000135
Converges to: X = 27.045003 Y = 0.199041 Z = 7.905934 A = 49.373632 B = 135.081469 G = 105.852333
Final Residual: 0.000119

Perturbation 2
Initial Approximation: X = 27.616606 Y = 1.156283 Z = 8.515274 A = 62.014290 B = 143.936524 G = 75.016287
Initial residual: 0.006061
Converges to: X = 28.680088 Y = -1.844146 Z = 2.067214 A = 54.653841 B = 144.879646 G = 89.487989
Final Residual: 0.000699

Perturbation 3
Initial Approximation: X = 27.859629 Y = 0.655798 Z = 7.165625 A = 21.156295 B = 167.445106 G = 82.417482
Initial residual: 0.083998
Converges to: X = 25.450806 Y = 1.372869 Z = 8.239886 A = 51.062101 B = 138.705948 G = 101.612622
Final Residual: 0.000369

Perturbation 4
Initial Approximation: X = 26.077001 Y = 1.317897 Z = 6.409784 A = 40.385445 B = 129.513913 G = 113.437770
Initial residual: 0.014336
Converges to: X = 27.045271 Y = 0.198829 Z = 7.905766 A = 49.373367 B = 135.081337 G = 105.852090
Final Residual: 0.000119

Perturbation 5
Initial Approximation: X = 29.030114 Y = 1.104930 Z = 9.535055 A = 32.482661 B = 140.126318 G = 103.367991
Initial residual: 0.035407
Converges to: X = 27.044877 Y = 0.199143 Z = 7.906034 A = 49.373738 B = 135.081517 G = 105.852440
Final Residual: 0.000119

Using perturbation #1
Initial Approximation: X = 27.445396 Y = 0.239184 Z = 7.772042 A = 49.397853 B = 135.214385 G = 105.643752
Initial residual: 0.000135
Converges to: X = 27.045003 Y = 0.199041 Z = 7.905934 A = 49.373632 B = 135.081469 G = 105.852333
Residual Vector = {-0.000048 0.000003 0.000006 0.000002 -0.000008 -0.000047 -0.000047 0.000014 0.000007 -0.000064 0.000001 0.000055 0.000000
0.000000 0.000000 0.000000}
Final residual: 0.000119
Stopping Criterion: 1
Number of function evaluations = 36

Data point # 24
==========

Perturbation 1
Initial Approximation: X = 27.045003 Y = 0.199041 Z = 7.905934 A = 49.373632 B = 135.081469 G = 105.852333
Initial residual: 0.000143
Converges to: X = 26.604183 Y = 0.148311 Z = 7.917939 A = 49.726440 B = 135.487274 G = 105.742715
Final Residual: 0.000123

Perturbation 2
Initial Approximation: X = 26.433176 Y = 1.931999 Z = 8.695594 A = 39.524495 B = 114.957967 G = 90.997949
Initial residual: 0.022680
Converges to: X = 26.604071 Y = 0.148396 Z = 7.918016 A = 49.726570 B = 135.487342 G = 105.742828
Final Residual: 0.000123

Perturbation 3
Initial Approximation: X = 27.819288 Y = 0.610350 Z = 6.166017 A = 32.029170 B = 107.693925 G = 116.324783
Initial residual: 0.001192
Converges to: X = 25.373919 Y = -0.811538 Z = 11.427737 A = 27.539333 B = 105.879665 G = 111.902318
Final Residual: 0.000665

Perturbation 4
Initial Approximation: X = 25.086623 Y = 1.195334 Z = 7.696745 A = 12.867274 B = 144.336207 G = 101.892061
Initial residual: 0.065302
Converges to: X = 28.348492 Y = 5.126245 Z = 12.313292 A = 85.310776 B = 160.037154 G = 109.504991
Final Residual: 0.000832

Perturbation 5
Initial Approximation: X = 28.926271 Y = 0.502900 Z = 7.136757 A = 32.095852 B = 163.873892 G = 103.846282
Initial residual: 0.069784
Converges to: X = 26.604060 Y = 0.148403 Z = 7.918016 A = 49.726588 B = 135.487354 G = 105.742839
Final Residual: 0.000123

Using perturbation #1
Initial Approximation: X = 27.045003 Y = 0.199041 Z = 7.905934 A = 49.373632 B = 135.081469 G = 105.852333
Initial residual: 0.000143
Converges to: X = 26.604183 Y = 0.148311 Z = 7.917939 A = 49.726440 B = 135.487274 G = 105.742715
Residual Vector = {-0.000050 0.000005 0.000009 0.000002 -0.000007 -0.000047 -0.000048 0.000017 0.000009 -0.000065 -0.000006 0.000058
0.000000 0.000000 0.000000 0.000000}
Final residual: 0.000123
Stopping Criterion: 1
Number of function evaluations = 36

Data point # 25
==========

Perturbation 1
Initial Approximation: X = 26.604183 Y = 0.148311 Z = 7.917939 A = 49.726440 B = 135.487274 G = 105.742715
Initial residual: 0.000142
Converges to: X = 26.175091 Y = 0.104642 Z = 7.985020 A = 49.810070 B = 135.585207 G = 105.713090
Final Residual: 0.000122

Perturbation 2
Initial Approximation: X = 27.443959 Y = 1.950947 Z = 9.539475 A = 58.678984 B = 168.906101 G = 106.934097
Initial residual: 0.031813
Converges to: X = 26.175010 Y = 0.104699 Z = 7.985067 A = 49.810189 B = 135.585274 G = 105.713183
Final Residual: 0.000122

Perturbation 3
Initial Approximation: X = 28.731902 Y = 0.558699 Z = 7.975792 A = 46.981267 B = 145.009217 G = 96.985868
Initial residual: 0.015150
Converges to: X = 26.174989 Y = 0.104710 Z = 7.985055 A = 49.810242 B = 135.585312 G = 105.713210
Final Residual: 0.000122

Perturbation 4
Initial Approximation: X = 25.572307 Y = 0.682607 Z = 7.702204 A = 67.698837 B = 149.801803 G = 144.807573
Initial residual: 0.055897
Converges to: X = 26.181338 Y = 0.101104 Z = 7.975721 A = 49.814062 B = 135.593716 G = 105.707762
Final Residual: 0.000123

Perturbation 5
Initial Approximation: X = 27.155285 Y = 0.969115 Z = 6.577142 A = 55.939513 B = 171.704819 G = 116.546345
Initial residual: 0.049267
Converges to: X = 26.174938 Y = 0.104769 Z = 7.985228 A = 49.810188 B = 135.585237 G = 105.713249
Final Residual: 0.000122

Using perturbation #1
Initial Approximation: X = 26.604183 Y = 0.148311 Z = 7.917939 A = 49.726440 B = 135.487274 G = 105.742715
Initial residual: 0.000142
Converges to: X = 26.175091 Y = 0.104642 Z = 7.985020 A = 49.810070 B = 135.585207 G = 105.713090
Residual Vector = {-0.000046 0.000004 0.000013 0.000003 -0.000008 -0.000047 -0.000048 0.000016 0.000009 -0.000065 -0.000007 0.000059
0.000000 0.000000 0.000000 0.000000}
Final residual: 0.000122
Stopping Criterion: 1
Number of function evaluations = 36

Data point # 26
==========

Perturbation 1
Initial Approximation: X = 26.175091 Y = 0.104642 Z = 7.985020 A = 49.810070 B = 135.585207 G = 105.713090
Initial residual: 0.000146
Converges to: X = 25.743842 Y = 0.102577 Z = 8.128432 A = 49.476469 B = 135.138552 G = 105.936775
Final Residual: 0.000126

Perturbation 2
Initial Approximation: X = 27.407795 Y = 1.024873 Z = 7.827055 A = 18.877595 B = 118.029512 G = 81.677114
Initial residual: 0.013760
Converges to: X = 25.983938 Y = 0.056717 Z = 8.189096 A = 48.476382 B = 135.057638 G = 104.274751
Final Residual: 0.000192

Perturbation 3
Initial Approximation: X = 24.638692 Y = 1.182843 Z = 6.430988 A = 65.721094 B = 147.300266 G = 142.784657
Initial residual: 0.051153
Converges to: X = 25.741791 Y = 0.105209 Z = 8.135207 A = 49.475746 B = 135.136864 G = 105.938547
Final Residual: 0.000126

Perturbation 4
Initial Approximation: X = 26.582903 Y = 1.311905 Z = 9.769656 A = 64.745216 B = 123.260610 G = 131.264077
Initial residual: 0.008296
Converges to: X = 25.743760 Y = 0.102637 Z = 8.128498 A = 49.476592 B = 135.138617 G = 105.936880
Final Residual: 0.000126

Perturbation 5
Initial Approximation: X = 24.973420 Y = 1.668388 Z = 8.428150 A = 82.176524 B = 160.144867 G = 73.751945
Initial residual: 0.002413
Converges to: X = 29.576688 Y = -5.508400 Z = 12.004908 A = 86.301561 B = 159.019772 G = 69.333418
Final Residual: 0.000771

Using perturbation #1
Initial Approximation: X = 26.175091 Y = 0.104642 Z = 7.985020 A = 49.810070 B = 135.585207 G = 105.713090
Initial residual: 0.000146
Converges to: X = 25.743842 Y = 0.102577 Z = 8.128432 A = 49.476469 B = 135.138552 G = 105.936775
Residual Vector = {-0.000048 0.000002 0.000015 0.000004 -0.000006 -0.000050 -0.000048 0.000017 0.000011 -0.000064 -0.000011 0.000062
0.000000 0.000000 0.000000 0.000000}
Final residual: 0.000126
Stopping Criterion: 1
Number of function evaluations = 36

Data point # 27
==========

Perturbation 1
Initial Approximation: X = 25.743842 Y = 0.102577 Z = 8.128432 A = 49.476469 B = 135.138552 G = 105.936775
Initial residual: 0.000154
Converges to: X = 25.238785 Y = 0.084329 Z = 8.191956 A = 49.707693 B = 135.337393 G = 105.992379
Final Residual: 0.000130

Perturbation 2
Initial Approximation: X = 23.678830 Y = 0.948759 Z = 9.721541 A = 51.027914 B = 95.302306 G = 96.613756
Initial residual: 0.058269
Converges to: X = 22.385279 Y = 0.810603 Z = 10.441754 A = 51.891744 B = 129.434493 G = 117.766710
Final Residual: 0.000630

Perturbation 3
Initial Approximation: X = 23.763123 Y = 0.576781 Z = 7.584872 A = 38.704353 B = 114.670613 G = 75.938634
Initial residual: 0.015838
Converges to: X = 28.281946 Y = -4.848414 Z = -0.226039 A = 43.091741 B = 132.991711 G = 87.603401
Final Residual: 0.000419

Perturbation 4
Initial Approximation: X = 26.764793 Y = 0.819947 Z = 8.022722 A = 55.136391 B = 112.176134 G = 128.381758
Initial residual: 0.014559
Converges to: X = 25.239555 Y = 0.083825 Z = 8.191437 A = 49.706276 B = 135.336625 G = 105.991227
Final Residual: 0.000130

Perturbation 5
Initial Approximation: X = 27.102449 Y = 0.201698 Z = 7.622891 A = 46.814756 B = 118.697894 G = 124.591483
Initial residual: 0.002321
Converges to: X = 25.351379 Y = 0.077360 Z = 8.380238 A = 47.892517 B = 133.257176 G = 106.690362
Final Residual: 0.000221

Using perturbation #4
Initial Approximation: X = 26.764793 Y = 0.819947 Z = 8.022722 A = 55.136391 B = 112.176134 G = 128.381758
Initial residual: 0.014559
Converges to: X = 25.239555 Y = 0.083825 Z = 8.191437 A = 49.706276 B = 135.336625 G = 105.991227
Residual Vector = {-0.000049 0.000002 0.000018 0.000003 -0.000005 -0.000052 -0.000049 0.000016 0.000013 -0.000062 -0.000012 0.000066
0.000000 0.000000 0.000000 0.000000}
Final residual: 0.000130
Stopping Criterion: 1
Number of function evaluations = 61

Data point # 28
==========

Perturbation 1
Initial Approximation: X = 25.239555 Y = 0.083825 Z = 8.191437 A = 49.706276 B = 135.336625 G = 105.991227
Initial residual: 0.000149
Converges to: X = 24.817063 Y = 0.043975 Z = 8.269070 A = 49.858674 B = 135.462418 G = 106.037355
Final Residual: 0.000128

Perturbation 2
Initial Approximation: X = 25.827887 Y = 1.332972 Z = 7.420812 A = 62.421969 B = 134.292942 G = 71.688326
Initial residual: 0.019971
Converges to: X = 24.804764 Y = 0.054055 Z = 8.285357 A = 49.876161 B = 135.474195 G = 106.055100
Final Residual: 0.000129

Perturbation 3
Initial Approximation: X = 25.870471 Y = 2.021705 Z = 9.645751 A = 64.063772 B = 161.346921 G = 79.170567
Initial residual: 0.012500
Converges to: X = 24.817535 Y = 0.043772 Z = 8.269140 A = 49.857361 B = 135.461527 G = 106.036616
Final Residual: 0.000128

Perturbation 4
Initial Approximation: X = 23.858613 Y = 2.196872 Z = 7.456978 A = 48.148883 B = 137.765718 G = 121.015325
Initial residual: 0.025894
Converges to: X = 24.816934 Y = 0.043973 Z = 8.268775 A = 49.859298 B = 135.462947 G = 106.037515
Final Residual: 0.000128

Perturbation 5
Initial Approximation: X = 23.425031 Y = 1.135297 Z = 9.049601 A = 59.814214 B = 117.663208 G = 88.721980
Initial residual: 0.053121
Converges to: X = 24.817013 Y = 0.044018 Z = 8.269163 A = 49.858719 B = 135.462412 G = 106.037447
Final Residual: 0.000128

Using perturbation #3
Initial Approximation: X = 25.870471 Y = 2.021705 Z = 9.645751 A = 64.063772 B = 161.346921 G = 79.170567
Initial residual: 0.012500
Converges to: X = 24.817535 Y = 0.043772 Z = 8.269140 A = 49.857361 B = 135.461527 G = 106.036616
Residual Vector = {-0.000048 -0.000001 0.000021 0.000003 -0.000002 -0.000050 -0.000051 0.000014 0.000017 -0.000061 -0.000012 0.000066
0.000000 0.000000 0.000000 0.000000}
Final residual: 0.000128
Stopping Criterion: 1
Number of function evaluations = 51

Data point # 29
==========

Perturbation 1
Initial Approximation: X = 24.817535 Y = 0.043772 Z = 8.269140 A = 49.857361 B = 135.461527 G = 106.036616
Initial residual: 0.000153
Converges to: X = 24.355842 Y = 0.046020 Z = 8.343546 A = 49.918299 B = 135.495525 G = 106.085597
Final Residual: 0.000126

Perturbation 2
Initial Approximation: X = 23.709031 Y = 1.928926 Z = 6.534408 A = 52.428358 B = 150.376395 G = 112.328717
Initial residual: 0.027189
Converges to: X = 24.355703 Y = 0.045981 Z = 8.343112 A = 49.919098 B = 135.496262 G = 106.085691
Final Residual: 0.000126

Perturbation 3
Initial Approximation: X = 22.890352 Y = 0.765932 Z = 6.692605 A = 46.331113 B = 144.067028 G = 134.018678
Initial residual: 0.061535
Converges to: X = 24.355691 Y = 0.046011 Z = 8.343230 A = 49.919020 B = 135.496152 G = 106.085750
Final Residual: 0.000126

Perturbation 4
Initial Approximation: X = 24.362057 Y = 1.459991 Z = 8.635667 A = 83.222842 B = 149.532819 G = 83.095176
Initial residual: 0.022924
Converges to: X = 21.007109 Y = -1.708898 Z = -1.042499 A = 66.596855 B = 152.321456 G = 75.904366
Final Residual: 0.000793

Perturbation 5
Initial Approximation: X = 23.596447 Y = 0.819113 Z = 8.069729 A = 24.756895 B = 112.596504 G = 136.743381
Initial residual: 0.050282
Converges to: X = 23.658590 Y = -0.084583 Z = 10.932289 A = 38.039958 B = 118.991364 G = 112.365293
Final Residual: 0.000511

Using perturbation #2
Initial Approximation: X = 23.709031 Y = 1.928926 Z = 6.534408 A = 52.428358 B = 150.376395 G = 112.328717
Initial residual: 0.027189
Converges to: X = 24.355703 Y = 0.045981 Z = 8.343112 A = 49.919098 B = 135.496262 G = 106.085691
Residual Vector = {-0.000047 -0.000000 0.000023 0.000000 -0.000001 -0.000045 -0.000047 0.000014 0.000020 -0.000059 -0.000021 0.000066
0.000000 0.000000 0.000000 0.000000}
Final residual: 0.000126
Stopping Criterion: 1
Number of function evaluations = 43

Data point # 30
==========

Perturbation 1
Initial Approximation: X = 24.355703 Y = 0.045981 Z = 8.343112 A = 49.919098 B = 135.496262 G = 106.085691
Initial residual: 0.000158
Converges to: X = 23.880401 Y = 0.004495 Z = 8.594262 A = 50.197012 B = 135.743827 G = 106.134610
Final Residual: 0.000126

Perturbation 2
Initial Approximation: X = 24.500626 Y = 1.835714 Z = 9.839416 A = 67.251597 B = 161.499678 G = 128.290821
Initial residual: 0.043297
Converges to: X = 23.912139 Y = 0.037522 Z = 8.562187 A = 50.042351 B = 135.618989 G = 106.098071
Final Residual: 0.000127

Perturbation 3
Initial Approximation: X = 25.205000 Y = 0.903180 Z = 9.280340 A = 58.965095 B = 150.311532 G = 119.171751
Initial residual: 0.025823
Converges to: X = 22.612318 Y = 0.050784 Z = 8.281390 A = 55.668486 B = 137.638861 G = 111.736646
Final Residual: 0.000279

Perturbation 4
Initial Approximation: X = 23.094776 Y = 1.155042 Z = 6.297301 A = 63.091340 B = 107.435335 G = 113.670957
Initial residual: 0.054427
Converges to: X = 23.880390 Y = 0.004516 Z = 8.594358 A = 50.196958 B = 135.743742 G = 106.134669
Final Residual: 0.000126

Perturbation 5
Initial Approximation: X = 24.578937 Y = 1.335410 Z = 7.452322 A = 21.470670 B = 129.485699 G = 93.436767
Initial residual: 0.027413
Converges to: X = 23.880370 Y = 0.004509 Z = 8.594290 A = 50.197078 B = 135.743853 G = 106.134682
Final Residual: 0.000126

Using perturbation #1
Initial Approximation: X = 24.355703 Y = 0.045981 Z = 8.343112 A = 49.919098 B = 135.496262 G = 106.085691
Initial residual: 0.000158
Converges to: X = 23.880401 Y = 0.004495 Z = 8.594262 A = 50.197012 B = 135.743827 G = 106.134610
Residual Vector = {-0.000043 0.000001 0.000025 -0.000002 -0.000002 -0.000048 -0.000049 0.000010 0.000021 -0.000055 -0.000020 0.000068
0.000000 0.000000 0.000000 0.000000}
Final residual: 0.000126
Stopping Criterion: 1
Number of function evaluations = 36

Data point # 31
==========

Perturbation 1
Initial Approximation: X = 23.880401 Y = 0.004495 Z = 8.594262 A = 50.197012 B = 135.743827 G = 106.134610
Initial residual: 0.000154
Converges to: X = 23.498337 Y = -0.002483 Z = 8.636739 A = 50.042079 B = 135.472788 G = 106.355252
Final Residual: 0.000129

Perturbation 2
Initial Approximation: X = 22.519037 Y = 0.286996 Z = 7.041637 A = 50.530083 B = 105.465240 G = 143.975114
Initial residual: 0.012979
Converges to: X = 20.741074 Y = 0.162611 Z = 12.420245 A = 55.998379 B = 121.189418 G = 130.396808
Final Residual: 0.000644

Perturbation 3
Initial Approximation: X = 23.160409 Y = 1.021611 Z = 7.069978 A = 83.426152 B = 115.626859 G = 86.754643
Initial residual: 0.079677
Converges to: X = 13.217088 Y = 7.907106 Z = 5.032295 A = 46.919410 B = 115.728580 G = 53.712779
Final Residual: 0.001531

Perturbation 4
Initial Approximation: X = 22.683237 Y = 0.635420 Z = 7.873797 A = 23.772839 B = 128.014197 G = 98.726768
Initial residual: 0.024004
Converges to: X = 23.498373 Y = -0.002477 Z = 8.636835 A = 50.041882 B = 135.472603 G = 106.355236
Final Residual: 0.000129

Perturbation 5
Initial Approximation: X = 24.749187 Y = 0.939457 Z = 8.517899 A = 56.807192 B = 114.437023 G = 128.338158
Initial residual: 0.014472
Converges to: X = 23.376399 Y = 0.048808 Z = 8.524630 A = 50.438327 B = 136.100505 G = 105.909693
Final Residual: 0.000127

Using perturbation #5
Initial Approximation: X = 24.749187 Y = 0.939457 Z = 8.517899 A = 56.807192 B = 114.437023 G = 128.338158
Initial residual: 0.014472
Converges to: X = 23.376065 Y = 0.048728 Z = 8.523851 A = 50.439953 B = 136.102050 G = 105.909785
Residual Vector = {-0.000049 -0.000001 0.000025 -0.000002 -0.000006 -0.000048 -0.000046 0.000008 0.000027 -0.000052 -0.000016 0.000069
0.000000 0.000000 0.000000 0.000000}
Final residual: 0.000127
Stopping Criterion: 1
Number of function evaluations = 57

Data point # 32
==========

Perturbation 1
Initial Approximation: X = 23.376065 Y = 0.048728 Z = 8.523851 A = 50.439953 B = 136.102050 G = 105.909785
Initial residual: 0.000158
Converges to: X = 22.992725 Y = -0.016917 Z = 8.766964 A = 50.360495 B = 135.751870 G = 106.418342
Final Residual: 0.000128

Perturbation 2
Initial Approximation: X = 22.108601 Y = 1.123635 Z = 10.267925 A = 38.203588 B = 158.547498 G = 107.823900
Initial residual: 0.057748
Converges to: X = 22.992777 Y = -0.016904 Z = 8.767116 A = 50.360217 B = 135.751589 G = 106.418355
Final Residual: 0.000128

Perturbation 3
Initial Approximation: X = 24.514183 Y = 0.839920 Z = 10.894055 A = 28.207479 B = 124.700400 G = 129.954054
Initial residual: 0.051318
Converges to: X = 20.968600 Y = 0.199505 Z = 12.934415 A = 53.520953 B = 129.782414 G = 119.142250
Final Residual: 0.000554

Perturbation 4
Initial Approximation: X = 23.765993 Y = 1.353532 Z = 8.677048 A = 48.879677 B = 103.117862 G = 75.845250
Initial residual: 0.045640
Converges to: X = 22.994085 Y = -0.016637 Z = 8.770297 A = 50.353769 B = 135.745355 G = 106.418163
Final Residual: 0.000128

Perturbation 5
Initial Approximation: X = 23.544551 Y = 1.534073 Z = 10.142371 A = 55.934275 B = 116.794244 G = 108.065753
Initial residual: 0.038691
Converges to: X = 22.992806 Y = -0.016898 Z = 8.767185 A = 50.360076 B = 135.751454 G = 106.418348
Final Residual: 0.000128

Using perturbation #1
Initial Approximation: X = 23.376065 Y = 0.048728 Z = 8.523851 A = 50.439953 B = 136.102050 G = 105.909785
Initial residual: 0.000158
Converges to: X = 22.992725 Y = -0.016917 Z = 8.766964 A = 50.360495 B = 135.751870 G = 106.418342
Residual Vector = {-0.000040 -0.000001 0.000030 -0.000006 0.000015 -0.000051 -0.000052 0.000001 0.000016 -0.000042 -0.000022 0.000077
0.000000 0.000000 0.000000 0.000000}
Final residual: 0.000128
Stopping Criterion: 1
Number of function evaluations = 36

Data point # 33
==========

Perturbation 1
Initial Approximation: X = 22.992725 Y = -0.016917 Z = 8.766964 A = 50.360495 B = 135.751870 G = 106.418342
Initial residual: 0.000174
Converges to: X = 22.504053 Y = -0.015998 Z = 8.878105 A = 50.357353 B = 135.573662 G = 106.738460
Final Residual: 0.000127

Perturbation 2
Initial Approximation: X = 21.743240 Y = -0.109197 Z = 10.955048 A = 47.865409 B = 123.211176 G = 105.067359
Initial residual: 0.018244
Converges to: X = 22.504037 Y = -0.016000 Z = 8.878085 A = 50.357416 B = 135.573712 G = 106.738481
Final Residual: 0.000127

Perturbation 3
Initial Approximation: X = 22.048315 Y = 1.515967 Z = 10.789949 A = 68.715965 B = 153.515015 G = 108.233574
Initial residual: 0.003224
Converges to: X = 22.497725 Y = -0.015259 Z = 8.857588 A = 50.402331 B = 135.629648 G = 106.727923
Final Residual: 0.000127

Perturbation 4
Initial Approximation: X = 22.956809 Y = 1.187227 Z = 7.765280 A = 73.938466 B = 129.937084 G = 118.679489
Initial residual: 0.028126
Converges to: X = 18.505149 Y = -7.260657 Z = 1.130155 A = 71.530270 B = 132.838529 G = 131.400598
Final Residual: 0.000662

Perturbation 5
Initial Approximation: X = 23.082543 Y = 1.792778 Z = 10.438543 A = 26.195558 B = 138.233209 G = 111.491104
Initial residual: 0.049569
Converges to: X = 22.504089 Y = -0.015990 Z = 8.878194 A = 50.357185 B = 135.573488 G = 106.738477
Final Residual: 0.000127

Using perturbation #1
Initial Approximation: X = 22.992725 Y = -0.016917 Z = 8.766964 A = 50.360495 B = 135.751870 G = 106.418342
Initial residual: 0.000174
Converges to: X = 22.504053 Y = -0.015998 Z = 8.878105 A = 50.357353 B = 135.573662 G = 106.738460
Residual Vector = {-0.000041 -0.000001 0.000030 -0.000006 0.000019 -0.000050 -0.000051 -0.000006 0.000014 -0.000036 -0.000023 0.000078
0.000000 0.000000 0.000000 0.000000}
Final residual: 0.000127
Stopping Criterion: 1
Number of function evaluations = 29

Data point # 34
==========

Perturbation 1
Initial Approximation: X = 22.504053 Y = -0.015998 Z = 8.878105 A = 50.357353 B = 135.573662 G = 106.738460
Initial residual: 0.000186
Converges to: X = 22.018701 Y = -0.013756 Z = 8.953371 A = 50.270757 B = 135.412507 G = 106.875805
Final Residual: 0.000128

Perturbation 2
Initial Approximation: X = 24.000141 Y = -0.208096 Z = 7.997085 A = 25.572643 B = 171.388340 G = 74.520312
Initial residual: 0.086260
Converges to: X = 22.018839 Y = -0.013721 Z = 8.953641 A = 50.270237 B = 135.411970 G = 106.875853
Final Residual: 0.000128

Perturbation 3
Initial Approximation: X = 20.908559 Y = 1.932458 Z = 9.034187 A = 61.355435 B = 145.064545 G = 99.380040
Initial residual: 0.007182
Converges to: X = 22.018533 Y = -0.013797 Z = 8.953053 A = 50.271388 B = 135.413147 G = 106.875770
Final Residual: 0.000128

Perturbation 4
Initial Approximation: X = 22.198606 Y = -0.471924 Z = 7.807051 A = 27.882006 B = 111.714014 G = 127.934200
Initial residual: 0.029626
Converges to: X = 22.356734 Y = -0.298374 Z = 10.445898 A = 44.034028 B = 124.384267 G = 113.905006
Final Residual: 0.000347

Perturbation 5
Initial Approximation: X = 24.167610 Y = 0.526639 Z = 7.864721 A = 34.089357 B = 136.056753 G = 68.189166
Initial residual: 0.034264
Converges to: X = 22.059397 Y = -0.000500 Z = 9.029533 A = 50.167915 B = 135.280107 G = 106.952017
Final Residual: 0.000130

Using perturbation #3
Initial Approximation: X = 20.908559 Y = 1.932458 Z = 9.034187 A = 61.355435 B = 145.064545 G = 99.380040
Initial residual: 0.007182
Converges to: X = 22.018533 Y = -0.013797 Z = 8.953053 A = 50.271388 B = 135.413147 G = 106.875770
Residual Vector = {-0.000046 -0.000001 0.000029 -0.000007 0.000019 -0.000050 -0.000052 -0.000016 0.000016 -0.000030 -0.000018 0.000078
0.000000 0.000000 0.000000 0.000000}
Final residual: 0.000128
Stopping Criterion: 1
Number of function evaluations = 50

Data point # 35
==========
Perturbation 1
Initial Approximation: X = 22.018533 Y = -0.013797 Z = 8.953053 A = 50.271388 B = 135.413147 G = 106.875770
Initial residual: 0.000209
Converges to: X = 21.407771 Y = -0.012021 Z = 9.018661 A = 50.568966 B = 135.595110 G = 107.073344
Final Residual: 0.000127

Perturbation 2
Initial Approximation: X = 19.873553 Y = 1.430266 Z = 9.836823 A = 29.658039 B = 133.799519 G = 126.572044
Initial residual: 0.058937
Converges to: X = 21.407805 Y = -0.012010 Z = 9.018715 A = 50.568871 B = 135.595004 G = 107.073368
Final Residual: 0.000127

Perturbation 3
Initial Approximation: X = 19.952017 Y = 1.585987 Z = 6.967251 A = 67.014883 B = 157.710651 G = 113.344548
Initial residual: 0.016588
Converges to: X = 21.428518 Y = -0.004505 Z = 9.050256 A = 50.517183 B = 135.532066 G = 107.099589
Final Residual: 0.000127

Perturbation 4
Initial Approximation: X = 23.020888 Y = 1.267189 Z = 8.473755 A = 10.549938 B = 146.005966 G = 132.042883
Initial residual: 0.110242
Converges to: X = 22.242728 Y = 7.060283 Z = 13.391232 A = 93.220824 B = 173.725117 G = 95.439083
Final Residual: 0.000908

Perturbation 5
Initial Approximation: X = 20.796397 Y = -0.153607 Z = 7.895804 A = 56.825411 B = 151.667358 G = 109.074136
Initial residual: 0.018101
Converges to: X = 21.407628 Y = -0.012067 Z = 9.018431 A = 50.569368 B = 135.595561 G = 107.073241
Final Residual: 0.000127

Using perturbation #5
Initial Approximation: X = 20.796397 Y = -0.153607 Z = 7.895804 A = 56.825411 B = 151.667358 G = 109.074136
Initial residual: 0.018101
Converges to: X = 21.407628 Y = -0.012067 Z = 9.018431 A = 50.569368 B = 135.595561 G = 107.073241
Residual Vector = {-0.000046 -0.000003 0.000031 -0.000009 0.000022 -0.000043 -0.000054 -0.000022 0.000017 -0.000025 -0.000018 0.000077
0.000000 0.000000 0.000000 0.000000}
Final residual: 0.000127
Stopping Criterion: 1
Number of function evaluations = 50

Data point # 36
==========

Perturbation 1
Initial Approximation: X = 21.407628 Y = -0.012067 Z = 9.018431 A = 50.569368 B = 135.595561 G = 107.073241
Initial residual: 0.000229
Converges to: X = 20.846301 Y = -0.065391 Z = 9.159704 A = 50.425210 B = 135.432115 G = 107.112263
Final Residual: 0.000128

Perturbation 2
Initial Approximation: X = 22.479404 Y = 1.637415 Z = 10.031945 A = 92.112471 B = 164.335049 G = 68.187227
Initial residual: 0.006927
Converges to: X = 19.538003 Y = -5.029307 Z = 11.703181 A = 116.603658 B = 123.186205 G = 44.900206
Final Residual: 0.000709

Perturbation 3
Initial Approximation: X = 23.073957 Y = 1.409392 Z = 7.923158 A = 21.351668 B = 107.382749 G = 81.311341
Initial residual: 0.002329
Converges to: X = 24.134806 Y = -0.689631 Z = 11.431772 A = 21.475410 B = 110.805654 G = 95.905003
Final Residual: 0.000651

Perturbation 4
Initial Approximation: X = 21.414725 Y = 1.752778 Z = 8.445350 A = 62.127738 B = 112.252171 G = 115.809875
Initial residual: 0.044858
Converges to: X = 21.172033 Y = 0.050178 Z = 9.538678 A = 48.724767 B = 133.053801 G = 108.466318
Final Residual: 0.000213

Perturbation 5
Initial Approximation: X = 21.512215 Y = 1.048880 Z = 7.968508 A = 61.071873 B = 112.418323 G = 133.443643
Initial residual: 0.014818
Converges to: X = 19.860335 Y = -4.321725 Z = 7.297893 A = 71.817441 B = 107.506172 G = 154.345719
Final Residual: 0.000898

Using perturbation #1
Initial Approximation: X = 21.407628 Y = -0.012067 Z = 9.018431 A = 50.569368 B = 135.595561 G = 107.073241
Initial residual: 0.000229
Converges to: X = 20.846301 Y = -0.065391 Z = 9.159704 A = 50.425210 B = 135.432115 G = 107.112263
Residual Vector = {-0.000049 -0.000001 0.000029 -0.000006 0.000013 -0.000049 -0.000059 -0.000030 0.000021 -0.000018 -0.000007 0.000072
0.000000 0.000000 0.000000 0.000000}
Final residual: 0.000128
Stopping Criterion: 1
Number of function evaluations = 29

Data point # 37
==========

Perturbation 1
Initial Approximation: X = 20.846301 Y = -0.065391 Z = 9.159704 A = 50.425210 B = 135.432115 G = 107.112263
Initial residual: 0.000241
Converges to: X = 20.288784 Y = -0.102192 Z = 9.305320 A = 50.212872 B = 135.086686 G = 107.353908
Final Residual: 0.000133

Perturbation 2
Initial Approximation: X = 20.595114 Y = 1.330051 Z = 8.338067 A = 90.275613 B = 113.906918 G = 104.732228
Initial residual: 0.077132
Converges to: X = 14.057467 Y = -0.162913 Z = 9.085932 A = 144.402127 B = 78.503621 G = 123.185946
Final Residual: 0.001036

Perturbation 3
Initial Approximation: X = 19.846922 Y = 1.892346 Z = 9.027765 A = 30.799470 B = 118.897995 G = 100.136979
Initial residual: 0.001094
Converges to: X = 20.525196 Y = 0.110496 Z = 9.699298 A = 49.778790 B = 133.179646 G = 109.873843
Final Residual: 0.000174

Perturbation 4
Initial Approximation: X = 20.556806 Y = 0.684714 Z = 10.530417 A = 67.642667 B = 155.274019 G = 88.332246
Initial residual: 0.003084
Converges to: X = 19.588380 Y = -0.371164 Z = 9.170436 A = 55.226652 B = 141.274055 G = 104.992765
Final Residual: 0.000242

Perturbation 5
Initial Approximation: X = 20.981788 Y = 0.899571 Z = 9.610902 A = 45.763383 B = 123.210309 G = 110.905357
Initial residual: 0.008605
Converges to: X = 20.288780 Y = -0.102194 Z = 9.305315 A = 50.212874 B = 135.086690 G = 107.353904
Final Residual: 0.000133

Using perturbation #5
Initial Approximation: X = 20.981788 Y = 0.899571 Z = 9.610902 A = 45.763383 B = 123.210309 G = 110.905357
Initial residual: 0.008605
Converges to: X = 20.288780 Y = -0.102194 Z = 9.305315 A = 50.212874 B = 135.086690 G = 107.353904
Residual Vector = {-0.000050 -0.000001 0.000030 -0.000004 0.000014 -0.000060 -0.000060 -0.000035 0.000016 -0.000012 -0.000002 0.000071
0.000000 0.000000 0.000000 0.000000}
Final residual: 0.000133
Stopping Criterion: 2
Number of function evaluations = 50

Data point # 38
==========

Perturbation 1
Initial Approximation: X = 20.288780 Y = -0.102194 Z = 9.305315 A = 50.212874 B = 135.086690 G = 107.353904
Initial residual: 0.000288
Converges to: X = 19.489953 Y = -0.242751 Z = 9.406935 A = 49.767463 B = 134.518886 G = 107.579375
Final Residual: 0.000134

Perturbation 2
Initial Approximation: X = 18.651122 Y = 0.355647 Z = 10.185660 A = 82.776650 B = 109.074975 G = 71.515774
Initial residual: 0.077710
Converges to: X = 19.312981 Y = -0.314560 Z = 9.284929 A = 50.202615 B = 134.937262 G = 107.598457
Final Residual: 0.000139

Perturbation 3
Initial Approximation: X = 21.555137 Y = 0.779353 Z = 10.712392 A = 40.958935 B = 126.970294 G = 97.422937
Initial residual: 0.005150
Converges to: X = 19.489968 Y = -0.242741 Z = 9.406947 A = 49.767473 B = 134.518883 G = 107.579398
Final Residual: 0.000134

Perturbation 4
Initial Approximation: X = 19.117589 Y = 1.184071 Z = 7.369644 A = 33.558724 B = 123.571147 G = 119.282855
Initial residual: 0.023959
Converges to: X = 19.489252 Y = -0.243232 Z = 9.406389 A = 49.766983 B = 134.519037 G = 107.578275
Final Residual: 0.000134

Perturbation 5
Initial Approximation: X = 18.953208 Y = 1.493847 Z = 9.946911 A = 82.631549 B = 137.392475 G = 96.319219
Initial residual: 0.043012
Converges to: X = 19.490110 Y = -0.242630 Z = 9.407057 A = 49.767585 B = 134.518857 G = 107.579638
Final Residual: 0.000134

Using perturbation #4
Initial Approximation: X = 19.117589 Y = 1.184071 Z = 7.369644 A = 33.558724 B = 123.571147 G = 119.282855
Initial residual: 0.023959
Converges to: X = 19.489252 Y = -0.243232 Z = 9.406389 A = 49.766983 B = 134.519037 G = 107.578275
Residual Vector = {-0.000058 0.000011 0.000025 0.000006 0.000004 -0.000068 -0.000067 -0.000028 0.000014 0.000002 0.000008 0.000060 0.000000 0.000000 0.000000 0.000000 0.000000}
Final residual: 0.000134
Stopping Criterion: 1
Number of function evaluations = 36

Data point # 39
==========

Perturbation 1
Initial Approximation: X = 19.489252 Y = -0.243232 Z = 9.406389 A = 49.766983 B = 134.519037 G = 107.578275
Initial residual: 0.000292
Converges to: X = 19.251919 Y = -0.185211 Z = 9.815174 A = 49.232447 B = 134.584654 G = 106.519588
Final Residual: 0.000147

Perturbation 2
Initial Approximation: X = 19.683222 Y = 0.687577 Z = 8.467319 A = 19.367131 B = 129.115457 G = 124.705618
Initial residual: 0.061229
Converges to: X = 19.251922 Y = -0.185202 Z = 9.815165 A = 49.232393 B = 134.584605 G = 106.519573
Final Residual: 0.000147

Perturbation 3
Initial Approximation: X = 18.757543 Y = -0.133020 Z = 6.964969 A = 28.374349 B = 146.061539 G = 123.253931
Initial residual: 0.076321
Converges to: X = 19.252135 Y = -0.185259 Z = 9.815251 A = 49.232270 B = 134.584600 G = 106.519363
Final Residual: 0.000147

Perturbation 4
Initial Approximation: X = 20.333633 Y = 1.121295 Z = 11.107569 A = 57.988151 B = 125.239327 G = 83.354963
Initial residual: 0.037279
Converges to: X = 19.251912 Y = -0.185209 Z = 9.815171 A = 49.232447 B = 134.584652 G = 106.519590
Final Residual: 0.000147

Perturbation 5
Initial Approximation: X = 17.682170 Y = 1.070915 Z = 7.974712 A = 46.803405 B = 133.605529 G = 111.684593
Initial residual: 0.008101
Converges to: X = 19.251973 Y = -0.185225 Z = 9.815199 A = 49.232423 B = 134.584655 G = 106.519543
Final Residual: 0.000147

Using perturbation #3
Initial Approximation: X = 18.757543 Y = -0.133020 Z = 6.964969 A = 28.374349 B = 146.061539 G = 123.253931
Initial residual: 0.076321
Converges to: X = 19.252135 Y = -0.185259 Z = 9.815251 A = 49.232270 B = 134.584600 G = 106.519363
Residual Vector = {-0.000050 0.000004 0.000020 0.000013 0.000003 -0.000093 -0.000067 -0.000036 0.000009 0.000003 -0.000006 0.000055 -0.000000 0.000000 0.000000 0.000000 0.000000}
Final residual: 0.000147
Stopping Criterion: 1
Number of function evaluations = 36

Data point # 40
==========

Perturbation 1
Initial Approximation: X = 19.252135 Y = -0.185259 Z = 9.815251 A = 49.232270 B = 134.584600 G = 106.519363
Initial residual: 0.000329
Converges to: X = 18.753529 Y = -0.225197 Z = 10.135808 A = 48.709197 B = 134.138754 G = 106.386375
Final Residual: 0.000167

Perturbation 2
Initial Approximation: X = 20.609254 Y = 1.081789 Z = 11.553021 A = 20.149441 B = 117.238577 G = 98.456916
Initial residual: 0.011328
Converges to: X = 18.753211 Y = -0.225343 Z = 10.135683 A = 48.708701 B = 134.138397 G = 106.386133
Final Residual: 0.000167

Perturbation 3
Initial Approximation: X = 19.462903 Y = 1.464160 Z = 12.027580 A = 59.861189 B = 123.298092 G = 120.756302
Initial residual: 0.018508
Converges to: X = 18.753217 Y = -0.225331 Z = 10.135687 A = 48.708728 B = 134.138397 G = 106.386182
Final Residual: 0.000167

Perturbation 4
Initial Approximation: X = 18.291689 Y = 1.399233 Z = 8.140558 A = 38.576292 B = 127.102619 G = 120.559353
Initial residual: 0.023373
Converges to: X = 18.754633 Y = -0.224277 Z = 10.136214 A = 48.711106 B = 134.138937 G = 106.389480
Final Residual: 0.000167

Perturbation 5
Initial Approximation: X = 19.943456 Y = 0.534540 Z = 9.205397 A = 43.404081 B = 159.013557 G = 133.332174
Initial residual: 0.087055
Converges to: X = 18.754260 Y = -0.224536 Z = 10.136227 A = 48.712012 B = 134.140774 G = 106.387808
Final Residual: 0.000167

Using perturbation #4
Initial Approximation: X = 18.291689 Y = 1.399233 Z = 8.140558 A = 38.576292 B = 127.102619 G = 120.559353
Initial residual: 0.023373
Converges to: X = 18.754633 Y = -0.224277 Z = 10.136214 A = 48.711106 B = 134.138937 G = 106.389480
Residual Vector = {-0.000049 0.000005 0.000012 0.000017 0.000011 -0.000122 -0.000070 -0.000029 -0.000004 -0.000014 -0.000015 0.000050 -0.000000 0.000000 0.000000 0.000000 0.000000}
Final residual: 0.000167
Stopping Criterion: 3
Number of function evaluations = 34

Data point # 41
==========

Perturbation 1
Initial Approximation: X = 18.754633 Y = -0.224277 Z = 10.136214 A = 48.711106 B = 134.138937 G = 106.389480
Initial residual: 0.000315
Converges to: X = 18.467129 Y = -0.110046 Z = 10.500275 A = 48.698117 B = 134.448686 G = 105.783859
Final Residual: 0.000175

Perturbation 2
Initial Approximation: X = 19.321232 Y = 0.553502 Z = 10.376636 A = 52.312950 B = 132.516069 G = 122.964435
Initial residual: 0.012673
Converges to: X = 18.467718 Y = -0.109011 Z = 10.500782 A = 48.704280 B = 134.453636 G = 105.786107
Final Residual: 0.000175

Perturbation 3
Initial Approximation: X = 18.198976 Y = 1.267706 Z = 12.126528 A = 61.368547 B = 140.502627 G = 78.050500
Initial residual: 0.013240
Converges to: X = 18.855413 Y = -0.548434 Z = 10.839760 A = 53.833416 B = 143.972709 G = 89.995612
Final Residual: 0.000530

Perturbation 4
Initial Approximation: X = 17.633415 Y = 1.895622 Z = 9.395901 A = 34.520849 B = 133.763562 G = 96.336336
Initial residual: 0.016964
Converges to: X = 18.465971 Y = -0.110577 Z = 10.500003 A = 48.695799 B = 134.446918 G = 105.782859
Final Residual: 0.000175

Perturbation 5
Initial Approximation: X = 20.124170 Y = 1.138765 Z = 9.968453 A = 49.174969 B = 108.492282 G = 118.454229
Initial residual: 0.024523
Converges to: X = 18.465802 Y = -0.110658 Z = 10.499962 A = 48.695461 B = 134.446666 G = 105.782704
Final Residual: 0.000175

Using perturbation #1
Initial Approximation: X = 18.754633 Y = -0.224277 Z = 10.136214 A = 48.711106 B = 134.138937 G = 106.389480
Initial residual: 0.000315
Converges to: X = 18.467129 Y = -0.110046 Z = 10.500275 A = 48.698117 B = 134.448686 G = 105.783859
Residual Vector = {-0.000046 0.000002 0.000002 0.000018 0.000021 -0.000134 -0.000070 -0.000014 -0.000019 -0.000036 -0.000019 0.000046 -0.000000 0.000000 0.000000 0.000000 0.000000}
Final residual: 0.000175
Stopping Criterion: 2
Number of function evaluations = 40

Data point # 42
==========

Perturbation 1
Initial Approximation: X = 18.467129 Y = -0.110046 Z = 10.500275 A = 48.698117 B = 134.448686 G = 105.783859
Initial residual: 0.000317
Converges to: X = 18.233088 Y = 0.062664 Z = 10.854362 A = 49.016208 B = 135.159554 G = 105.011242
Final Residual: 0.000200

Perturbation 2
Initial Approximation: X = 18.649256 Y = 0.500029 Z = 9.461556 A = 17.513881 B = 130.176773 G = 120.184999
Initial residual: 0.057852
Converges to: X = 18.228499 Y = 0.059671 Z = 10.853441 A = 48.997320 B = 135.147732 G = 104.997550
Final Residual: 0.000200

Perturbation 3
Initial Approximation: X = 19.270707 Y = 0.898493 Z = 10.318772 A = 37.491837 B = 129.769859 G = 119.005402
Initial residual: 0.027395
Converges to: X = 18.234612 Y = 0.063308 Z = 10.854037 A = 49.012880 B = 135.157278 G = 105.009197
Final Residual: 0.000200

Perturbation 4
Initial Approximation: X = 19.027369 Y = 0.204313 Z = 9.088873 A = 59.946013 B = 99.226950 G = 106.221761
Initial residual: 0.064561
Converges to: X = 18.233469 Y = 0.061831 Z = 10.853765 A = 49.007098 B = 135.153753 G = 105.004771
Final Residual: 0.000200

Perturbation 5
Initial Approximation: X = 18.723697 Y = 1.345294 Z = 8.573789 A = 22.178341 B = 160.123116 G = 105.993520
Initial residual: 0.081788
Converges to: X = 18.234998 Y = 0.062439 Z = 10.853837 A = 49.010268 B = 135.155825 G = 105.006896
Final Residual: 0.000200

Using perturbation #5
Initial Approximation: X = 18.723697 Y = 1.345294 Z = 8.573789 A = 22.178341 B = 160.123116 G = 105.993520
Initial residual: 0.081788
Converges to: X = 18.234998 Y = 0.062439 Z = 10.853837 A = 49.010268 B = 135.155825 G = 105.006896
Residual Vector = {-0.000040 -0.000010 -0.000004 0.000011 0.000029 -0.000152 -0.000071 -0.000002 -0.000032 -0.000069 -0.000025 0.000049 -0.000000 0.000000 0.000000 0.000000}
Final residual: 0.000200
Stopping Criterion: 2
Number of function evaluations = 48

Data point # 43
==========

Perturbation 1
Initial Approximation: X = 18.234998 Y = 0.062439 Z = 10.853837 A = 49.010268 B = 135.155825 G = 105.006896
Initial residual: 0.000268
Converges to: X = 18.016987 Y = 0.178269 Z = 11.122625 A = 49.589354 B = 136.062528 G = 104.325337
Final Residual: 0.000212

Perturbation 2
Initial Approximation: X = 18.466037 Y = 1.187547 Z = 10.816093 A = 47.048282 B = 96.370353 G = 81.002164
Initial residual: 0.049899
Converges to: X = 18.022708 Y = 0.179649 Z = 11.121487 A = 49.598514 B = 136.065889 G = 104.337131
Final Residual: 0.000212

Perturbation 3
Initial Approximation: X = 18.541152 Y = 1.076727 Z = 11.017665 A = 26.146227 B = 138.404697 G = 121.397446
Initial residual: 0.063664
Converges to: X = 18.017327 Y = 0.179639 Z = 11.122693 A = 49.594955 B = 136.064353 G = 104.333085
Final Residual: 0.000212

Perturbation 4
Initial Approximation: X = 19.004193 Y = 2.194054 Z = 12.176859 A = 48.298753 B = 138.992833 G = 63.419811
Initial residual: 0.021327
Converges to: X = 20.431585 Y = 0.182189 Z = 11.348368 A = 46.520633 B = 136.604420 G = 88.550463
Final Residual: 0.000482

Perturbation 5
Initial Approximation: X = 16.067987 Y = 0.558518 Z = 10.871809 A = 71.435598 B = 143.847683 G = 85.776424
Initial residual: 0.024239
Converges to: X = 18.018215 Y = 0.178557 Z = 11.122405 A = 49.591126 B = 136.063151 G = 104.327670
Final Residual: 0.000212

Using perturbation #5
Initial Approximation: X = 16.067987 Y = 0.558518 Z = 10.871809 A = 71.435598 B = 143.847683 G = 85.776424
Initial residual: 0.024239
Converges to: X = 18.018215 Y = 0.178557 Z = 11.122405 A = 49.591126 B = 136.063151 G = 104.327670
Residual Vector = {-0.000036 -0.000020 -0.000001 -0.000001 0.000031 -0.000152 -0.000065 0.000013 -0.000039 -0.000100 -0.000017 0.000053 -0.000000 0.000000 0.000000 0.000000}
Final residual: 0.000212
Stopping Criterion: 2
Number of function evaluations = 61

D.7 RUN067 With Motion Constraining Residual Add-on

The plots below refer to the discussion of section 4.3.1.1. The computed X, Y and Z position of the tracking sphere using the data of RUN067 is presented below. The first set of plots are the X, Y and Z when

$$F1 = 2.0e\text{-}05 \quad \text{and} \quad F2 = 0.$$

These figures represent a minor "penalty" as the distance the tracking moves from iteration to iteration increases. No restriction is placed on the angular displacement because the run in angle invariant. We do not expect to see large angle variations. The second set of plots correspond to

$$F1 = 3.5e\text{-}05 \quad \text{and} \quad F2 = 0.$$

These figures represent a large "penalty" as the tracking sphere's displacement increases from iterate to iterate.

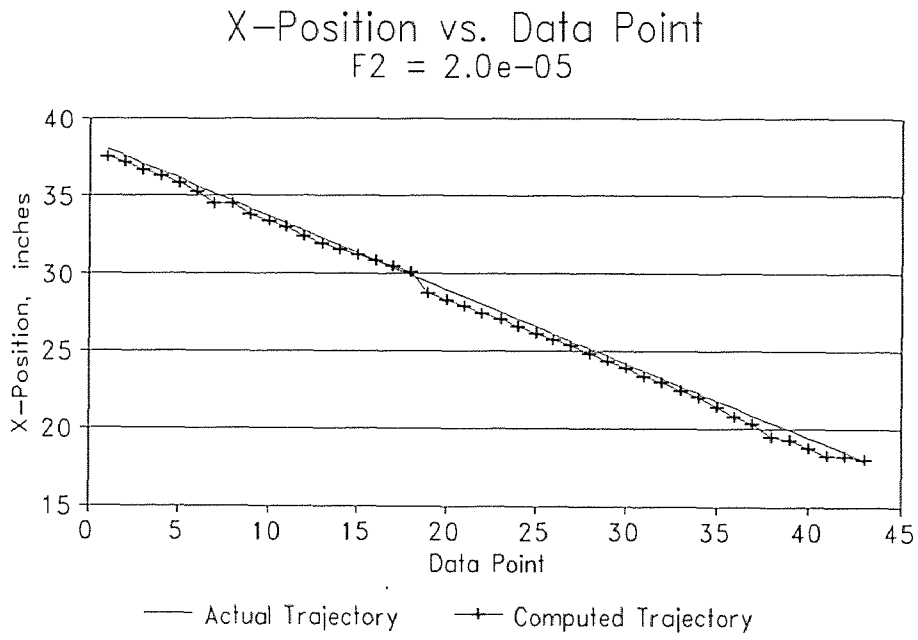

Figures D.27 X-Solution, $F1=2.0e^{-05}$

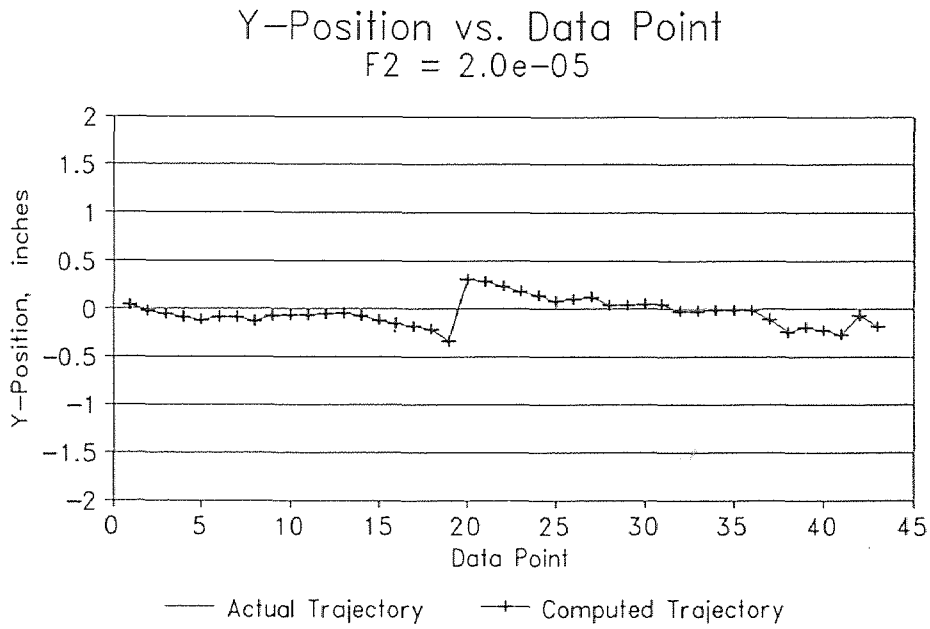

Figures D.28 Y-Solution, F1=2.0e^{-05}

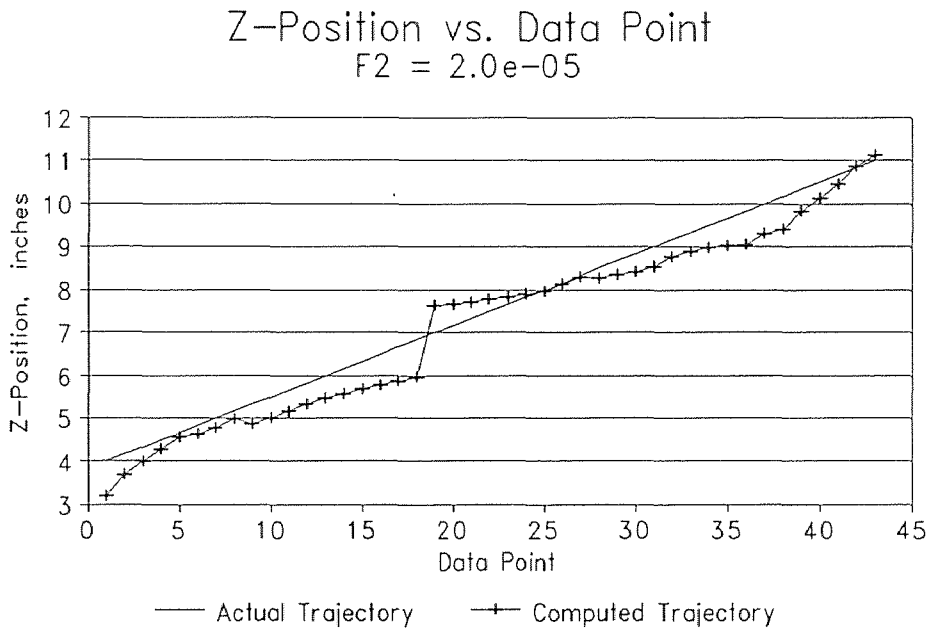

Figures D.29 Z-Solution, F1=2.0e^{-05}

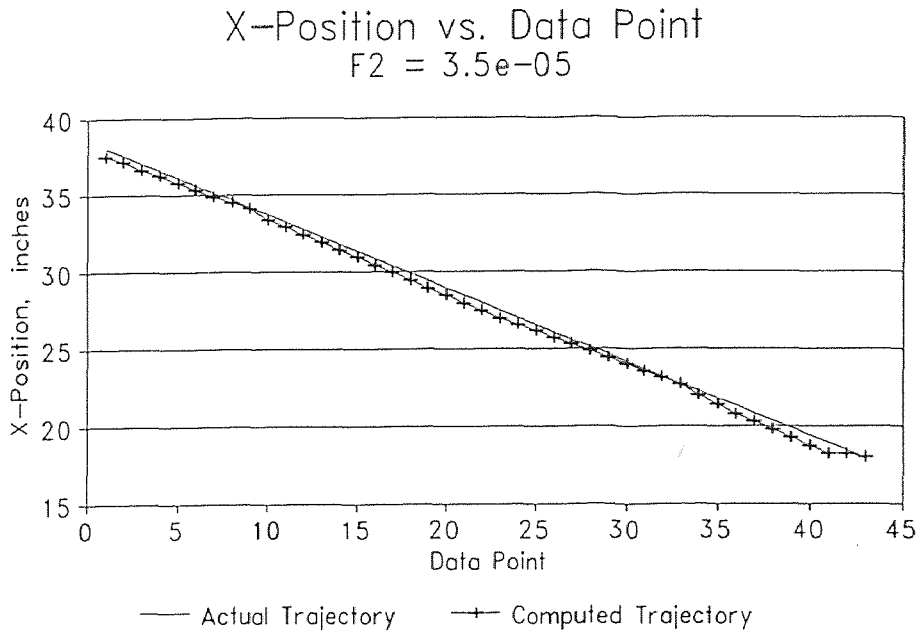

Figures D.30 X-Solution, F1=3.5e^{-05}

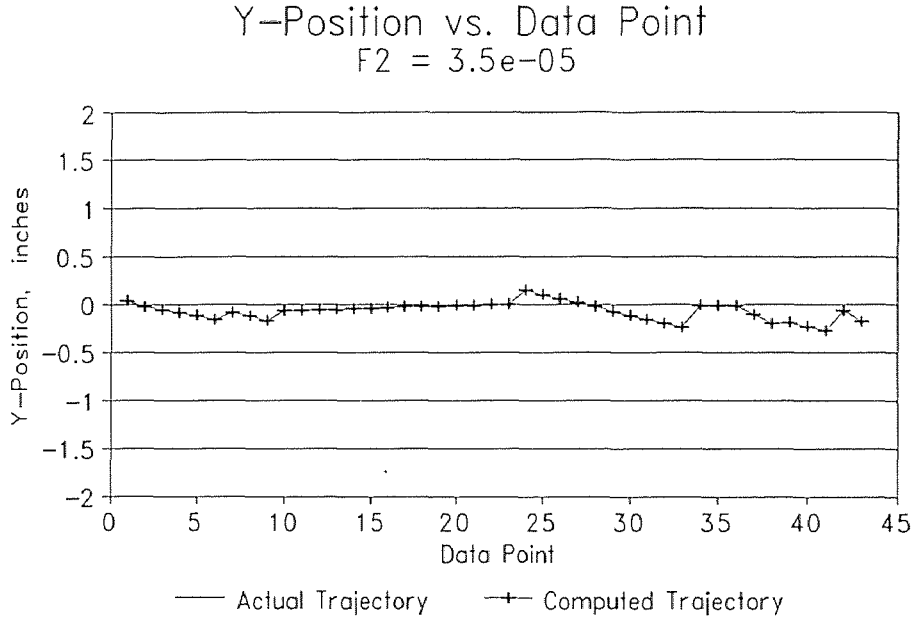

Figures D.31 Y-Solution, F1=3.5e^{-05}

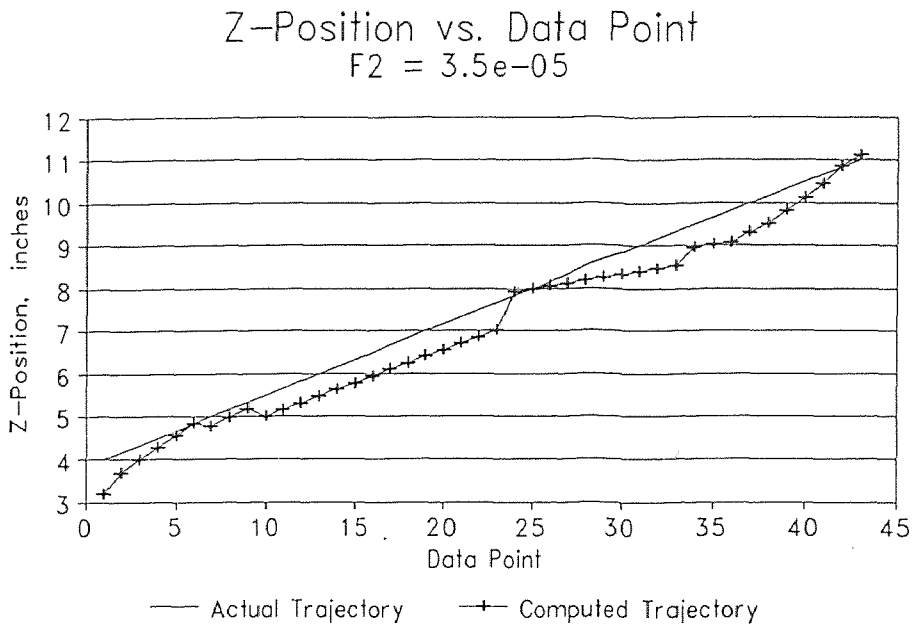

Figures D.32 Z-Solution, F1=3.5e^{-05}

APPENDIX E
Experimental Results

The data presented in this appendix are the results of several trajectories taken in the development of this technique. Trajectories are selected for presentation if they are useful illustration tools for the arguments in the body of this text. However, the results presented are typical of the successes of the tracking system as it stands at the date of this document.

E.1 Fixed-Angle Runs

The following fixed-angle runs will be presented in the proceeding sections:

- RUN038: Straight line
- RUN068: Straight line
- RUN251: Straight line

E.1.1 Solution to RUN038

The data of figures E.1 to E.4 are for the fixed-angle, straight-line trajectory RUN038. The starting and ending points of this trajectory are as follows:

Start:	X = 29.0"	Y= 2.0"	Z = 9.4"	α = 45.0°	β= 45.0°	γ = 90.0°
End:	X = 7.0"	Y= 2.0"	Z = 9.4"	α = 45.0°	β= 45.0°	γ = 90.0°

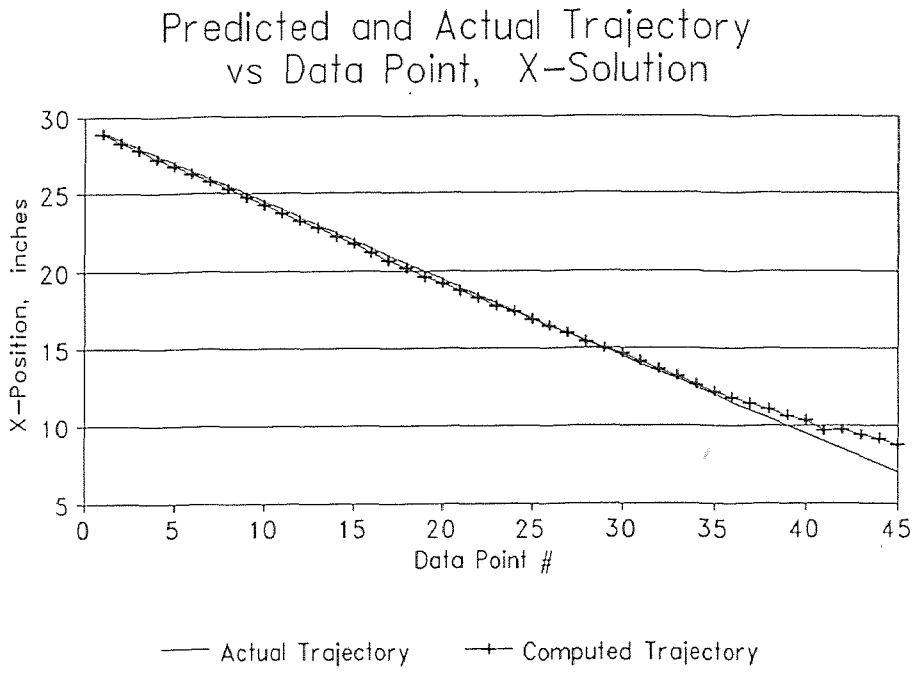

Figure E.1 X-Solution (RUN038).

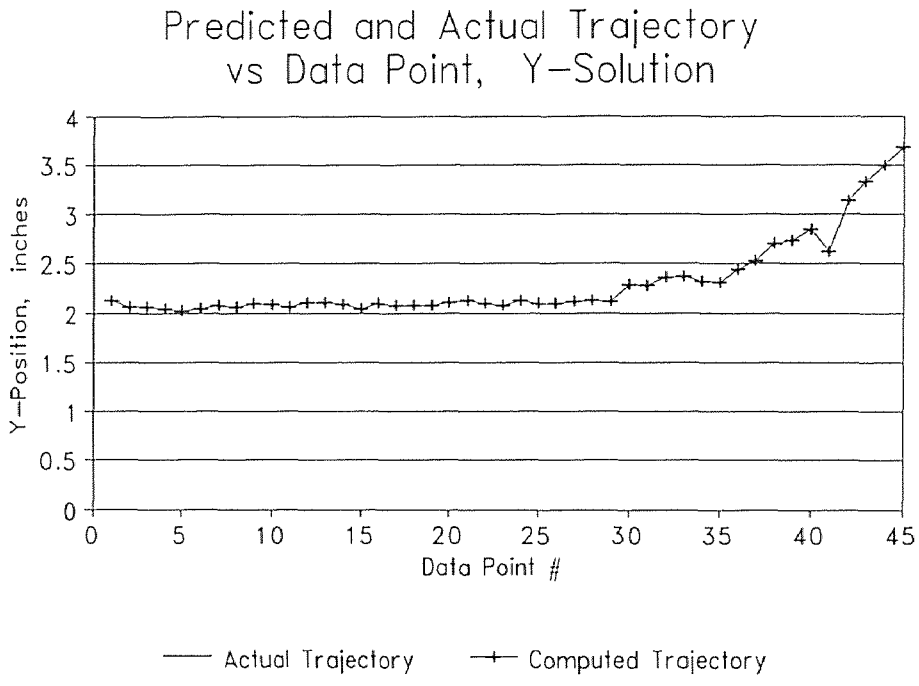

Figure E.2 Y-Solution (RUN038).

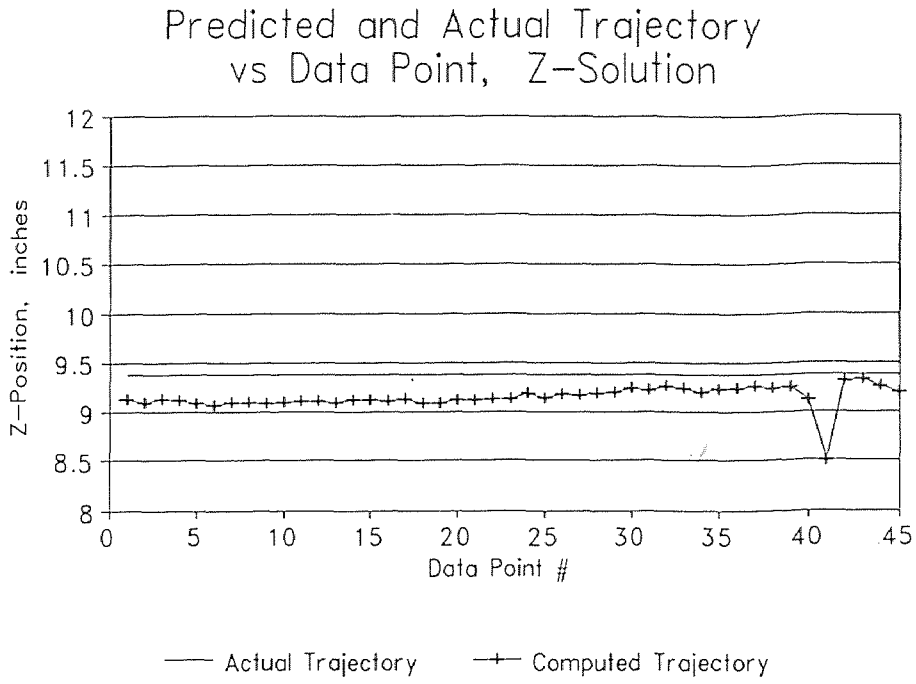

Figure E.3 Z-Solution (RUN038).

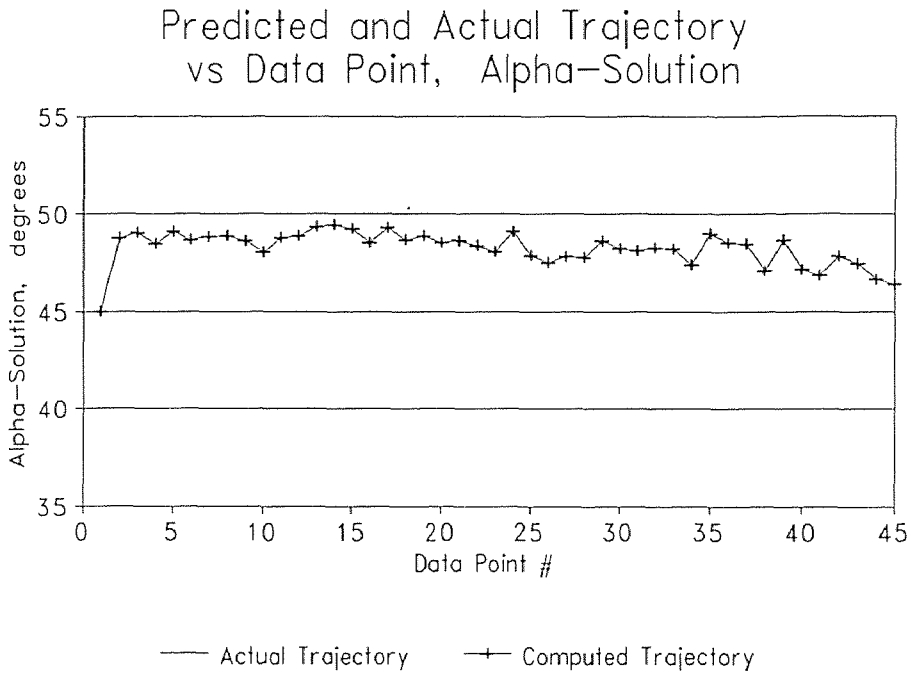

Figure E.4 Alpha-Solution (RUN038).

E.1.2 Solution to RUN068

The data of figures E.5 to E.8 are for the fixed-angle, straight-line trajectory RUN068. The starting and ending points of this trajectory are as follows:

Start: X = 3.0" Y = 0.0" Z = 4.0" $\alpha = 48.0°$ $\beta = 135.5°$ $\gamma = 77.0°$

End: X = 3.0" Y = 0.0" Z = 4.0" $\alpha = 48.0°$ $\beta = 135.5°$ $\gamma = 77.0°$

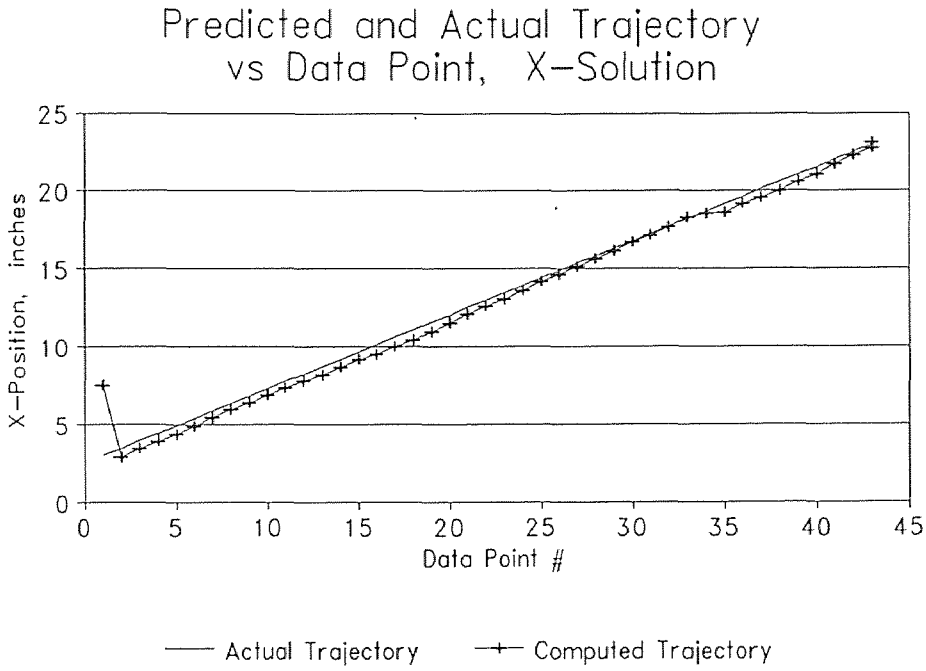

Figure E.5 X-Solution (RUN068).

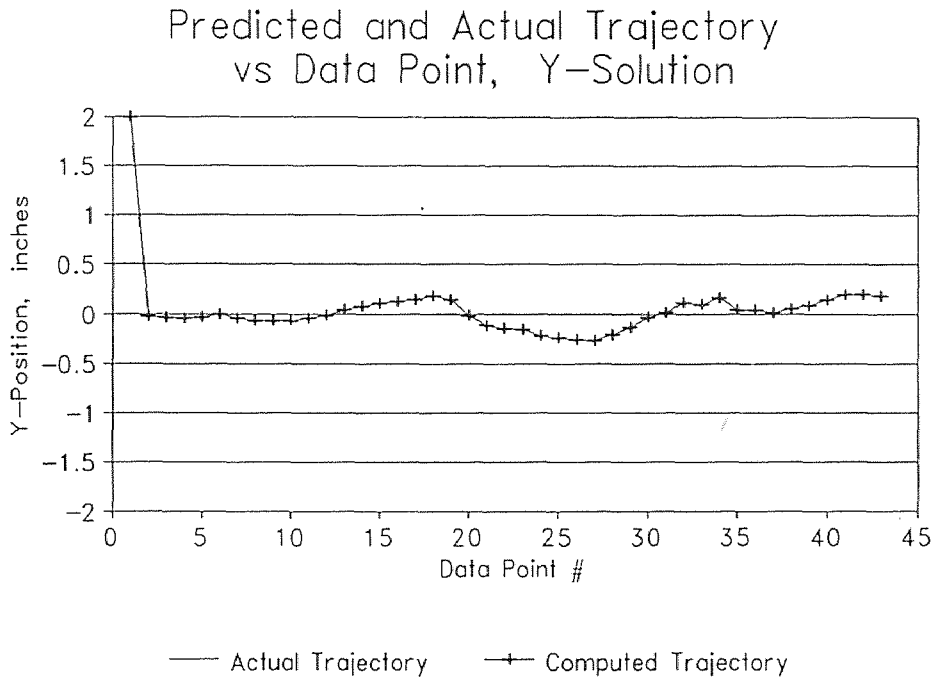

Figure E.6 Y-Solution (RUN068).

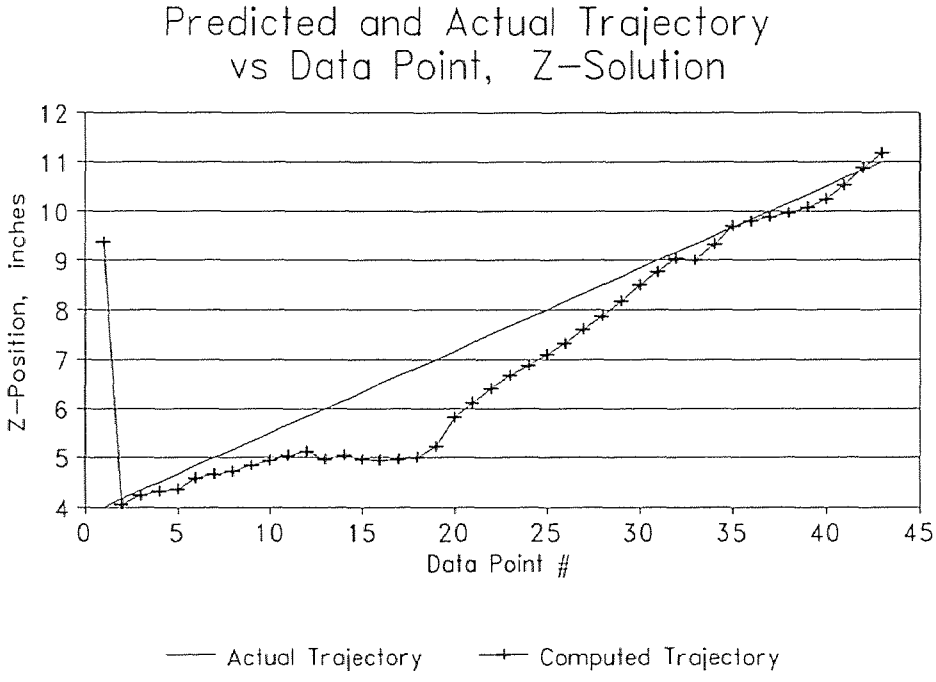

Figure E.7 Z-Solution (RUN068).

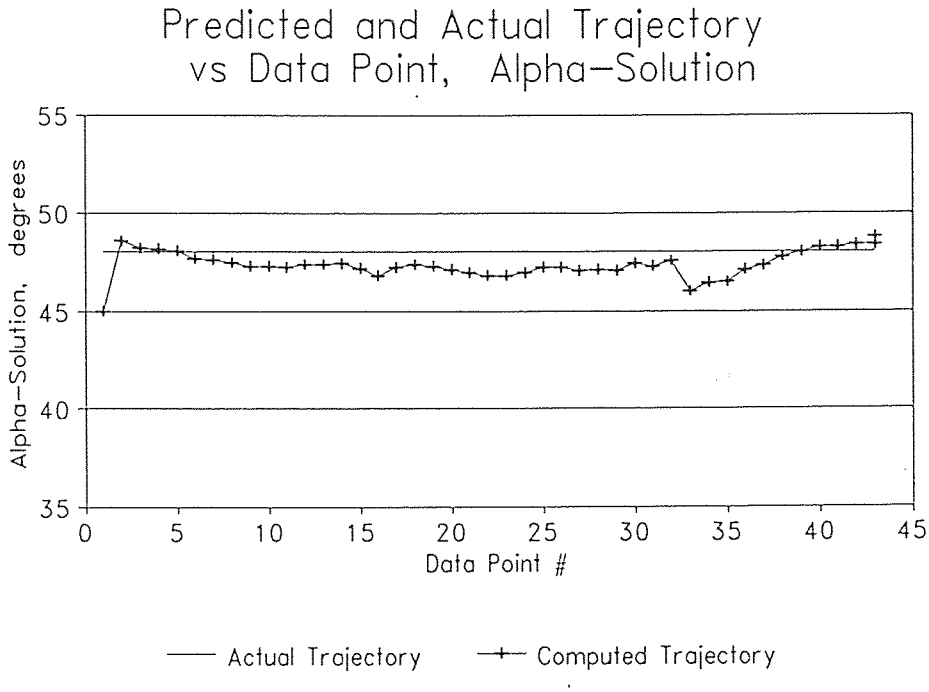

Figure E.8 Alpha-Solution (RUN068).

E.1.3 Solution to RUN251

The data of figures E.9 to E.12 are for the fixed-angle, straight-line trajectory RUN251.

The starting and ending points of this trajectory are as follows:

Start:	X = 53.0"	Y = 3.0"	Z = 10.5"	α = 46.0°	β = 82.5°	γ = 45.0°
End:	X = 53.0"	Y = -3.0"	Z = 10.5"	α = 46.0°	β = 82.5°	γ = 45.0°

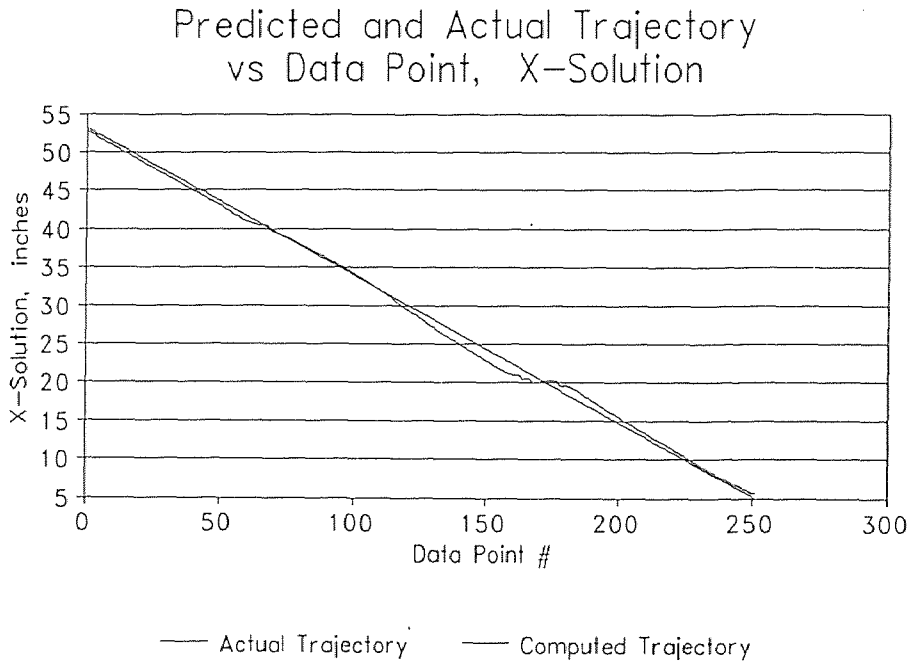

Figure E.9 X-Solution (RUN251)

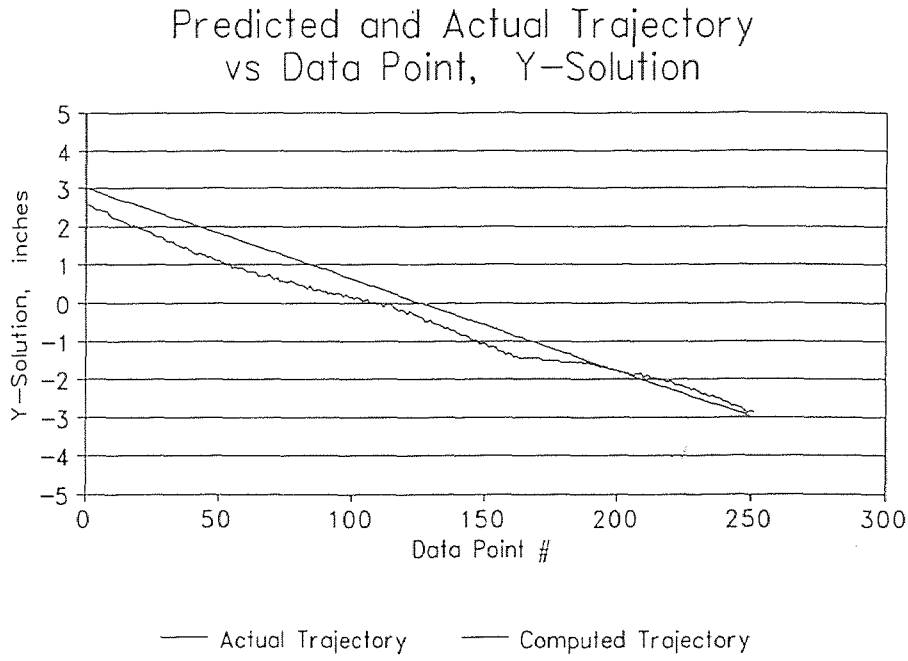

Figure E.10 Y-Solution (RUN251)

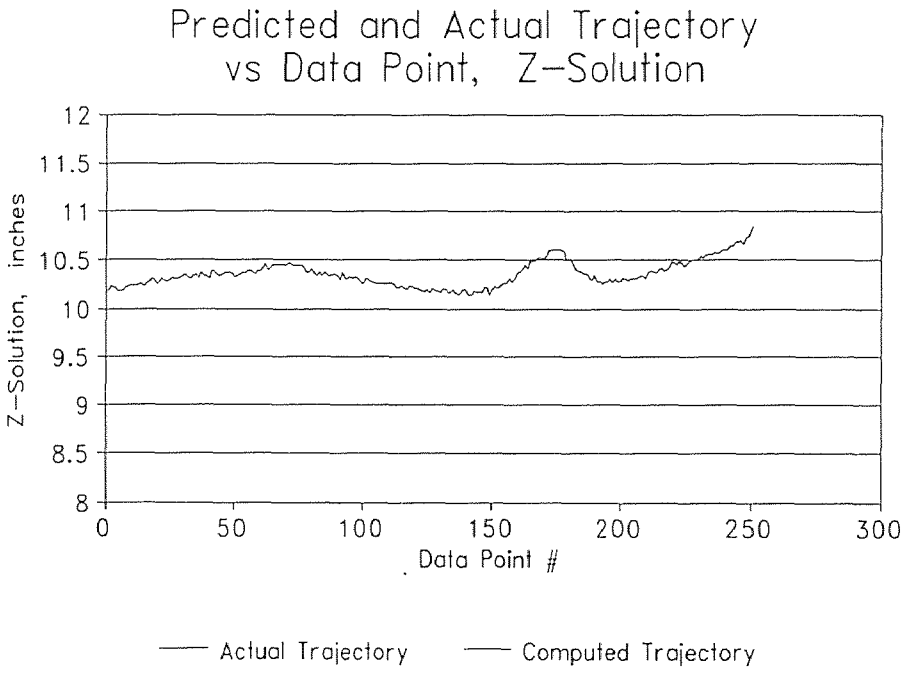

Figure E.11 Z-Solution (RUN251)

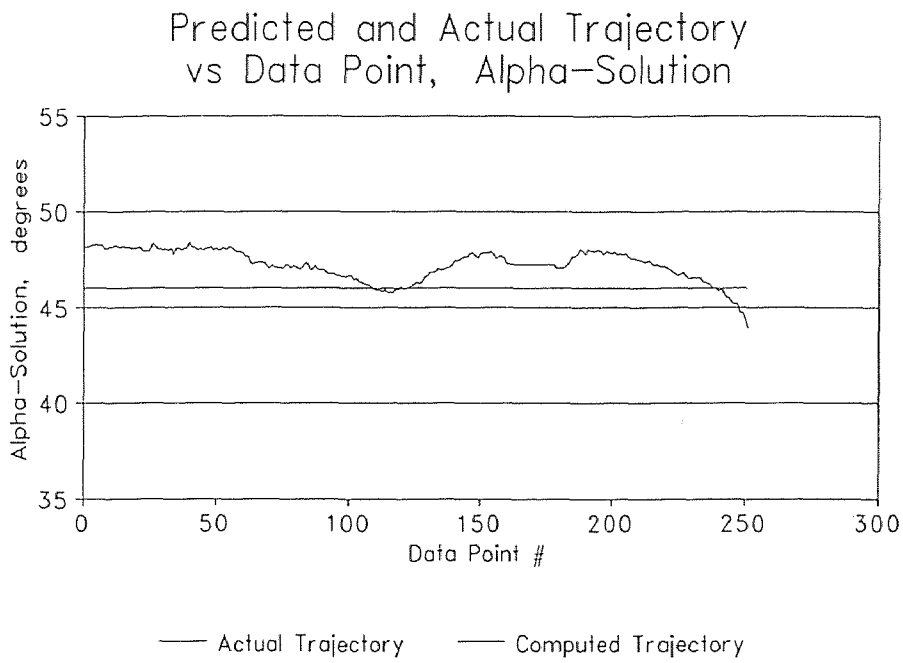

Figure E.12 Alpha-Solution (RUN251)

E.2 Simulated Roll

The data in this section is representative of the "simulated roll" (RUN061) described in section 5.1.2.

The starting and ending points of this trajectory are as follows:

Start:	X = 34.0"	Y = 0.0"	Z = 6.4"	$\alpha = 121°$	$\beta = 59°$	$\gamma = 47.0°$
End:	X = 15.5"	Y = 0.0"	Z = 6.4"	$\alpha = 59°$	$\beta = 121°$	$\gamma = 47.0°$

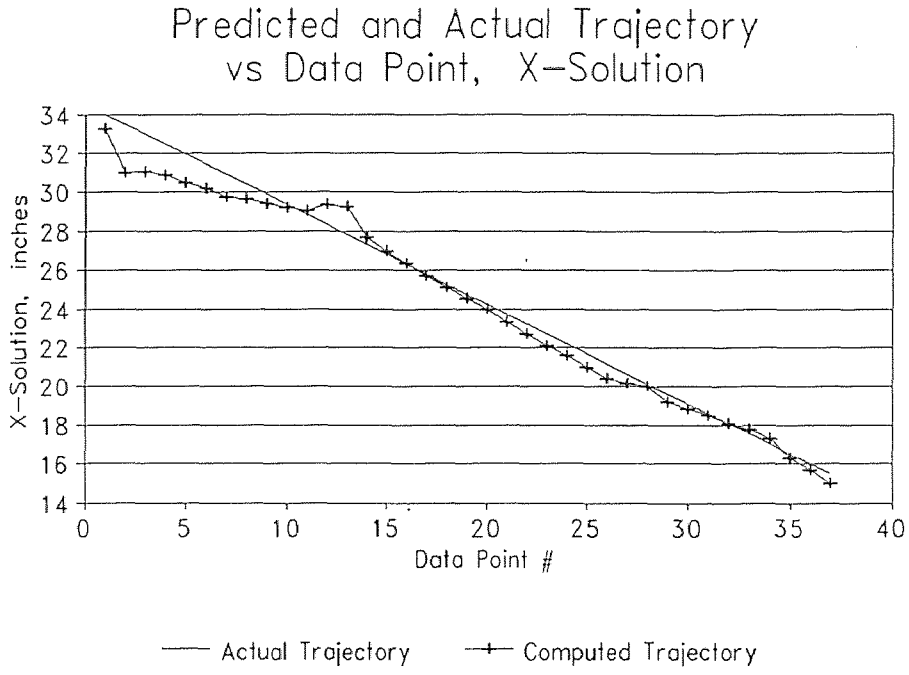

Figure E.13 X-Solution (RUN061)

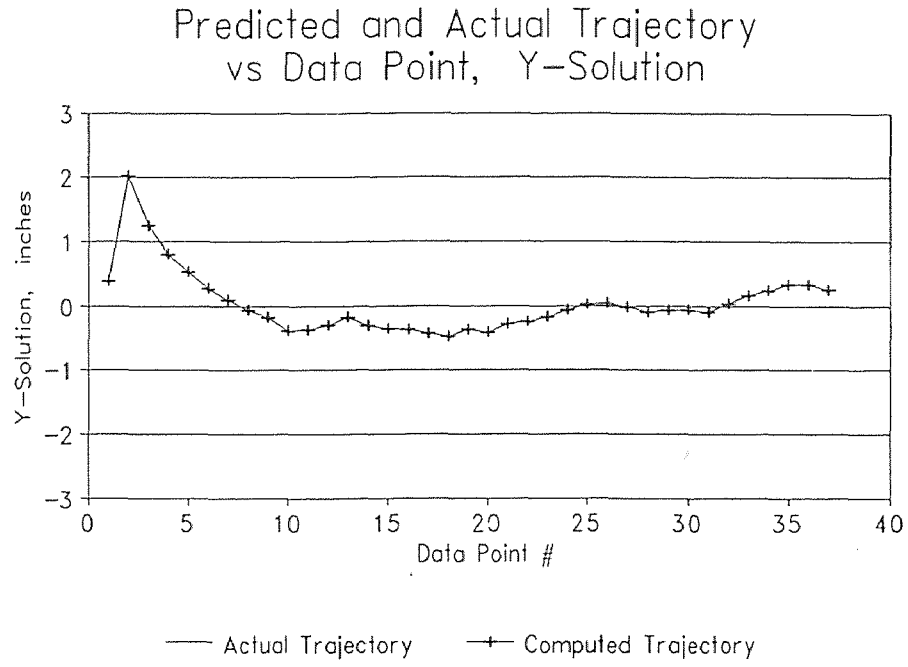

Figure E.14 Y-Solution (RUN061)

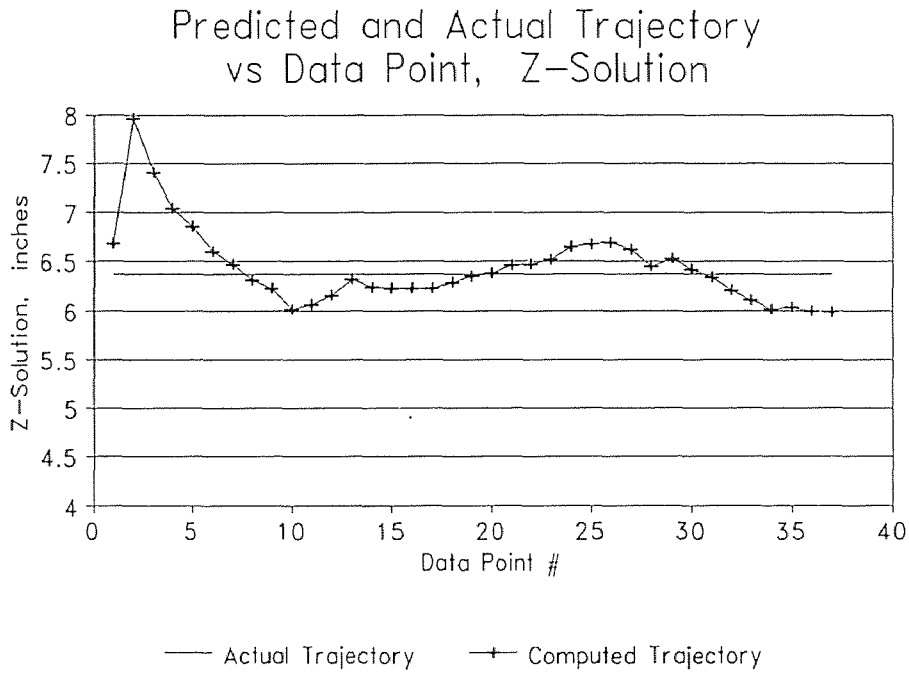

Figure E.15 Z-Solution (RUN061)

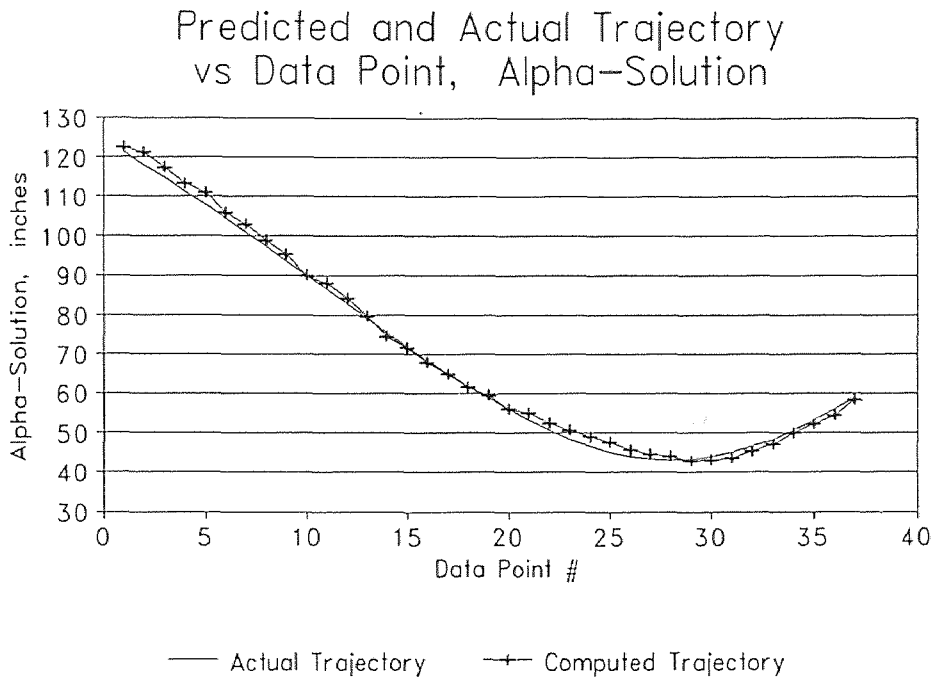

Figure E.16 Alpha-Solution (RUN061)

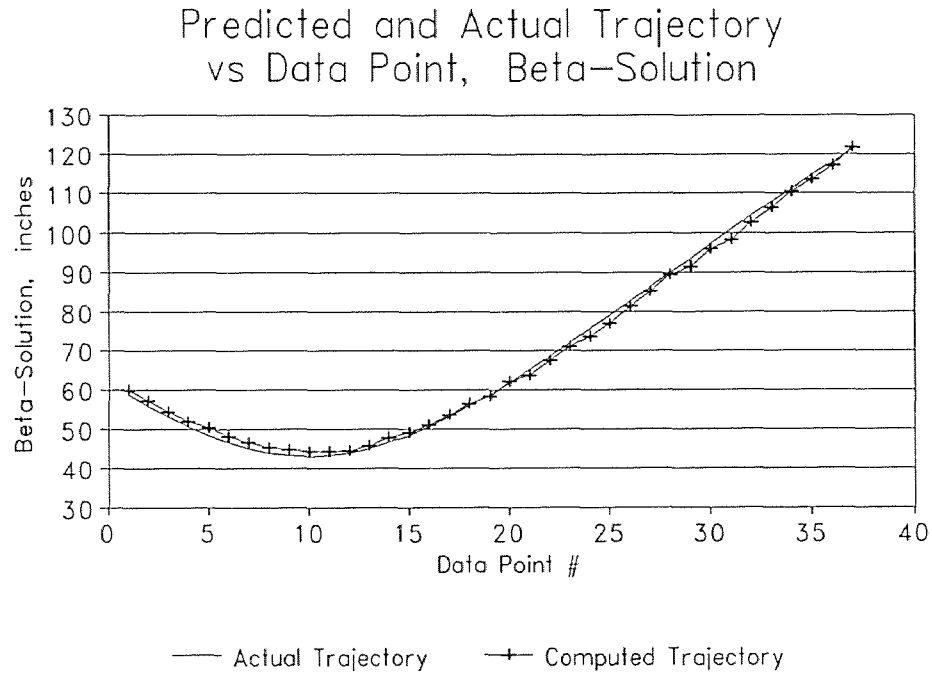

Figure E.17 Beta-Solution (RUN061)

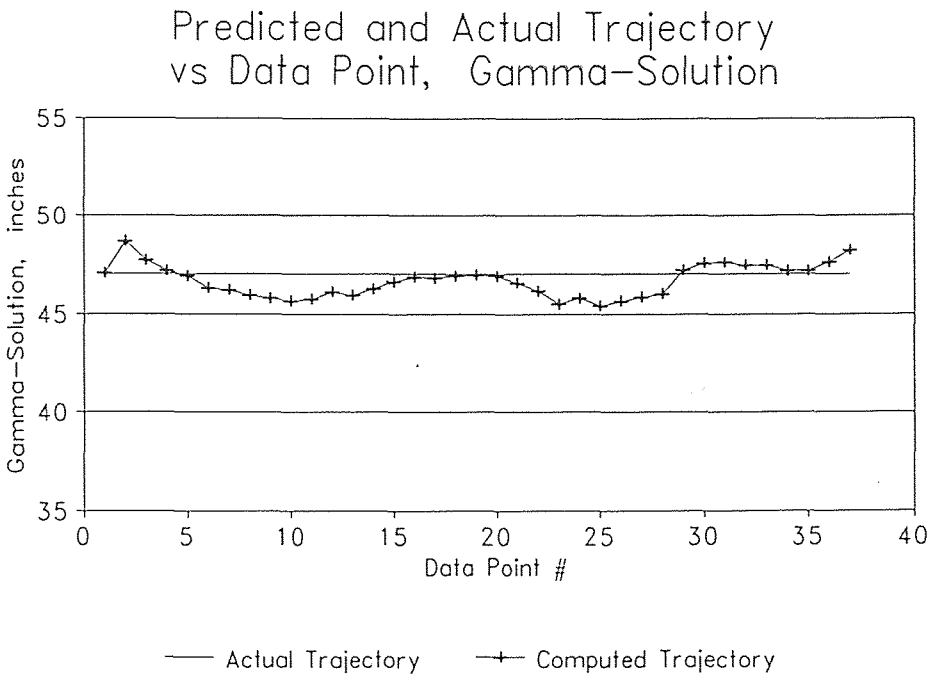

Figure E.18 Gamma-Solution (RUN061)

APPENDIX F
Materials, Equipment and Algorithms

The contents of this appendix is a description of trade names and supplier names for the various materials and tools used in this research.

Extren: Extren is a high-strength fiberglass reinforced thermalset polyester or vinyl ester resin. The Extren trade name is a registered trademark of Morrison Molded Fiber Glass Company, Bristol, Virginia.

AT-MIO-16: The AT-MIO-16 is a high-performance multifunction analog, digital and timing input/output board for the IBM PC AT and compatibles. The AT-MIO-16 is a product of the National Instruments Corporation, Austin, Texas.

AT-MUX-64: The AMUX-64T is a front-end analog multiplexer that quadruples the number of analog input signals that can be digitized with a National Instruments AT-MIO-16 board. The AMUX-64T is a product of National Instruments Corporation, Austin, Texas.

Marconi Radio Communications Test Set: 2955R: The Marconi 2955R Radio Communications Test Set is an instruments capable of combining all the measurement facilities required for testing mobile radio transceivers in the range up to 1000MHz. It is a product of Marconi Instruments Ltd., United Kingdom.

MINPACK: MINPACK refers to a FORTRAN package developed by Jorge More, Burt Garbow and Kell Hillstrom at Argonne National Laboratory used to solve systems of nonlinear equations and nonlinear least squares problems. The algorithms proceed either from an analytic specification of the Jacobian matrix or directly from the problem functions. The paths include facilities for systems of equations with a banded Jacobian matrix, for least squares problems with a large amount of data, and for checking the consistency of the Jacobian matrix with the functions.

LMDIF: One of five principle algorithms from the MINPACK package. The purpose of lmdif is to minimize the sum of the squares of m nonlinear functions in n variables by a modification of the levenberg-marquardt algorithm. the user must provide a subroutine which calculates the functions. The Jacobian is then calculated by a forward-difference approximation.

REFERENCES

1 Ashok, A. S., "Computational Aspects of a Three Dimensional Non-Intrusive Particle Motion Tracking System", Thesis submitted to the faculty of New Jersey Institute of Technology (1992).

2 Carr, W. N. and A. Parasar, Private Communications, New Jersey Institute of Technology (1992).

3 Dave, R. N., Ashok, A. S., Bukiet, B. G., On the Development of a Three Dimensional Particle Motion Tracking System", *Proceedings to the ASME Winter Annual Meeting*, (1992).

4 La Rosa, A., Private Communications, New Jersey Institute of Technology (1992).

5 Parasar, A., Lab notes, New Jersey Institute of Technology (1992).

6 Savage, S. B., "Flows of Granular Materials with Applications to Geophysical Problems", Lectures for the *Continuum Mechanics in the Environmental Sciences and Geophysics* (1992) 1-3.

7 Troiano, A., Private Communications, New Jersey Institute of Technology (1992).

8 Tuzun, U., G. T. Houlsby, R. M. Nedderman, and S. B. Savage, "The Flow of Granular Materials - II", *Chem. Eng. Sci.* vol 37(12), 1691-1709, 1982.

9 Van Valkenberg, M. E., Network Analysis, pg. 258, Prentice-Hall, Englewood Cliffs, New Jersey, 1974.

10 Woodcock, C. R. and J. S. Mason, Bulk Solids Handling: An Introduction to the Practice and Technology, Blackie & Son Limited, London (1987) iii-iv.

GLOSSARY

background reading or **background noise**: the finite signal measured by the data acquisition system when all local transmitters are shut off.

backward model: the mathematics that allow us to compute the transmitter's position given the signal levels in a set of antennae.

backward solution or inverse solution: the computed position and orientation of the transmitter(s) given the signal levels in a set of antennae.

bulk solid or granular mass: class of substances characterized by a collection of discrete particles dispersed in a fluid continuum.

count: trademark of National Instruments -- a count is a unit of measuring potential difference. 204.8 counts correspond to 1 volt.

coupling: phenomenon whereby the receiver antennae with high signal levels behave as secondary transmitters. An adjacent antenna affected by the transmitting antenna is said to be *coupled* with the transmitting antenna.

cubic tessellation: method arranging square antennae about the flow space such that the loop antennae form the outline of stacked cubes.

DAQ System: Data AcQuisition System. The data acquisition in the composite multiplexer, analog to digital converter and PC-based data collecting system used to collect data from the band-pass amplifier system.

decoupling: process of reversing the effect of antenna-to-antenna inductions.

forward model: mathematics used to compute voltages induced in a loop antenna as a function of transmitter position and orientation.

forward solution: Theoretical voltages computed for a given transmitter position and orientation.

inverse solution or backward solution: the computed position and orientation of the transmitter(s) given the signal levels in a set of antennae.

iteration: One step of the Levenberg-Marquardt algorithm, resulting in an advancement toward a local or global minimum.

orientation: orientation typically refers to the orientation of the transmitting coil in space. Because the transmitter is fixed in the tracking sphere, its orientation is an indication of the orientations of the orientation of the tracer particle. The parameters that define the transmitting coil's orientation are α, β and γ as defined in the figure below.

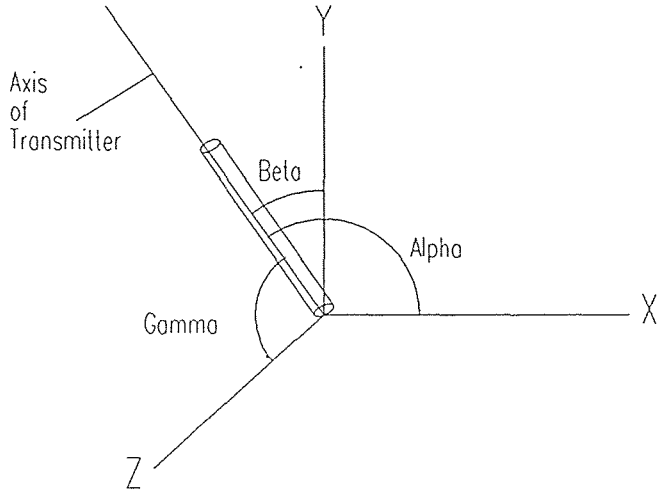

orthogonality condition: condition wherein the axis of the transmitter is 90° with respect to the axis of an antenna. The result of such an occurrence is typically a low reading in the orthogonal antenna.

perturbation: process by which alternate initial-guesses are selected as a seed for the numerical algorithm. Once the numerical algorithm converges to a solution, the solution vector $\bar{x} = \{x, y, z, \alpha, \beta, \gamma\}^T$ is randomly perturbed such that a new initial guess $\bar{x}_0 = \{x + \Delta x, y + \Delta y, z + \Delta z, \alpha + \Delta\alpha, \beta + \Delta\beta, \gamma + \Delta\gamma\}^T$ is selected and the iteration process is repeated. This is done any number of time. The iteration sequence resulting in the least residual is selected at the global minimum.

tessellation: system or arranging antennae about the flow space.

tracking sphere: the packaged transmitter. The tracking sphere is the powered transmitter embedded within a 1" acrylic sphere typical of those in the flowing mass.

voltage model: Mathematical model that allows us to compute voltages given the position and orientation of the transmitting source.